Roles of Acyl-CoA:Diacylglycerol Acyltransferases 1 and 2 in Triacylglycerol Synthesis and Secretion in Hepatocytes

by

Chen Li

A thesis submitted in partial fulfillment of the requirements for the degree of

Master of Science

Department of Cell Biology
University of Alberta

Abstract

Triacylglycerol (TG) metabolism with its high-energy potential is stringently regulated. Unbalanced TG regulation, either too much TG that overwhelms cellular storage capacity or too little TG due to defects in adipogenesis, is associated with various metabolic disorders. TG can be exported from liver in very-low density lipoprotein (VLDL). Although compelling evidence suggests that the majority of TG in VLDL is derived from re-esterification of lipolytic products released by endoplasmic reticulum-associated lipases, little is known about the roles of enzymes that catalyze the re-esterification reaction, acyl-CoA:diacylglycerol acyltransferases (DGATs). In mammals, two DGAT enzymes (DGAT1 and DGAT2) with no homology in primary amino acid sequences are encoded by genes belonging to distinct gene families and perform non-redundant physiological functions. The research goal was to investigate the contribution of DGAT1 and DGAT2 to lipid metabolism and lipoprotein secretion in primary mouse and human hepatocytes.

Highly selective small-molecule inhibitors of DGAT1 and DGAT2 were used to track storage and secretion of lipids synthesized *de novo* from [^{3}H]acetic acid and from exogenously supplied [^{3}H]oleic acid. Inactivation of an individual DGAT did not affect incorporation of either radiolabeled precursor into intracellular TG, whereas combined inactivation of both DGATs severely attenuated TG synthesis. However, inhibition of DGAT2 augmented fatty acid oxidation, whereas inhibition of DGAT1 increased TG secretion, suggesting preferential channeling of separate DGAT-derived TG pools to distinct metabolic pathways. Inactivation of DGAT2 impaired cytosolic lipid droplet expansion, whereas DGAT1 inactivation promoted large lipid droplet formation. Moreover,

inactivation of DGAT2 attenuated expression of lipogenic genes. Finally, TG secretion was significantly reduced upon DGAT2 inhibition without altering extracellular apoB levels.

The data suggest that DGAT1 and DGAT2 can compensate for each other to synthesize TG, but TG synthesized by DGAT1 is preferentially channeled to oxidation, while DGAT2 synthesizes TG destined for VLDL assembly.

Preface

This thesis is an original work by Chen Li. Chemical inhibitors of DGAT1 and DGAT2 were supplied by our collaborator, Dr. Bryan Goodwin, Pfizer Global Research and Development, CVMED Research Unit, Cambridge, MA, USA. Human liver samples used for hepatocyte isolation were obtained from patients undergoing operations for therapeutic purposes at the Service of Digestive Tract Surgery, University of Alberta, by Jamie Lewis and Dr. Norman Kneteman, Department of Surgery, University of Alberta. Primary mouse hepatocytes were prepared with the assistance of Lena Li, a technician in Lehner Lab. Project conception and experimental designs in Chapters 3 and 4 were proposed by me and Dr. Richard Lehner. Acquisition of data and analysis and interpretation of data in Chapters 3 and 4 are my original work, as is the literature review in Chapter 1. Chapter 3 of this thesis is adapted from the published work by Chen Li, Lena Li, Jihong Lian, et al. "Roles of Acyl-CoA:Diacylglycerol Acyltransferases 1 and 2 in Triacylglycerol Synthesis and Secretion in Primary Hepatocytes," *Arteriosclerosis, Thrombosis, and Vascular Biology*, 35.5 (2015): 1080-1091. I am responsible for the data collection and analysis, as well as the manuscript composition. Dr. Richard Lehner is the supervisory author and involved with concept formation and manuscript editing.

Acknowledgements

The most important person to thank is my supervisor, Dr. Richard Lehner. Thank you for giving me this invaluable opportunity to learn from and work with you. Not only did you teach me knowledge, experimental and writing skills, scientific thinking, and also the importance and ways of collaboration in research, a sense of humor, and an optimistic and persistent attitude towards life and career.

I would like to thank my committee members: Dr. Richard Lehner, Dr. Paul Melançon and Dr. Dawei Zhang for your helpful discussions and comments throughout my Master program, and the review of my thesis.

I also appreciate all the help of my dearest senior lab members: Dr. Jihong Lian, Lena Li, Russ Watts, and Randy Nelson. Without your technical support and guidance, I would not be able to conduct this project. I also owe big thanks to my past and present lab mates: Jianfeng Huang and Wesam Bahitham. Your company and inspiring talks have colored every second of my mundane days. I would also like to thank my student, Marc Spiess. Thank you for your efforts and faith that initiate and drive a very demanding project forward, and also a precious friendship. Besides every one in the Lehner lab, I also appreciate the guidance, encouragement, and suggestions from every member of the Molecular and Cell Biology of Lipid (MCBL) group, and especially I am very grateful to Dr. Dennis Vance and Dr. Dawei Zhang for your big supports in helping me to pursue my future study and academic career.

Thank you to my peers and office staff at the Department of Cell Biology for all your kind supports and graciousness that always made me feel warmly welcomed.

Last, but not least, I would like to dedicate my greatest thanks to my parents and my boyfriend for their understanding, support, encouragement and unconditional love!

Table of Contents

List of Tables

List of Figures

List of Abbreviations

2-MG	2-monoacyl-*sn*-glycerol
ABHD5	alpha/beta-hydrolase-containing 5
ACC	acetyl-CoA carboxylase
AGPAT2	acylglycerol-3-phosphate O-acyltransferase 2
apo	apolipoprotein
Arf	ADP-ribosylation factor
ASM	acid-soluble metabolite
ASO	antisense oligonucleotide
ATGL	adipose TG lipase
ATP	adenosine triphosphate
BSA	bovine serum albumin
BSCL2	Berardinelli–Seip congenital lipodystrophy 2
CIDE	cell death-inducing DFFA-like effector
COPI	coatomer
CPT-1	carnitine palmitoyltransferase 1
CTP	cytidine triphosphate

CVD	cardiovascular disease
DG	diacylglycerol
DGAT	acyl-CoA:diacylglycerol acyltransferase
DMEM	Dulbecco's modified Eagle's medium
DMSO	dimethyl sulfoxide
DNL	*de novo* lipogenesis
dNTPs	deoxynucleotide triphophates
EDTA	ethylene diaminetetraacetic acid disodium salt
ER	endoplasmic reticulum
FA	fatty acid
FAS	fatty acid synthase
FBS	fetal bovine serum
GBF1	Golgi brefeldin-A-resistant guanine nucleotide exchange factor 1
GCA	Golgicide A
GLUT4	glucose transporter type 4
GPAT	glycerol-3-phosphate acyltransferase
GPL	glycerophospholipid

HDL	high-density lipoprotein
IRS	insulin receptor substrate
LD	lipid droplet
LDL	low-density lipoprotein
LPA	lysophosphatidic acid
LPL	lipoprotein lipase
MBOAT	membrane-bound O-acyltransferase
McA	McArdle rat hepatoma 7777
MGAT	acyl-CoA:monoacylglycerol acyltransferase
MTP	microsomal triacylglycerol transfer protein
NAFLD	nonalcoholic fatty liver disease
NASH	non-alcoholic steatohepatitis
NEFA	non-esterified fatty acid
PA	phosphatidic acid
PAP	phosphatidic acid phosphatase
PBS	phosphate buffered saline
PC	phosphatidylcholine

PE	phosphatidylethanolamine
PG	phosphatidylglycerol
PI	phosphatidylinositol
PL	Phospholipid(s)
PPAR	peroxisome proliferator-activated receptor
PS	phosphatidylserine
qPCR	quantitative polymerase chain reaction
SCD	stearoyl-CoA desaturase
SDS	sodium dodecyl sulphate
SREBP	sterol regulatory element binding protein
TBS	tris buffered saline
TG	triacylglycerol
TLC	thin-layer chromatography
TTBS	tris buffered saline with Tween®20
VLDL	very-low-density lipoprotein
WAT	white adipose tissue

CHAPTER I INTRODUCTION

1.1 Pathologies Associated with Abnormal TG Metabolism

Carbohydrates and triacylglycerol (TG) constitute the major energy sources for mammals. Energy balance is driven by a dynamic equation of the rate of energy intake and expenditure. Digestion of dietary fat is initiated in the stomach by acid-stable gastric lipases and amplified in the duodenum/jejunum by a synergic action of colipase-dependent pancreatic lipase and bile acids, releasing 2-monoacyl-*sn*-glycerol [2-(MG)] and free fatty acid (FA). These glycerolipid building blocks are then rapidly taken up by enterocytes via passive diffusion and active transport catalyzed by specific transport proteins. Within the enterocytes 2-MG and FA are re-esterified to TG and assembled into a TG-rich lipoprotein, termed chylomicron. Chylomicrons are transported through lymph vessels into the circulation, mainly delivering lipids to the adipose tissue for storage. In the fasted state, TG breakdown (lipolysis) in white adipose tissue (WAT) is stimulated, and the released FA is delivered to peripheral tissues for energy consumption. In the liver, the WAT-derived FA is re-synthesized into TG, some of which is stored in cytosolic lipid droplets (LDs) of hepatocytes, while the rest is assembled into hepatic TG-rich lipoprotein, termed very-low-density lipoprotein (VLDL). VLDL enters the bloodstream, where the TG component is hydrolyzed, releasing FA to oxidative tissues for fuel consumption, or WAT for storage (Figure 1-1).

TG metabolism with its high-energy potential is stringently regulated. Although nearly all types of eukaryotic cells are capable of storing TG, their storing capacities vary considerably. In mammals, the majority of TG is stored in

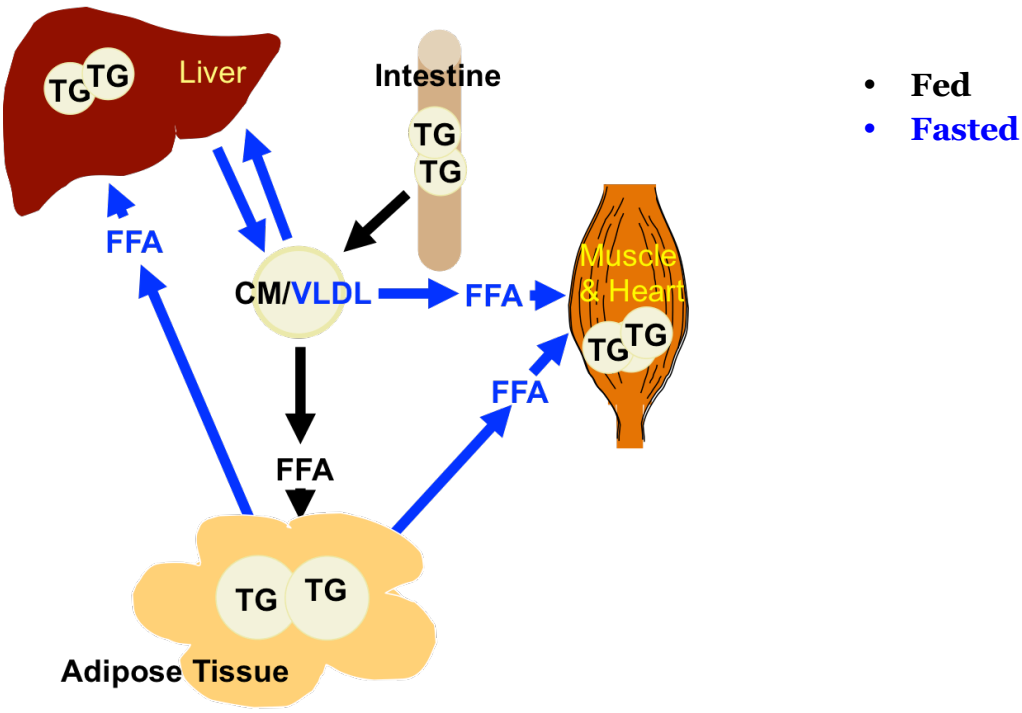

Figure 1-1. Mammalian TG metabolism in fed and fasted states. In the fed state (black arrows), TG is digested and absorbed into enterocytes, where the hydrolyzed products are resynthesized into TG that packaged into chylomicron (CM). CM is transported through lymph vessels into the circulation. CM-TG is hydrolyzed by lipoprotein lipase attached to the luminal surface of endothelial cells in capillaries. The majority of free fatty acid (FFA) is taken up by the adipose tissue, and resynthesized to TG for storage. In the fasted state (blue arrows), adipose lipolysis is activated, releasing FFA to peripheral tissues, such as muscle and liver. Besides glycogenolysis, liver depends on this exogenous FFA to meet its own energy demands, and utilizes the excess FFA to produce TG, some of which is stored in hepatocytes in cytosolic lipid droplets, while the rest is secreted into the circulation system in very-low density lipoprotein (VLDL). VLDL-TG is hydrolyzed by lipoprotein lipase, releasing FFA to oxidative tissues for fuel consumption, or adipose tissue for storage. VLDL remnants are then taken up by the liver for further metabolism and recycling. Illustration was adapted from Dr. Richard Lehner, University of Alberta.

WAT. Saturating or overwhelming the physiological capacity of fat accommodation is directly correlated with various metabolic disorders, such as hyperlipidemia, insulin resistance, hepatic steatosis and cardiovascular disease (CVD). On the other hand, chronic or acute loss of fat storage due to inherited or acquired defects in adipogenesis, lipolysis and overall TG homeostasis often results in comparable metabolic complications. Here, I briefly discuss diseases associated with abnormal TG metabolism, reviewing their molecular, cellular and physiological etiologies.

1.1.1 Obesity-Related Metabolic Diseases

A sedentary lifestyle combined with high fat and carbohydrate diets leads to positive energy balance that eventually results in obesity. Body mass index (weight in kilograms/height^2 in meters) is used as a crude assessment of obesity. A person with a body mass index of 30 or more is generally considered obese. However, a high body mass index is not always correlated to obesity-associated metabolic disorders, as obesity is a complex condition with respect to regional distribution and biological properties of fat depots.[1] Visceral or abdominal fat is considered unhealthy and more closely associated with various metabolic diseases than peripheral or subcutaneous fat. Thus metabolic aberrations would be predicted more critically by the distribution of fat reservoirs rather than the absolute fat mass alone.[2] Description and characterization of different body fat patterning have been developed for its potential prognostic values of metabolic abnormalities, but the molecular mechanisms underlying the co-occurrence of those metabolic aberrances and visceral obesity are largely unknown.[2]

Delicate neurohumoral regulatory mechanisms have evolved to maintain a constant body weight. The key is a crosstalk between the brain and its targeted peripheral centers, including the liver, WAT, intestine and skeletal muscle.[3] The overall nutritional status was implied by circulating glucose, non-esterified fatty acid (NEFA) and hormones such as insulin, leptin, adiponectin, etc., which function as neuronal sensitizers; these signals are then transported to different centers of the brain by activated neurons, where they are processed and integrated, leading to behavioral and metabolic responses. Alternatively, these signals are directly recognized by receptors expressed in local (autocrine/paracrine) or distant (endocrine) organs. However, during a prolonged positive energy balance (obesity), plasma glucose levels remain high, which is clinically identified as hyperglycemia. Hyperglycemia stimulates drastic and incessant insulin and leptin secretion, which, paradoxiacally, blunt the corresponding responses in peripheral tissues, and in a long term, leads to apoptosis of overwhelmed pancreatic β cells and low-grade inflammation of WAT, and eventually type 2 diabetes, fatty liver and CVD.[4]

1.1.1.1 Insulin Resistance

Insulin resistance is largely due to the elevation of plasma NEFA levels that is frequently present in obese individuals, especially with ectopic visceral fat storage.[4] Excess of circulating NEFA is due to surplus ingested fat and to overactivated lipolysis in enlarged WAT.[4] Excess circulating NEFA is the key to hypertriglyceridemia through increased secretion of TG-rich lipoproteins: VLDL and chylomicron from liver and small intestine, respectively.[4]

Skeletal muscle plays a crucial role in insulin-mediated glucose disposal after a meal.[5] Approximately two thirds of ingested glucose is taken up by the skeletal muscle in lean healthy subjects,[5] and about 80% of the total glucose is absorbed by skeletal muscle in euglycemic hyperinsulinemic conditions.[6] Therefore, type 2 diabetes is thought to be primarily caused by the insulin resistance in this particular tissue, followed by β-cell dysfunction and hyperlipidemia.[7] Glucose is transported into myocytes via glucose transporter type 4 (GLUT4), and immediately phosphorylated by hexokinase II. Approximately 70% of the resulting intramuscular glucose-6-phosphate is diverted to the glycogen synthetic pathway, while the rest enters the glycolytic pathway to generate adenosine triphosphate (ATP).[8] A high concentration of saturated FA in blood attenuates glucose uptake into skeletal muscle by impairing GLUT4 function, thereby reducing glucose oxidation and glycogen synthesis in myocytes.[9] High levels of saturated FA dampen myocellular insulin signaling through decreased tyrosine phosphorylation and activation of insulin receptor substrate (IRS) 1 and PI3-kinase activity.[10-12] The mechanism of saturated FA-mediated reduction of myocellular insulin signaling is believed to be the result of accumulation of highly toxic metabolic intermediates, such as diacylglycerol (DG) and ceramides and activation of protein kinase C.[13-15] Saturated FA also indirectly influences insulin sensitivity via activation of inflammatory signaling pathways and inhibition of mitochondrial biogenesis and oxidative capacity.[16-18]

WAT markedly expands to accommodate storage of excess TG, but the capacity of WAT lipid loading is not infinite. Once the TG storage limitation is exceeded, adipocytes become dysfunctional and insulin-resistant, leading to accelerated TG lipolysis that liberates large amounts of FA that enter the

circulation and contribute to deterioration of all the features of metabolic syndrome.[19] Therefore, increasing adipose TG storage capacity may ameliorate metabolic complications. For instance, agonists of peroxisome proliferator-activated receptor (PPAR) γ, thiazolidenediones (TZDs), stimulate adipogenesis and have been shown to improve lipid metabolism and insulin sensitivity in human trials.[20] On the other hand, enlarged WAT in obesity presented an altered secretion profile of adipokines with increased leptin and resistin and decreased adiponectin.[21,22] Changes in the levels of adipokines may play key roles in obesity-related metabolic diseases. For example, exaggerated resistin secretion is associated with adipose pro-inflammation and systemic insulin resistance, as resistin increases production of several adipocyte-derived chemotactic molecules and pro-inflammatory cytokines in adipocytes, and dampens insulin sensitivity via inactivation of GLUT4 and IRS 1/2.[23] On the contrary, decreased adiponectin in obese patients exacerbates the metabolic syndrome, as adiponectin acts to ameliorate insulin resistance by inhibiting adipose lipolysis and improving lipid metabolism in skeletal muscle and liver through activation of 5' AMP-activated protein kinase and PPARα signaling pathways.[24,25]

1.1.1.2 Nonalcoholic Fatty Liver Disease

Obesity is intimately linked to a spectrum of hepatic disorders, known as nonalcoholic fatty liver disease (NAFLD), a clinical manifestation of ectopic TG accumulation (>5% of liver volume, or weight; or histologically defined as >5% of hepatocytes containing visible LDs) in the absence of significant chronic alcohol consumption.[26,27] Fifteen-45% of adult population are afflicted with NAFLD in the modern society, and is even higher in obese populations, particularly in

subjects with visceral obesity.[28] NALFD is classified into several stages, with the majority of patients remaining asymptomatic. The initial stage (steatosis) caused by increased hepatic TG content is reversible by weight reduction through lifestyle intervention.[28] However, 20% of NAFLD individuals can progress to non-alcoholic steatohepatitis (NASH), where progressive inflammation (lobular and portal) is present in addition to steatosis and elevated plasma levels of liver enzymes (aspartate aminotransferase and alanine aminotransferase.[29] Although NASH is a non-fatal disease, some cases may deteriorate to cirrhosis, where functional liver tissues become fibrotic, and may lead to hepatocellular carcinoma.[29,30] Despite the high prevalence of NASH, causal determinants that facilitate the progression from steatosis to NASH are poorly understood.

A "two hit" mechanism was originally proposed to explain the pathogenesis of NAFLD/NASH progression.[30-32] Steatosis has been identified as the first hit. Steatosis occurs due to lipotoxicity: high-fat meal derived TG-rich lipoprotein remnants and enhanced lipolysis in insulin-resistant WAT lead to excess FA delivery to the liver. Additionally, obese subjects with NAFLD exhibited increased gene expression of hepatic lipase and hepatic lipoprotein lipase (LPL),[33,34] and fatty acid transporter/CD36 that increases FA influx into hepatocytes.[35,36] Furthermore, enhanced hepatic *de novo* lipogenesis (DNL) has been frequently observed in NAFLD patients.[37] Hepatic DNL is stimulated by glycolysis in the presence of a high concentration of circulating glucose. Additionally, fructose can promote hepatic DNL to a larger extent due to its unique metabolic properties. Fructose is rapidly absorbed into liver and phosphorylated by fructokinase, thus escaping the key regulatory step on phosphofructokinase that commonly occurs during glycolysis.[38,39] The mechanisms of how increased hepatic DNL triggers

ectopic TG accumulation in liver are largely unknown, because DNL quantitatively contributes only to a minor portion of the overall hepatic FA input.

One possibility is through the modulation on FA β-oxidation by some of the intermediates or products generated during DNL. Studies have shown that *de novo* synthesized FA may serve as a distinct pool of endogenous activators of PPARα, regulating energy homeostasis.[40] Moreover, carnitine palmitoyltransferase 1 (CPT-1) activity is allosterically inhibited by malonyl-CoA, a key intermediate formed during the FA *de novo* synthesis, thereby decreasing FA import into mitochondria and thus FA β-oxidation. Nevertheless, FA β-oxidation in NAFLD patients is more likely to increase rather than decrease, based on measurements of plasma β-hydroxybutyric acid (a type of ketone bodies) concentration.[32,41] This is perhaps not surprising, because although the expression and activity of CPT-1 are suppressed, expression of other genes involved in FA β-oxidation was reported to be increased.[42,43] Moreover, tricarboxylic acid cycle was shown to be around two-fold induced in subjects with high intrahepatic TG, implying active oxidative metabolism in mitochondria.[41] Paradoxically, mitochondrial paracrystalline inclusions have been described in the NASH patients, reminiscent of mitochondrial atrophies due to mutations in genes encoding electron transport chain complex.[32,44,45] These mitochondrial defects may suggest a segregation of oxidative phosphorylation and ATP generation. Congruent with this interpretation, obese mice exhibited impaired recovery from hepatic energy depletion as their fatty liver disease deteriorated.[46] Furthermore, the gene expression of uncoupling protein 2 was increased in steatotic liver, suggesting energy stored in the mitochondrial membrane potential was more likely to dissipate as heat.[43] Therefore, NAFLD/NASH-related

mitochondrial abnormalities may provide a protective mechanism in the liver against excessive lipid burden.[27] Furthermore, these mitochondrial abnormalities are proposed to occur in a yet undetermined fraction of the total mitochondrial population, and no mitochondrial insufficiency has been reported.[32]

Finally, secretion of VLDL was increased in subjects with NAFLD, allowing a partial removal of hepatic TG, which, however, was insufficient to compensate for the rapid TG production.[27] Pathophysiological increase of VLDL secretion *per se* may be unable to reverse steatosis in obesity; however, genetic ablation of VLDL secretion, such as inactivation of microsomal triglyceride transfer protein (MTP), often leads to NAFLD.[47,48]

Uncoupling oxidation enables liver to undertake extensive FA β-oxidation, thus enhancing liver tolerance towards excessive lipid burden, which on the other hand facilitates lipid peroxidation and production of reactive oxygen species.[30] This detrimental side effect triggers the second hit of NASH pathogenesis: reactive oxygen species excess and lipotoxic metabolites such as DG and ceramides that induce oxidative stress, pro-inflammatory responses and subsequent apoptosis and necrosis. Dietary or adipose lipolysis-derived saturated FA, cytokines that are mainly synthesized and secreted from Kupffer cells (liver macrophages) and liver-infiltrating monocyte-derived macrophages initiate NAFLD progression.[49-51] NAFLD progression is also pathologically linked to dilated and pro-inflammatory WAT, circulating chemokines, cytokines and innate immune cells and compositional changes of the gut microbiota.[28,32,52,53]

1.1.1.3 CVD

Obesity, abdominal fat in particular, is an independent risk factor for CVD.[54] However, the mechanisms of how visceral obesity increases cardiac morbidity and mortality are not well understood. Here I briefly introduce a model linking dyslipidemia to the pathogenesis of CVD.

Dyslipidemia is characterized by increased circulating TG-rich lipoproteins with their major lipid constituents (TG, cholesterol and cholesteryl esters), formation of small dense low-density lipoprotein (LDL), and less high-density lipoprotein (HDL) particles with their associated cholesterol. LDL-cholesterol is an established and widely accepted cardiovascular risk marker, and measurement of apolipoprotein (apo)B molecule and LDL particle numbers has been included into clinical lipid examination.[55] LDL population is heterogeneous, consisting of lipoprotein particles with densities ranging from 1.006 to 1.063 kg/L. LDL is originally generated from VLDL through LPL-catalyzed TG hydrolysis and cholesteryl ester transfer protein-mediated exchange of phospholipids (PL) and neutral lipids. LDL oxidation occurs in the subendothelial space after crossing the endothelial fenestrations.[56] The oxidized-LDL, known as the bad cholesterol, is taken up by macrophages through scavenger receptor-mediated endocytosis, leading to foam cell formation and secretion of various cytokines that accelerate atherosclerosis.[56] Escalated synthesis and secretion of VLDL (LDL precursor) were often found in hepatic steatosis and other insulin resistance-related syndromes, as illustrated in previous sections. Moreover, the clearance of VLDL might decline in men with visceral obesity, as plasma levels of ApoC-III (a natural inhibitor of LPL) are elevated, suggesting decreased catabolism of apoB-containing particles.[57] Subjects with insulin resistance were presented with increased activities of

cholesteryl ester transfer protein and PL transfer protein, suggesting dysregulated lipid transfer among lipoproteins and impaired HDL formation.[58] HDL, known as the good cholesterol, regresses atherosclerotic lesion by transporting cholesterol from foam cells to the liver, where it is further processed and excreted into bile through a pathway known as reverse cholesterol transport. The liver takes up HDL-cholesterol either directly via scavenger receptor B1, or through cholesteryl ester transfer protein-mediated cholesteryl esters/TG exchange between HDL and apoB-containing lipoproteins, followed by LDL receptor-mediated endocytosis.

1.1.2 Genetic Defects in Lipid Storage: Lipodystrophies

Lipodystrophies are clinically characterized with selective body fat loss and often associated with metabolic complications, such as insulin resistance, hyperlipidemia and hepatic steatosis.[59] This disorder is quite heterogeneous with respect to patterns and phenotypes. Congenital generalized lipodystrophy (autosomal recessive) and familial partial lipodystrophy (autosomal dominant) are the most common types of genetic lipodystrophies.[59] A dozen genetic loci have been identified in patients with inherited lipodystrophies, including genes encoding fundamental enzymes in TG and PL biosynthesis, LD dynamics and adipocyte differentiation.[59]

Adipogenesis is a process in which fibroblast-like precursor cells undergo growth arrest and subsequent differentiation into mature adipocytes with a large unilocular LD occupying most of the cytoplasm. Loss-of-function in certain genes disrupts this process and leads to lipodystrophic phenotypes. Subjects with dominant-negative single point mutations in PPARγ lack subcutaneous WAT,

particularly in limb and hip depots, while preserving visceral fat.[60] These patients also manifest severe insulin resistance, dyslipidemia, and hepatic steatosis. Other gene mutations responsible for partial lipodystrophies include a homozygous nonsense mutation in the *death-inducing DFFA-like effector (CIDE)C* gene, encoding a LD-coat protein,[61] and two frame-shift mutations in the gene that encodes the C-terminus of perilipin1.[62,63] Notably, the above gene variances account for a relatively small portion of the inherited partial lipodystrophies, the most common one of which is caused by mutations in the *LMNA* gene, encoding a protein lamin A/C that is required for the integrity of the nuclear envelope.[64] Pre-lamin A has been reported to co-localize and interact with SREBP1 at the nuclear envelope, thus sequestering the active form of SREBP1 from inducing adipogenesis.[65] However, the reasons why the lamin A/C regulates SREBP1 selectively in WAT remain largely unexplained.

Generalized lipodystrophies were caused by several loss-of-function mutations, such as in the Berardinelli–Seip congenital lipodystrophy 2 (BSCL2) gene.[66] BSCL2, also termed seipin, intercalates into the ER membrane by a hairpin-like transmembrane domain.[67] In 3T3-L1 cells, *Bscl2* gene expression was remarkably increased during adipose differentiation; on the contrary, knockdown of *Bscl2* prevented this process, possibly through downregulation of PPARγ.[66] Moreover, BSCL2 has been suggested to play a crucial role in the biogenesis, expansion, distribution and mobilization of lipid droplets (LDs).[67] Deletion of *Bscl2* orthologue in yeast formed enlarged or aggregated LDs, whereas null allele of *Bscl2* in *Drosophila* exhibited defects in lipid storage with strikingly shrunk LDs in larval fat bodies and young adult fat cells.[68,69] Although knocking out *Bscl2* gene expression in the two model animals led to distinct, or more precisely,

opposite phenotypes of LDs, an essential role of BSCL2 in PL metabolism has been proposed in both models. Ablation of this gene altered acyl chain profiles of several PL in yeast and increased levels of total phosphatidic acid (PA) and most PA species in *Drosophila*.[68,69]

Homozygous mutations in the gene that encodes acylglycerol-3-phosphate O-acyltransferase 2 (AGPAT2) account for a large subset of patients with congenital generalized lipodystrophies, possibly due to inhibition of TG biosynthesis and adipocyte differentiation.[70] Finally, systemic lipodystrophy was caused by a bi-allelic nonsense mutation in the gene encoding caveolin-1, possibly through a collapse of cholesterol-rich microdomains in the plasma membrane. These microdomains (lipid drafts) are engaged in FA intake, GLUT4 translocation and insulin signaling in adipocytes.[67,70]

1.2 TG Biosynthesis in Mammals

TG serves as the major fat source of energy for most living organisms, and protects cells from excess FA-induced toxicity, and provides substrates for PL synthesis. TG is assembled into lipoproteins that deliver dietary and endogenously synthesized FA to peripheral tissues to satisfy a whole-body energy demand. In addition, TG contributes to epidermal barrier protection.[71] Intermediates of TG metabolism, such as FA, lysophosphatidic acid (LPA), PA and DG, may serve as essential regulators of FA oxidation, adipogenesis and hormone signaling.[72] TG consists of a glycerol backbone with hydroxyl groups esterified by three FAs that vary in carbon numbers and degrees of desaturation. Two major pathways of mammalian TG biosynthesis have been elucidated: the

sn-glycerol-3-phosphate pathway, also known as the Kennedy pathway, and the MG pathway (Figure 1-2). Most of the acylation reactions are catalyzed by enzymes of multiple isoforms that in some cases, encoded by genes that belong to distinct gene families, while in others, are derived from alternative splicing and post-translational modifications.[72]

1.2.1 The MG Pathway of TG Synthesis

While the glycerol 3-phosphate pathway is present in all tissues, only tissues of high capacity of TG synthesis employ the MG pathway, such as the small intestine, liver, and WAT.[73] The MG pathway plays an essential role in fat absorption in the small intestine. It has been demonstrated that 75–80% of TG synthesis in enterocytes is conducted through the MG pathway during the post-prandial state.[74] TG contained in dietary fat is first hydrolyzed to 2-MG and FA by pancreatic lipases in the lumen of the small intestine followed by solubilization in bile acid micelles. FA and 2-MG are then absorbed into the intestinal enterocytes, where they are re-esterified first into DG by acyl coenzyme A:monoacylglycerol acyltransferases (MGATs), and the resulting DG is subsequently converted to TG by acyl coenzyme A:diacylglycerol acyltransferases (DGATs). TG is either stored in cytosolic LDs or assembled into chylomicrons that are secreted into circulation through lymph ducts and function as a lipid source for peripheral tissues.

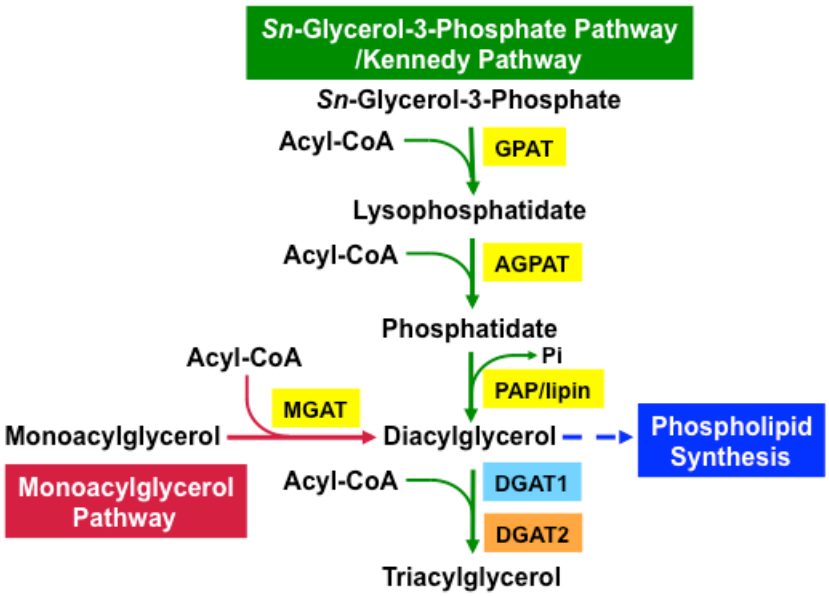

Figure 1-2. TG biosynthesis in mammals. Two major pathways of mammalian TG biosynthesis have been elucidated: the *sn*-glycerol-3-phosphate pathway, also known as the Kennedy pathway, and the monoacylglycerol pathway. The reactions are shown in a stepwise manner, with essential substrates, intermediates and products, and key enzymes illustrated. MGAT: acyl-coenzyme A:monoacylglycerol acyltransferase; GPAT: *sn*-glycerol-3-phosphate acyltransferase; AGPAT: *sn*-1-acyl-glycerol-3-phosphate acyltransferase; PAP: phosphatidic acid phosphatase; DGAT: acyl-coenzyme A:diacylglycerol acyltransferase.

1.2.1.1 MGATs

MGATs synthesize DG by catalyzing the acylation of MG. Three isoforms of MGATs have been identified and all are ER membrane proteins. The first reported MGAT (MGAT1) encoding gene (*Mogat1*) was identified based on sequence homology to members of the *Dgat2* gene family, and is ubiquitously expressed in tissues except small intestine.[75] In contrast, MGAT2 is most abundantly expressed in the small intestine.[76] MGAT2-deficient mice exhibited less than half of intestinal MGAT activity, and were protected against diet-induced obesity and the related metabolic disorders, including insulin resistance, hypercholesterolemia and hepatic steatosis.[77] Chylomicrons were secreted at a reduced rate from mice lacking MGAT2, but no fat malabsorption was observed.[77] The protective metabolic phenotype of MGAT2-deficient mice against high-fat diet was possibly due to increased energy expenditure and thermogenesis.[77] The metabolic consequences of *Mogat2* global deletion were recently confirmed in intestine-specific *Mogat2*$^{-/-}$ mice, suggesting that the predominant activity of rodent MGAT2 is concentrated in the intestine.[78] Moreover, the adult-onset genetic ablation of *Mogat2* was sufficient to confer resistance to diet-induced obesity and glucose intolerance.[79] Finally, the *Mogat3* gene is only expressed in the gastrointestinal tract in humans and not rodents.[80] MGAT3 uses both MG and DG as substrates, and shares higher sequence similarity with DGAT2 than the other two MGAT enzymes.[80]

1.2.2 The *sn*-Glycerol-3-Phosphate, or Kennedy, Pathway

The *sn*-glycerol-3-phosphate/Kennedy pathway is present in most cells, and ~90% of total TG in hepatocytes has been reported to be produced through this

pathway.[72] First, a hydroxyl group at the *sn*-1 position is esterified by glycerol-3-phosphate acyltransferases (GPATs), generating LPA, followed by a second esterification reaction at the *sn*-2 position, catalyzed by *sn*-1-acyl-glycerol-3-phosphate acyltransferases (AGPATs) to form a key intermediate, PA. Next, the phosphate group of PA is removed by phosphatidic acid phosphatase (PAP), also known as lipin, generating *sn*-1,2-DG. Finally, DGATs catalyze the last and only committed step of the two TG biosynthetic pathways, converting DG to TG. There are two branch points in the pathway, one at the level of PA and the other at the level of DG. A condensation of PA and cytidine triphosphate (CTP) generates CDP-DG that is used in the synthesis of phosphatidylglycerol (PG), phosphatidylinositol (PI), and cardiolipin. *sn*-1,2-DG can be diverted to phosphatidylcholine (PC), phosphatidylethanolamine (PE) synthesis, with PC and PE can be further converted to phosphatidylserine (PS).

1.2.2.1 GPATs

GPATs catalyze the first step of glycerolipid biosynthesis, acylating *sn*-glycerol-3-phosphate to LPA. The backbone molecule, *sn*-glycerol-3-phosphate, is mainly generated through glycolysis, or to a lesser extent in certain tissues such as the liver via direct phosphorylation of glycerol. FA taken up into cells is activated by (very) long-chain acyl-CoA synthetases, generating acyl-CoA molecules that are channeled to complex lipid synthesis or oxidation.

Four GPAT enzymes have been identified, each encoded by a separate gene. Mammalian GPATs are integral membrane proteins with active sites exposed to the cytosol.[72] However, the four GPATs exhibit distinct enzymatic and cellular characteristics, including their subcellular locations, substrate

preferences and sensitivity to sulfhydryl group modifiers such as *N*-ethylmaleimide (NEM).[73]

GPAT1 is located on the outer mitochondrial membrane, and is enriched in junction sites between the mitochondria and the ER. The enzyme favors saturated FA, palmitic acid in particular, and is insensitive to sulfhydryl reagents.[73,81] Thirty-50% of hepatic GPAT activity has been ascribed to GPAT1.[82] Adenovirus-mediated overexpression of GPAT1 in chow-fed rats resulted in elevated hepatic glucose production, hyperlipidemia, steatosis and insulin resistance.[83] The essential role of GPAT1 in hepatic TG synthesis was further confirmed in *Gpat1*$^{-/-}$ mice fed high-fat diet, as these mice displayed remarkably lower TG contents and improved hepatic insulin sensitivity.[84]

GPAT2 is also located on the mitochondrial outer membrane, but is different from GPAT1, as it is sensitive to NEM and shows no preference for saturated acyl-CoAs. GPAT2 is most abundantly expressed in testis and may play an essential role in spermatogenesis and cell proliferation.[85,86]

The genes encoding GPAT3 and GPAT4 share ~80% identity, and the proteins are ER-bound, NEM-sensitive and are responsible for the majority of total GPAT activity in mammals.[87] Insulin stimulated both GPAT3 and GPAT4 activity in 3T3-L1 adipocytes, but only *Gpat3* gene expression was dramatically upregulated during PPARγ agonist-initiated adipocyte differentiation.[88] The predominant role of GPAT3 during adipogenesis was further confirmed by global deletion of *Gpat3* in mice, as 80% of adipose GPAT activity was eliminated in these mice.[89] GPAT4 is also highly expressed in WAT and exerts different effects from GPAT3 on adipocyte differentiation, reflected by GPAT4-deficient mice.[73] *Gpat4*$^{-/-}$ mice exhibited less TG accumulation in WAT and the mice had shrunk

adipocytes, though this lipodystrophic feature did not lead to metabolic disorders.[84,90] Moreover, GPAT4, similar to GPAT1, plays a critical role for hepatic TG synthesis, as Gpat4$^{-/-}$ mice had 50% reduction of liver TG content.[73,90]

1.2.2.2 AGPATs

AGPATs catalyze the second acylation reaction, esterifying LPA to PA. AGPAT1-3 have been experimentally demonstrated to exhibit authentic AGPAT activity, though many other enzymes that have similar structures with identical catalytic motifs are named AGPATs.[73]

AGPAT1 is expressed in most mammalian tissues, and is enriched in the liver, heart, skeletal muscle and pancreas.[91,92] *Agpat2* shows a different tissue distribution, with the highest mRNA levels found in WAT. Mutations in the *Agpat2* gene have been identified in the congenital generalized lipodystrophy.[93] AGPAT3 is an ER- and Golgi-localized transmembrane protein with four conserved acyltransferase motifs; specifically, motif II is partially buried within the membrane, followed by motifs III and IV that constitute a long loop oriented towards luminal space, and motif I, on the other side, is extruded into cytosol.[94] AGPAT3 regulates Golgi structure and protein trafficking. Overexpression of *Agpat3* impaired the integrity of the Golgi and both anterograde and retrograde protein trafficking possibly through modulation of PA levels.[95] It has been suggested that AGPAT3 possesses a strong lysophosphatidic acid (LPA) and a moderate lysophosphatidylinositol acyltransferase activity, with polyunsaturated fatty acyl-CoAs, such as 22:6-CoA and 20:4-CoA as preferential substrates.[96,97] Thus AGPAT3 may function in both *de novo* and remodeling pathways (Lands' cycle, working in concert with phospholipase A2) of PL synthesis.[97]

Proteins containing the PIsC domain are named AGPAT in the GenBank, but the PIsC domain not only defines the protein family of LPA acyltransferase but also a more distantly related family (MBOAT) that includes DGAT1, thus many of the so-called AGPAT proteins do not exhibit LPA acyltransferase activity.[73] On the other hand, some proteins that share poor homology with the AGPAT family, can catalyze the conversion of LPA to PA. Interestingly, ABHD5, besides functioning as a co-activator of ATGL, has been reported to exhibit a LPA acyltransferase acitivity using palmitoyl- and oleoyl-CoAs as preferential substrates.[98]

1.2.2.3 PAPs

PAPs, also known as lipins, translocate from the cytosol to the ER membrane, where they convert AGPAT-derived PA to DG.[99] The lipin protein family consists of three members, lipin-1, -2 and -3; and lipin-1 is comprised of two isoforms, lipin-1α and lipin-1β that are generated by alternative mRNA splicing.[100] This family of proteins is highly conserved in eukaryotes, particularly at the amino-terminal and carboxy-terminal regions.[100] Lipins exhibit unique, though to some extent overlapping, tissue expression patterns, implying their nonredundant physiological functions. Lipin-1 is primarily expressed in WAT, skeletal muscle, and testis; while lipin-2 is preferentially enriched in the liver, brain and kidney; and lipin-3 is more frequently found in the liver and the gastrointestinal tract.[73,99]

Lipin-1-deficient mice initially develop fatty liver and hypertriglyceridemia, and subsequently present with lipodystrophic features, characterized by impaired adipogenesis, decreased TG storage in adipocytes and comprehensive insulin resistance.[101] Human patients with *LPIN1* mutations do

not develop lipodystrophy, however, the molecular basis underlying the species variability remains unclear.[101] Nevertheless, both humans and mice showed commensurate correlations between *LPIN1*/*lipin-1* expression in WAT and systemic insulin sensitivity, suggesting a conserved and fundamental role of lipin-1 in adipocyte function and differentiation.[101] Separate and specific overexpression of lipin1 in the WAT and skeletal muscle promoted obesity, yet through different mechanisms: in mature adipocytes lipin-1 upregulated the expression of several adipogenic genes, whereas a muscle-specific expression of *lipin-1* reduced oxygen consumption and energy expenditure.[102] Finally, Mammalian lipin-1 was found to localize in the nucleus of adipocytes and hepatocytes where lipin-1 functioned as a component of the transcriptional machinery.[99] The subcellular localization of lipin-1 may be regulated by hormone (insulin and epinephrine)-mediated (de)phosphorylation.[103]

Lipin-2 is highly expressed in the liver, though it is also expressed in preadipocytes where it precedes lipin-1 expression in differentiating 3T3-L1 adipocytes. Lipin-2 could not rescue defective adipocyte differentiation upon lipin-1 depletion, and loss of lipin-2 exerted little effects on adipogenesis.[104] Lipin-2 may primarily function in the liver, as hepatic *lipin-2* expression was upregulated in neonatal lipin-1-deficient mice, and accompanied with a dramatic TG accumulation in the liver.[105]

1.2.2.4 DGATs

DGATs catalyze the terminal and only committed step of the two pathways of TG biosynthesis, esterifying DG to TG with one molecule of acyl-CoA. Inasmuch as DG acts as a precursor for the synthesis of several glycerophospholipid (GPL)

species, DGATs determine the branch point of DG metabolism. DG is generated either from hydrolysis of PA, a key intermediate of the glycerol-3-phosphate pathway, or by esterification of MG during a pathway essential for absorption of dietary fat in the small intestine. The first report of DGAT activity was in the 1950s, however, subsequent attempts to purify this enzyme to homogeneity proved difficult.[71,106] Only at the end of the last century was the first *Dgat* gene (*Dgat1*) cloned, based on sequence similarity analysis to acyl-CoA:cholesterol acyltransferase.[107] A second *Dgat* gene (*Dgat2*) was later identified.[108,109] The two DGAT enzymes are ubiquitously expressed in eukaryotes, and categorized to distinct gene families, with *Dgat1* belonging to a large family of MBOAT and Dgat2 classified into a seven-member gene family, *DAGAT*,[107,109] and recent phylogenetic analyses have confirmed their separate evolutionary pathes.[110]

1.2.2.4.1 Catalytic Functions of DGATs

Besides their common catalytic function esterifying DG to TG, DGAT1 possesses several other acyltransferase activities. First, DGAT1 can synthesize retinyl esters from retinol (vitamin A) and fatty acyl-CoA. *Dgat1*$^{-/-}$ mice exhibited markedly reduced acyl-CoA:retinol acyltransferase activities in several tissues and perturbed retinol homeostasis in the liver of mice on a high-retinol diet.[111] Both pharmacological inhibition of DGAT1 activity and genetic deletion of intestinal *Dgat1* gene resulted in significantly decreased vitamin A absorption in the small intestine.[112] Second, membranes from insect cells or homogenates from COS7 cells overexpressing DGAT1 exhibited a MGAT activity and wax monoester and diester synthase activities.[111] These findings suggest that DGAT1 possesses a less discriminating substrate binding domain than that of DGAT2, as the former

esterifies not only DG, but also retinol, MG and fatty alcohols, though with different affinities.

1.2.2.4.2 Topology and Cell Biology of DGATs

DGAT1 is integrated with the ER membrane by multiple transmembrane domains: 8 based on algorithmic prediction, and 3 determined experimentally.[113] The C-terminal region of DGAT1 was proposed to extrude into the ER lumen and accounts for approximately half of the protein. The C terminus, which is essential for its catalytic activity, contains a highly conserved histidine residue, while the N-terminus may be responsible for its di/tetramerization.[113] DGAT1 has been demonstrated to have a dual topology within the ER in HepG2 cells, exhibiting comparable activities on both the cytosolic and lumenal sides of the ER membrane.[114]

DGAT2 is an integral membrane protein with one or two predicted transmembrane domains forming a hairpin-like structure with both N- and C-termini oriented towards the cytosol.[115] A four-amino acid sequence (His-Pro-His-Gly) was conserved in the active sites of the DGAT2 and other characterized family members, including MGAT1–3 and wax synthase 1 and 2, with the two histidines catalytically indispensable.[115] Biochemical fractionation revealed that DGAT2 was enriched in mitochondria-associated membranes and was found to co-localize with mitochondria and LDs upon oleate loading of cells.[116] The ER-targeting signal of DGAT2 is present within the first transmembrane domain; however, deletion of both transmembrane domains maintained DGAT2 interaction with LDs and the efficiency of TG synthesis.[117] DGAT2 was also found localized on the surface of LDs in *Caenorhabditis elegans* intestinal segments

and *Drosophila melanogaster* Schneider 2 cells, where it has been suggested to promote LD expansion via local TG synthesis.[118,119] The mechanism of substrate channeling onto LDs for DGAT2-catalyzed reaction is unknown but may involve ADP-ribosylation factor/coatomer (Arf)/COPI machinery-mediated connection between the ER and the LDs.[120,121] Co-expression of DGAT2 and MGAT2 in nephritic cell lines revealed extensive co-localization of the two enzymes in the ER and mitochondria-associated membranes, and on the surface of LDs upon oleate supplementation, suggesting that DGAT2 efficiently utilizes MG-derived DG as a substrate for TG synthesis.[122] On the other hand, DGAT2 was also shown to interact with stearoyl-CoA desaturase (SCD)1, an enzyme required for desaturation of *de novo* synthesized FA, thus DGAT2 may preferentially incorporate the autonomously synthesized FA into TG.[123]

1.2.2.4.3 Physiological Roles of DGATs

Genetic ablation of individual *Dgat* genes in adipocytes failed to interfere with the TG synthesis and LD formation, suggesting a compensatory function of DGAT1 and DGAT2 in adipose TG production.[124] Moreover, TG accumulation and LD biogenesis were abolished in the adipocytes that were differentiated from *Dgat1*$^{-/-}$/*Dgat2*$^{-/-}$ mouse embryonic fibroblasts, suggesting the two DGATs in combination accounted for the vast majority of TG production in the murine WAT.[124] Despite the seemingly redundant roles of DGAT1 and DGAT2 in the TG synthesis in the murine WAT, their physiological functions vary greatly with distinct tissue expression patterns. *Dgat1* and *Dgat2* genes are expressed ubiquitously, with the former expressed the highest in small intestine, liver,

adipose tissue, and mammary gland, and the latter showed the highest expression in liver and adipose tissue.[71]

Whole-body DGAT1-deficient mice are lean, resistant to diet-induced obesity, which may be attributed to an increased metabolic rate, a higher level of physical activity, and mildly impaired lipid absorption due to delayed gastric emptying and suppressed chylomicron secretion.[71,125] Neither intervention in food intake nor detectable fat malabsorption was observed.[125] Higher levels of thermogenesis may also contribute to enhanced energy expenditure, as the body temperature was increased and the expression of uncoupling protein 1 was upregulated by ~70% in brown adipose tissue of *Dgat1*$^{-/-}$ mice.[126,127] To support this speculation, *Dgat1*$^{-/-}$ mice suffered from hypothermia and low plasma glucose levels when challenged with caloric restriction and cold challenge.[126] TG content was substantially decreased in WAT, skeletal muscle, liver and mammary epithelial tissue in the DGAT1-deficient mice fed with high-fat diet, accompanied with enhanced insulin and leptin sensitivity.[125,127] Moreover, absence of DGAT1 in cardiac muscle prevented buildup of lipotoxic intermediates, such as DG and ceramide, possibly through decreased FA delivery into cardiomyocytes due to reduced mRNA levels of *Cd36* and *Lpl*.[128] DGAT1 deficiency did not appear to affect metabolic flexibility, as DGAT1-deficient muscle took up more glucose as a compensatory source of energy, therefore resulting in improved insulin sensitivity. The expression of all three *Ppar* genes (α, β/δ, γ) was downregulated, as well as a number of their target genes involved in FA oxidation, while expression of glucose transporters was increased.[128]

A study in *Dgat1*$^{-/-}$ mice suggested TG resynthesis in mouse intestine thus chylomicron assembly did not require DGAT1 activity, as TG accumulated in

large cytosolic LDs and chylomicron-sized particles in the lumen of the ER and the Golgi apparatus in enterocytes.[129] Plasma TG levels in *Dgat1*$^{-/-}$ mice decreased at 1 h, but not at 4 h following intragastric administration of a bolus of corn oil, suggestive of a delayed fat absorption but no malabsorption.[129] Additional experiments in mice and rats suggested that attenuated postprandial serum TG levels were largely due to the DGAT1 deficiency-induced delay of chylomicron secretion.[112,130]

A selective, competitive DGAT1 inhibitor, T863, markedly delayed the intestinal fat absorption, blunted an immediate postprandial excursion of plasma TG after an acute lipid challenge, and promoted TG accumulation in distal small intestinal fragments, reminiscent of the phenotypes from the global genetic abrogation of *Dgat1* expression.[131] Prolonged DGAT1 inhibition (2 weeks) in high-fat-diet-induced obese mice showed enhanced insulin sensitivity with upregulated phosphorylation of hepatic IRS2 and protein kinase B, ameliorated steatosis and increased glucose uptake in differentiated 3T3-L1 adipocytes.[131] This chronic DGAT1 inhibition in obese mice also resulted in a moderate decrease of weight gain, despite no difference in food intake between inhibitor-treated and vehicle-treated control mice.[131] In contrast, a rapid and significant decrease of food intake was observed upon acute DGAT1 inhibition in diet-induced obesity, accompanied with increases of intestinal FA oxidation and ketogenesis.[130]

Additionally, *Dgat1*$^{-/-}$ mice exhibited elevated secretion of gut hormones, including glucagon-like peptide-1 and peptide tyrosine-tyrosine when fed with normal chow or a high-fat diet.[132] Alterations in gastrointestinal peptides upon DGAT1 inhibition may contribute to the beneficial effects on appetite and energy expenditure. However, these results begged the question whether the reduction of

chylomicron secretion in DGAT1-deficient mice is due to a delayed gastric emptying via glucagon-like peptide-1 overproduction or a lack of TG synthesis via DGAT1 inactivation. Recent studies have found that chylomicron secretion was reversibly blocked or permanently hampered upon pharmacological inhibition of DGAT1 or intestine-specific deletion of *Dgat1* gene, respectively, independent of gastric emptying, as neither bypassing the stomach through duodenal oil injection, nor inhibiting the glucagon-like peptide-1 receptor by an antagonist, exendin (9-39), failed to correct the reduced chylomicron secretion.[112] Finally, ablation of *Dgat1* expression in apoE knockout mice reduced atherosclerosis, foam cell formation and aortic inflammation, ameliorated hyperlipidemia, and improved intestinal and macrophage cholesterol metabolism.[133]

All the above beneficial observations suggested that DGAT1 inhibition could be used to treat lipid metabolic disorders in humans. However, loss-of-function mutations in the human DGAT1 have been reported to cause extreme congenital diarrheal disorders.[134] A further investigation uncovered that human small intestine expresses only DGAT1,[135] while rodents also express DGAT2. Therefore, DGAT1 inactivation in humans might potentially result in severe side effects.

Despite all the advantages conferred by DGAT1 deficiency in mice either by genetic or chemical modulation, overexpression of *Dgat1* did not lead to opposite phenotypes. For example, athletic training naturally increased TG storage in heart and skeletal muscle, accompanied with an enhanced DGAT1 activity, and improved lipotoxicity and insulin sensitivity.[128,136] Similar metabolic benefits were observed in several transgenic mouse models. Myocellular overexpression of DGAT1 mitigated the toxic effects of free FA and DG by channeling them into TG

synthesis, so that the DG-induced protein kinase C signaling pathway and several downstream effectors were suppressed, leading to increased IRS1/protein kinase B activation and GLUT4 translocation.[136] Similarly, cardiomyocyte-specific *Dgat1* transgenic mice exhibited a doubling in TG content and reduced cardiac DG, free FA and ceramide levels.[128] Crossing these mice with mice overexpressing long-chain acyl-CoA synthetase 1, a model of cardiomyopathy, significantly improved cardiac function and survival rates.[128] In addition, overexpression of *Dgat1* in macrophages and adipocytes (aP2-*Dgat1* transgenic mice) showed enhanced glucose metabolism and reduced inflammation.[137] The relative contributions of adipocytes and macrophages to these beneficial phenotypes were discriminated by bone marrow transplantation of an aP2-*Dgat1* transgenic mouse into irradiated wild-type mice.[137] Interestingly, the selective overexpression of *Dgat1* in monocyte-derived macrophages was sufficient to protect mice against diet-induced insulin resistance and attenuated activation and accumulation of inflammatory M1 macrophage in the WAT.[137]

In contrast, DGAT2-mediated TG synthesis is indispensable for mouse perinatal development, as DGAT2-deficient mice died within a few hours after birth.[138] The carcass TG contents of *D*gat2$^{-/-}$ mice were reduced by ~90%, suggesting a whole-body TG deprivation may contribute to the early mortality.[138] Another determinant of the early death was defective epidermal barrier protection, which resulted in rapid dehydration.[138] Therefore, DGAT2 plays an obligatory role in the antenatal period. Despite DGAT2 accounting for only a small portion (~20%) of the total DGAT activity in an *in vitro* assay, its pivotal role may lie in the *in vivo* TG synthesis.[71,114]

In addition, DGAT2 appeared to exert a highly rate-limiting effect on *de novo* TG synthesis, as biased pharmacological inhibition of DGAT2 or genetic suppression of *Dgat2* expression dramatically (~70%) reduced incorporation of ^{3}H-glycerol and ^{14}C-acetate, but not ^{14}C-oleate into cellular and secreted TG; as glycerol and acetate contribute to the *de novo* synthesized pool of TG, while oleate represents the exogenous source of FA for TG synthesis.[114,139] Similarly, inactivation of DGAT2 by selective small molecule inhibitors (JNJ-DGAT2-A and –B) or siRNA knockdown significantly attenuated incorporation of isotope-labeled glycerol, but not oleate, into TG.[139]

Several antisense oligonucleotide (ASO) studies suggested an essential role of DGAT2 in hepatic TG metabolism and apoB-containing lipoprotein secretion. ASO reduced *Dgat2* mRNA levels solely in WAT and liver, with correspondingly decreased DGAT activity in the liver but not the WAT.[140] The ASO-mediated downregulation of hepatic DGAT2 activity led to marked changes in hepatic lipid metabolism, including a dramatic reduction of liver TG, decreased expression of several lipogenic genes, increased FA oxidation, and impaired VLDL secretion.[140] Another group using an identical ASO to abrogate *Dgat2* expression also reported decreased hepatic TG contents, a reduction of apoB-containing lipoprotein particles in number but not size, and improvement of metabolic disorders induced by leptin deficiency.[140,141]

Furthermore, studies in *Dgat2* transgenic mice further confirmed DGAT2 as a critical regulator of hepatic TG metabolism. Liver-specific overexpression of *Dgat2* increased levels of various lipid intermediates, such as DG, ceramides and free FA (16:1, 18:1 and 18:2), but they were protected from high-fat-diet-induced inflammation and ER stress.[142] These *Dgat2* transgenic mice developed steatosis,

but exhibited normal glucose tolerance and insulin signaling transduction, with increased expression of genes involved in hepatic lipogenesis and FA oxidation.[142] However, whether and how the increased hepatic *Dgat2* expression affects VLDL secretion is unknown.

1.3 Liver TG Metabolism

Liver is composed of parenchymal cells (hepatocytes) and nonparenchymal cells (Kupffer cells, hepatic stellate cells and sinusoidal endothelial cells), with the former occupying ~80% of the total liver volume.[143] Liver plays an important role in energy balance, detoxification, immune response and protein synthesis. From a perspective of energy homeostasis, liver intricately coordinates and synchronizes carbohydrate and lipid metabolism according to changes in nutritional states. In the fed state, glucose serves as the major energy supply for the liver. Active glycolysis generates acetyl-CoA, the basic substrate for *de novo* FA synthesis. Excess FA is incorporated into a variety of glycerolipids, with the neutral lipids stored in cytosolic LDs in hepatocytes as a physiological reservoir of energy to support acute and extended periods of nutrient deprivation.

During the early stage of fasting, hepatic glycogenolysis provides the primary source of energy, which is supplemented by gluconeogenesis during a prolonged fasting when glycogen reserves are exhausted. Additionally, FA oxidation is stimulated to produce acetyl-CoA, supplying substrates for both gluconeogenesis and ketogenesis. Besides hydrolysis of endogenous TG pools in hepatocytes, exogenous FA generated from adipose lipolysis is delivered to the liver. The excess FA is reesterified to TG, which can be stored in LDs or secreted

in VLDL. Hepatic TG biosynthesis, consumption and secretion are of great significance to the whole body energy homeostasis; however, the regulation of TG metabolism is largely unclear. Hepatocellular TG stored in distinct depots (cytosol or ER lumen) is highly dynamic, undergoing robust lipolysis and reesterification cycle. This TG turnover can provide FA for oxidation and up to 60-80% of VLDL-TG.[144]

1.3.1 Lipid Storage in Hepatocytes

TG in hepatocytes is distributed into three subcellular compartments: cytosolic LDs, ER lumenal LDs and apoB-containing primordial lipoprotein particles. Cytosolic LDs are the major intracellular lipid reservoir in hepatocytes, providing substrates for energy metabolism, membrane synthesis and production of lipid-derived molecules, such as bile salts and hormones.[147] This dynamic organelle is also involved in cellular events that are irrelevant to lipids *per se*, such as sequestration of hydrophobic proteins destined for degradation and hepatitis C virus assembly.[145,146]

LDs comprise a neutral lipid core (TG and cholesteryl esters) surrounded by a polar lipid monolayer that, in mammals, mainly consist of PC.[147] The lipid composition varies in hepatocellular LDs under nutritional or genetic stresses.[148,149] Specific proteins that possess amphipathic α-helices bind to LDs and regulate lipid synthesis, metabolism and lipoprotein assembly in hepatocytes.[147] In eukaryotes, LDs primarily arise from the ER and remain linked to this organelle, but the molecular mechanisms of LD biogenesis are not fully understood.[150] Several models of LD formation have been proposed. Generally, TG synthesized within the ER bilayer may form a lens-like structure, and as TG

accumulating in the ER intramembranous space, LDs grow, mature and may eventually bud off.[150] Alternatively, the entire LDs are excised from the ER bilayer through a bicelle formation mechanism.[147,151]

LDs grow by expansion and coalescence to accommodate more TG. Neutral lipids might be synthesized locally at LDs, or transferred from ER through membrane connections and interorganelle transport. Lack of surfactants on LD surfaces destabilizes the oil phase boundary, resulting in high surface tension that predisposes LDs to coalescence.[147] However, LD fusion may only occur by experimental manipulations, such as genetic ablation of CTP: phosphocholine cytidyltransferase alpha, the rate-limiting enzyme in PC synthesis.[152-154]

Besides the ER, other organelles were found in close proximity to LDs, such as mitochondria, endosomes and peroxisomes, suggesting an essential role of LDs in energy homeostasis, lipid trafficking and membrane lipid synthesis.[147] Rab GTPases are required for vesicular trafficking and membrane fusion. Rab18 was found to localize particularly on small LDs and mediate the connections between LDs and the ER, thus facilitating TG translocation and mobilization.[155,156] Moreover, Rab18 co-localized with perilipin 2 in HepG2 cells, but their expression levels were regulated in a reciprocal manner.[155] Endogenous Arf1 GTPase and coatomer (COPI) complex were found localized on the surface of LDs in *Drosophila* Schneider 2 cells and mammalian NRK cells,[120] and identified in a LD proteomic study in CHO K2 cells.[157] The Arf1/COPI machinery is required for bidirectional membrane trafficking and was found to be critical for LD targeting of specific proteins that are involved in lipid synthesis and lipolysis.[120,158] Depletion of Arf1/COPI complex in *Drosophila* Schneider 2 cells resulted in defects in lipolysis and a more dispersed distribution of LDs.[159]

1.3.2 *De Novo* FA Synthesis

Liver uses glucose not only for acute energy demands but also for glycogenesis; when the latter is replenished, excess glucose is shunted to FA *de novo* synthesis during the fed state. Cytosolic acetyl-CoA is the initial substrate for mammalian FA biosynthesis. Carboxylation of acetyl-CoA generates malonyl-CoA by acetyl-CoA carboxylase (ACC) in a biotin-dependent mode. Mammals have two isoforms of ACC, ACC1 and ACC2, encoded by separate genes, *Acaca* and *Acacb*. ACC1 and ACC2 share considerable sequence similarities and an identical catalytic domain, but show distinct tissue distributions, with the former highly expressed in lipogenic tissues, such as liver and adipose tissue, while the latter primarily found in heart and skeletal muscle, and also to a lesser extent in the liver.[160,161] Seven molecules of malonyl-CoA and one molecule of acetyl-CoA form palmitic acid (16:0) via 7 rounds of the Claisen condensation, reduction and dehydration reactions, which are all undertaken by a multifunctional enzyme: fatty acid synthase (FAS). Palmitic acid is elongated by fatty acyl-CoA elongases in the ER to generate long-chain FA, which can be further desaturated by SCDs.

ACCs and FAS are rate-limiting enzymes in FA *de novo* synthesis, and thus under tight regulations by hormones and nutrients.[61] ACCs are switched on/off via reversible dephosphorylation and phosphorylation on a single serine residue, respectively.[162] The phosphoryl group is mounted by 5'-AMP-activated protein kinase that is activated when energy charge is low, and removed by phosphatases. Palmitoyl-CoA also inhibits ACCs, serving as a feedback control.[162]

FAS is mainly regulated at the transcriptional level, essentially by SREBP1.[61] Hepatic expression of *Srebf1c* and the nuclear translocation of its mature form were remarkably induced by refeeding fasted animals with a high-carbohydrate diet, which led to increased expression of lipogenic genes, including *Acaca*, *Fas*, *Scd1*, *Gpat* and genes encoding key enzymes involved in cytosolic acetyl-CoA and NADPH production.[163] Specific deletion of the first exon of the *Srebf1c* gene with the *Srebf1a* transcript intact diminished but did not completely eliminate the refeeding-stimulated enhancement in *Acaca* and *Fas* gene expression.[164] As a matter of fact, SREBP1a is a much stronger activator of hepatic lipogenesis, as the *Srebf1a* transgenic mice exhibited four-times increased expression of *Acaca* and *Fas* genes in the liver than the *Srebf1c* transgenic mice.[165] Moreover, the livers in the *Srebf1a* transgenic mice were only slightly enlarged with a moderate increase in TG, but not cholesterol, whereas the liver expansion of the *Srebf1c* transgenic mice appeared to be tremendous, owing to an accumulation of both TG and cholesterol.[165]

1.3.3 FA Oxidation

Liver FA oxidation is suppressed in the fed state, and stimulated in the fasted state, providing energy for itself as well as the extrahepatic tissues by generating ketone bodies (β-hydroxybutyric acid, acetoacetic acid, and acetone) that are transported through the circulation. In mammals, mitochondria and peroxisomes take the major responsibility for FA β-oxidation, while γ-oxidation is restricted to the smooth ER.[166]

The mitochondrion is responsible for all short (<C8), medium (C8~C12) and the majority of the long (>C12) chain FA β-oxidation.[167] Acyl-CoA is first transported into the mitochondria via the carnitine shuttle that is comprised CPTI, CPTII and a translocase. CPTI catalyzes the formation of fatty acyl-carnitine for translocation across the mitochondrial inner membrane. CPTI is transcriptionally activated by PPARα and allosterically inhibited by malonyl-CoA, especially by the ACC2-derived, locally produced malonyl-CoA. Each cycle of β-oxidation is initiated by a dehydrogenation reaction to form a *trans*-double bond between the carbon-2 and carbon-3, which is catalyzed by the long-chain acyl-CoA dehydrogenase, followed by hydration, oxidation of a hydroxyl group to a keto group, and thiolysis. The cycle continues until the entire even-numbered saturated FA is decomposed into basic subunits of acetyl-CoA, with concomitant production of reducers, $FADH_2$ and NADH.

In mammals, the peroxisome takes an exclusive responsibility for very long-chain FA (>C20) β-oxidation, and can also utilize long-chain FA as a substrate.[167] However, because acyl-CoA oxidase, the first and rate-limiting enzyme of the mammalian peroxisomal β oxidation, is incapable of processing medium-chain FA, thus the chain-shortened acyl-CoA is exported to mitochondria for complete oxidation.[167]

1.3.4 VLDL Assembly and Secretion

TG, due to its hydrophobicity, is assembled into TG-rich lipoproteins for their transport through the circulatory system. Differences in FA compositions of hepatic intracellular TG and plasma VLDL-TG revealed an indirect transfer of TG

for VLDL maturation.[168] It has been established that the majority (60-80%) of TG in VLDL is derived from mobilization of hepatic TG storage via lipolysis and re-esterification cycle.[144,153] This sinuous supply of TG for VLDL maturation overcomes the inability of TG stored in the cytosolic LDs to cross the lipid bilayer of the ER and provides a mechanism for the regulation of VLDL secretion independently of plasma FA and intracellular TG concentration.[169]

Nascent VLDL forms by co-translational lipidation of the apoB molecule with cholesteryl esters and TG to generate a neutral lipid core that is surrounded by amphiphilic lipids, including PL and cholesterol, and other associated-apolipoproteins, apoE and apoC-I (Figure 1-3). The availability of lipids, TG in particular, in proximity to VLDL assembly sites is crucial for VLDL maturation, as insufficient TG supply results in apoB misfolding and degradation. This process that initially generates small, dense, lipid-poor primordial apoB particles is facilitated by MTP. MTP is a heterodimer composed of a large (97 kDa) lipid transfer protein and a small (55 kDa) multifunctional enzyme-protein disulfide isomerase.[170,171] Dissociation of these two subunits resulted in the abrogation of MTP activity.[170] MTP is encoded by *Mttp*, a gene predominantly expressed in hepatocytes and enterocytes, where it participates in the assembly of VLDL and chylomicrons, respectively. However, the subcellular location of MTP remains a matter of controversy. Both the large and small subunits have been observed to localize in the rough ER membrane and the Golgi apparatus using electron and confocal microscopies, and the localization was confirmed by immunoprecipitation of the Golgi fractions.[170,172] Genetic ablation of hepatic *Mttp* inhibited TG transfer into the ER lumen, leading to drastically impaired VLDL assembly and hypolipidemia,[48] whereas adenovirus-mediated 3-fold overexpression of *Mttp* elevated VLDL secretion by more than 70%.[173]

The primordial VLDL is further lipidated with a bulk of TG to form mature secretion-competent VLDL, and this process has been suggested to be independent of MTP.[174,175] Inactivation of MTP in murine primary hepatocytes resulted in a significant reduction of apoB100 in the microsomal lumenal compartment as well as in the culture medium, whereas only a slight decrease of secreted apoB48 with less TG associated was observed.[176] The disparate effects of MTP inhibition on apoB48 and apoB100 secretion suggest distinct roles of MTP in two stages of VLDL maturation: on the first stage, MTP is required for TG transfer onto a lipid-free apoB polypeptide during its translation/translocation to form a poorly (partially) lipidated primordial apoB particle, but on the second stage, a further lipidation to form a mature secretion-competent VLDL is independent of MTP.[176]

Several cytosolic LD-associated proteins also influence VLDL maturation. For instance, adenovirus-mediated overexpression of perilipin 2 in primary rat hepatocytes increased cytosolic TG storage and concomitantly decreased secretion of TG, apoB100 and apoB48.[177] In contrast, siRNA-mediated knockdown of perilipin 2 significantly dampened cytosolic LD accumulation, while increasing the secretion of apoB48 in VLDL of relatively larger diameters.[177] Deficiency of CIDEB, a protein found on the ER membrane and the surface of LDs, increased cytosolic TG deposition and diminished size but not number of VLDL particles.[178] ABHD5, a modulator of lipolysis that resides on the surface of LDs and/or in the cytosol, has been reported to promote mobilization of cytosolic TG for VLDL secretion in hepatoma cells, which was dependent on E600-sensitive TG lipase(s).[179,180] ASO-mediated ablation of *Abhd5* expression significantly decreased hepatic TG hydrolase activity and neutral lipid secretion.[181] On the other hand, liver-specific knockout of *Abhd5* also reduced

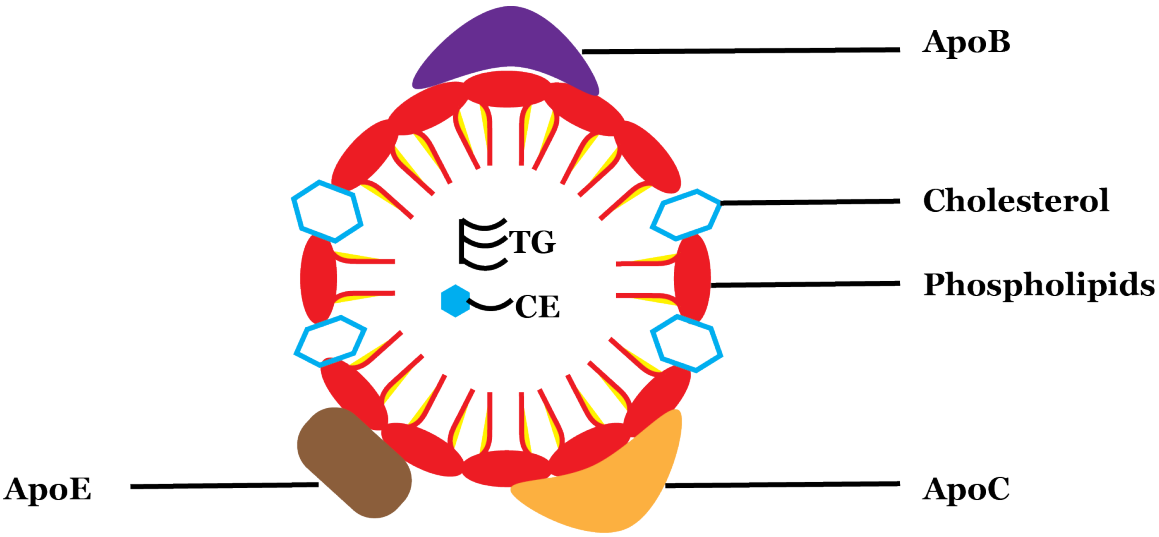

Figure 1-3. Schematic illustration of VLDL structure. VLDL is composed of a bolus of neutral lipids [triacylglycerol (TG) and cholesteryl ester (CE)] that are surrounded by a monolayer of amphiphilic lipids, including phospholipids and cholesterol, with specific apolipoproteins associated, initially ApoB, ApoE and ApoC-I. ApoC-II is later donated by high-density lipoprotein in the circulation.

hepatic TG hydrolase activity, but the VLDL-TG secretion was comparable with that of wild-type mice.[182] The discrepancies of the effects of ABHD5 on VLDL secretion in the two mouse models require further investigation. Moreover, it would be important to identify which TG hydrolase is activated by ABHD5 if the involvement of ABHD5 in the VLDL assembly is confirmed. Notably, gain- or loss-of-function of ATGL, currently the only known target of ABHD5, failed to exert any effect on hepatic TG secretion, suggesting a dispensable role of ATGL in the VLDL maturation.[183-185]

An ER-lumen-localized TG hydrolase (TGH), termed carboxylesterase 1d, has been suggested to play a role in the VLDL secretion. The hydrolysis of hepatocellular TG destined for VLDL assembly was significantly augmented or dampened by activation or inhibition of TGH activity, respectively, in both *in vitro* and *in vivo* experiments.[186-190] Another ER-localized lipase, arylacetamide deacetylase, which is homologous to hormone-sensitive lipase, may also contribute to the VLDL maturation based on preliminary transfection studies in hepatoma cells.[191,192]

Finally, vesicular trafficking proteins also contribute to VLDL secretion, as nascent and/or mature VLDL demands transport from the ER to the Golgi for exocytosis. The COPII complex facilitates ER budding, and functions in the anterograde transport of apoB100 and other typical hepatic secretory proteins, such as albumin and transferrin.[193] The COPII complex consists of five major subunits, including the Sar1b GTPase. Transfection of dominant-negative Sar1b in McA cells inhibited anterograde trafficking of apoB to a certain extent.[193] Mutations of Sar1b have been identified in humans, and were associated with reduced chylomicron production and severe fat malabsorption due to impaired

activation of COPII complex.[194] In contrast, COPI vesicles are classically known to transport retrograde cargoes from the Golgi to the ER. Recent studies have also suggested their engagement in the bidirectional transport, trafficking small anterograde cargoes forward (from *cis* to *trans* face) within the cisternae of Golgi.[195,196] The localization of COPI at the Golgi and the anterograde transport were impaired by an Arf1 mutant that is restricted to its GDP-bound inactive form, leading to decreased secretion of apoB100-VLDL of higher Svedberg flotation rate.[197] Consistently, chemical inhibition of the Golgi brefeldin-A-resistance guanine nucleotide exchange factor 1 (GBF1) by brefeldin A blocked the Arf-mediated recruitment and activation of COPI complex, resulting in decreased VLDL assembly and secretion.[198] Moreover, Arf1 has been reported to activate phospholipase D that catalyzes a conversion of PC to PA.[199] Overexpression of phospholipase D significantly increased secretion of VLDL at both maturation stages, but with a stronger effect on the second stage of VLDL maturation.[197,200] Notably, phospholipase D activity was required for Sar1b-mediated recruitment of COPII complex and ER export, therefore a modulation of lipid composition might be pre-requisite for vesicle formation and secretion.[201]

1.4 Thesis Objectives, Rationale and Hypotheses

VLDL assembly is largely regulated by the availability of TG in hepatocytes. Although compelling evidence indicates the majority of TG in VLDL is derived from re-esterification of lipolytic products released by ER-localized lipases, little is known about roles of the two DGATs in this process. Based on the different phenotypes of *Dgat1*$^{-/-}$ and *Dgat2*$^{-/-}$ mice, these two DGAT enzymes appear to

perform non-redundant physiological functions. To dissect the distinct contributions of DGAT1 and 2 in lipid metabolism and lipoprotein secretion in liver cells, I inactivated DGAT1 and 2 separately or in combination with highly-selective, small-molecule inhibitors of DGAT1 and DGAT2 in primary mouse and human hepatocytes, tracked the storage and secretion of lipids with radioisotope labeling, and performed secretory apoB analysis.

LDs synthesized through the DGAT1- or DGAT2-dependent pathways may be predisposed to different uses. To distinguish the potential differences of DGAT1- and DGAT2- derived LDs, I inactivated DGAT1 and 2 individually or in combination during TG synthesis, and labeled LDs with a fluorescent FA analogue for morphological analysis or with radioisotopes for metabolic studies, including FA oxidation and TG secretion. I hypothesized that DGAT1- and 2-synthesized TG undergo preferential metabolic use in oxidation, storage or secretion, and the cytosolic LDs containing DGAT1- or DGAT2-derived TG may exhibit distinct morphologies in primary hepatocytes.

CHAPTER II MATERIALS AND METHODS

2.1 Materials

2.1.1 Chemicals and Reagents

Chemicals and reagents used in this thesis are listed in Table 2-1.

Table 2-1. Chemicals and Reagents

NAME OF CHEMICAL	SOURCE
[^{3}H]Acetic acid (0.1 Ci/mmol)	Perkin Elmer
[9,10(n)-^{3}H]Oleic acid (54.6 Ci/mmol)	Perkin Elmer
[1-^{14}C]Oleic acid (56.3 mCi/mmol)	Perkin Elmer
70% perchloric acid	Sigma-Aldrich
Acetone	Fisher Scientific
Albumin Standard	Thermo Scientific
Amersham ECL Western Blotting Detection Reagent	GE Healthcare
Ammonium Chloride	Sigma-Aldrich
Bodipy 493/503 Dye	Molecular Probes
Bodipy FL C12	Molecular Probes
Bovine Serum Albumin [(BSA), FA free]	Sigma-Aldrich
Bradford Protein Assay Reagent	Bio-Rad Laboratories
Chloroform	Sigma-Aldrich

Collagenase, Type IV	Sigma-Aldrich
Complete™ Protease Inhibitor Cocktail Tablets	Roche Diagnostics
Cupric Sulphate	Fisher Scientific
CytoScint™-ES Liquid Scintillation Cocktail	MP Biomedicals
deoxynucleotides triphophates (dNTPs)	Invitrogen
DGAT1 Inhibitor (PF-04620110)	Pfizer
DGAT2 Inhibitor (Example 109B)	Pfizer
Dimethyl Sulfoxide (DMSO)	Sigma-Aldrich
DNAse I	Invitrogen
Dulbecco's Modified Eagle's Medium (DMEM)	Gibco
DMEM, high glucose, no glutamine, no methionine, no cysteine	Gibco
EasyTag™ EXPRESS^{35}S Protein Labeling Mix, [^{35}S], 11mCi/ml	Invitrogen
Ethylene Diaminetetraacetic Acid Disodium Salt (EDTA)	Fisher Scientific
Ethylene Glycol Tetraacetic acid (EGTA)	Sigma-Aldrich
Fetal Bovine Serum (FBS)	Gibco
Formaldehyde, 16% EM Grade	Thermo Scientific
Fumed Silica (Cab-O-Sil)	Sigma-Aldrich

G418 (Geneticin)	Invitrogen
Glycerol	Fisher Scientific
Golgicide A	Sigma-Aldrich
HEPES	Sigma-Aldrich
Heptane	Fisher Scientific
Horse Serum	Gibco
Isopropyl Ethanol	Fisher Scientific
Magnesium Chloride	BDH
Methanol	Fisher Scientific
Oligo dT Primers	Invitrogen
Penicillin Streptomycin (Pen Strep)	Gibco
Platinum® SYBR® Green qPCR SuperMix-UDG	Invitrogen
Ponceau S Solution	Sigma-Aldrich
Potassium Bromide	BDH
Prestained SDS-PAGE Standards (low/high range)	Bio-Rad Laboratories
ProLong® Gold Antifade Mountants	Molecular Probes

RPMI-1640 Medium	Sigma-Aldrich
Saponin	Sigma-Aldrich
Sodium Chloride	BDH
Sodium Dodecyl Sulphate (SDS)	Bio-Rad Laboratories
Sucrose	Fisher Scientific
SuperScript® II Reverse Transcriptase	Invitrogen
SuperSignal™ West Dura Extended Duration Substrate	Invitrogen
Triton X-100	Fisher Scientific
TRIzol® Reagent	Invitrogen
UltraPure™ Tris Buffer (powder format)	Invitrogen

2.1.2 Antibodies

Antibodies used in this thesis are listed in Tables 2-1 and 2-2.

Table 2-2. Primary Antibodies

ANTIGEN NAME	IgG SPECIES	DILUTION	SOURCE
ApoB	Goat	1:5,000	Chemicon
MTP	Rabbit	1:5,000	Dr. David Gordon

Calnexin	Rabbit	1:10,000	Stressgen
SREBP1	Rabbit	1:1,000	Drs. M. Brown and J. Goldstein
Lamin A/C	Rabbit	1:2,000	Cell Signaling
GAPDH	Rabbit	1:10,000	Abcam
Golgi α-Mannosidase II	Rabbit	1:500	Dr. Tom Hobman

Table 2-3. Secondary Antibodies

NAME
Horseradish Peroxidase-Conjugated Goat-Anti-Rabbit IgG
Horseradish Peroxidase-Conjugated Mouse-Anti-Goat IgG
Texas Red-Conjugated Donkey-Anti-Rabbit IgG (H+L)

The first two secondary antibodies were used for immunoblotting at 1: 5,000 dilutions and were from Pierce Biotech; the last secondary antibody was used for immunofluorescence staining at 1:100 dilution and was from Jackson ImmunoResearch.

2.1.3 Primer Sequences

Primer sequences used for real-time PCR in this thesis are listed in Table 2-3.

Table 2-4. Primer Sequences for Real-Time PCR Analysis

GENE	SYMBOL	FORWARD	REVERSE
DGAT1	*Dgat1*	GGATCTGAGGTGCCATCGT	CCACCAGGATGCCATACTTG
DGAT2	*Dgat2*	GGCTACGTTGGCTGGTAACTT	TTCAGGGTGACTGCGTTCTT
Cyclophilin	*Ppia*	TCCAAAGACAGCAGAAAACTTTCG	TCTTCTTGCTGGTCTTGCCATTCC
ACC1	*Acaca*	GGCGACTTACGTTCCTAGTTG	AGGTGTCGATAAATGCGGTCC
FAS	*Fasn*	TTCCGTCACTTCCAGTTAGAG	TTCAGTGAGGCGTAGTAGACA
SCD1	*Scd1*	CACCTCCCTCCGGAAAT	AGCGCTGGTCATGTAGTAGAAA
SREBP1c	*Srebf1c*	ATGGATTGCACATTTGAAGAC	CTCTCAGGAGAGTTGGCACC

2.1.4 Buffers And Solutions

Compositions of buffers and solutions used in this thesis are listed in Table 2-4.

Table 2-5. Buffers and Solutions

NAME	COMPOSITION
Perfusion Buffer	1X Hank's Balanced Salt Solution (no calcium, no magnesium, no phenol red), 20mM glucose, 4.0 mM $NaHCO_3$, 2.5 mM HEPES, 0.5 mM EGTA, pH 7.4
Collagenase Buffer	1X Hank's Balanced Salt Solution (calcium, magnesium, no phenol red), 20mM glucose, 4.0 mM $NaHCO_3$, 2.5 mM HEPES, 100 collagenase U/mL, pH 7.4

Phosphate Buffered Saline (PBS)	137 mM NaCl, 2.7 mM KCl, 10 mM Na_2HPO_4, 2 mM KH_2PO_4, pH 7.4
Tris Buffered Saline (TBS)	20 mM Tris-HCl, 150 mM NaCl, pH 7.4
Tris Buffered Saline with Tween®20 (TTBS)	20 mM Tris-HCl, 150 mM NaCl, pH 7.4, 0.1% (v/v) Tween 20
Tris-Glycine SDS Running Buffer	10 g of SDS, 30.3 g of Tris base, 144.1 g Glycine, dissolved in 1 L ddH_2O, pH 8.3
Tris-Glycine SDS Transfer Buffer	192 mM Glycine, 24 mM Tris, 20% (v/v) Methanol, pH ~8.3
4X SDS-PAGE Loading Buffer	200 mM Tris-HCl, pH 6.8, 8% SDS, 40% (v/v) Glycerol, 40% 2-mercaptoethanol (v/v), 0.4% Bromophenol Blue
Ponceau Red Buffer	0.2% (v/v) Ponceau Solution, 3% (w/v) Trichloroacetic acid, 3% (w/v) Sulfosalicylic Acid
Methionine/Cysteine-free DMEM	500 ml DMEM with high glucose, no glutamine, no methionine, no cysteine; 1 mM Sodium Pyruvate
Homogenization Buffer	250 mM Sucrose, 50 mM Tris-HCl, 1 mM EDTA, pH 7.4

Hypertonic Buffer	10 mM HEPES, 420 mM NaCl, 1.5 mM $MgCl_2$, 2.5% (v/v) Glycerol, 1 mM EDTA, 1 mM EGTA, 1 mM DTT, pH 7.4
RIPA Buffer	50 mM Tris-HCl, 50 mM NaCl, 0.5% Sodium Deoxycholate, 0.1% SDS, 1% (v/v) Triton X-100, pH 8.0

2.2 Animals

All animal procedures were approved by the University of Alberta's Animal Care and Use Committee and were in accordance with guidelines of the Canadian Council on Animal Care. All mice used in this study were 2-3 months old C57BL/6J females maintained on chow diet (PicoLab Rodent Diet 20; LabDiet, Richmond, IN) with *ad libitum* access to distilled water. Unless otherwise stated, all mice were fasted overnight before experiments.

2.3 General Methodology

2.3.1 Preparation And Culture of Primary Mouse Hepatocytes

Primary mouse hepatocytes were isolated by collagenase perfusion of livers from wild type C57BL/6J mice based on a method published previously.[202] Mice were deeply anesthetized before a midline incision was made to separate the skin from abdominal muscle. Then the hepatic portal vein was exposed by carefully moving

the intestines away from the abdominal cavity with a cotton swab. Next ligatures were made loosely around the portal vein and the lower vena cava. A proper cut was made on the portal vein to insert a feeding needle, which was then repositioned and held in place by tying the ligature above. While the liver was perfused at 1.5 mL/min, the left side of the rib cage and the diaphragm were cut to expose the heart. Then another ligature around the upper vena cava was loosely made. Then the first ligature around the lower vena cava was untied to allow the perfusate to run out of the heart until no blood was visible. At this time the upper vena cava was tied off to swell the liver for two minutes. The liver was then digested by addition of collagenase solution for about 5 minutes until the liver appeared granulated and inelastic. The fully digested liver was then removed from the mouse and transferred to a 60-mm dish, further minced with scissors and suspended in pre-warmed DMEM supplemented with 15% FBS by pipetting up and down twelve times. Cells were then filtered through a sterilized coarse filter, centrifuged at 200 x g for 2 min, and resuspended in the same medium, followed by a finer filtration and resuspension. Cells were counted with a hemocytometer, and plated on 60-mm collagen-coated dishes (BD BioCoat™) at a confluence of 2.0 X 10^6 cells/dish for the following metabolic studies, or on collagen-coated coverslips (BD BioCoat™) in six-well plates at 2.0 X 10^5 cells/well for microscopic analysis. Cell were incubated for 4 h for attachment at 37 °C in humidified air containing 5% CO2 before experimental procedures.

2.3.2 Preparation of Primary Human Hepatocytes

The procedure was performed at the Service of Digestive Tract Surgery, University of Alberta. Briefly, human liver samples were obtained from resection

specimens far away from the tumor margin in patients undergoing operations for therapeutic purposes. Ethical approval was obtained from the University of Alberta's Faculty of Medicine Research Ethics Board, and all patients consented to participate in the study. Primary human hepatocytes were isolated and purified by collagenase-based perfusion of the liver fragments (~20 g). Isolated primary hepatocytes were plated on 60-mm collagen-coated dishes at a density of 1.5 × 10^6 cells/dish and kept at 37 °C in humidified air containing 5% CO2 for 4 h in RPMI-1640 culture medium containing 15% FBS before changing to experimental medium.

2.3.3 Subcellular Fractionation of Primary Hepatocytes

Mouse hepatocytes were washed with ice-cold PBS twice, 5 min each time, and suspended in ice-cold homogenization buffer (Table 2.1.5) containing the Complete Protease Inhibitor Cocktail (1 tablet/20 mL), 2 mL/sample, and disrupted with a homogenizer bearing a 15.6-μm clearance ball (Isobiotec, Heidelberg, Germany) for 30 strokes. One mL of homogenate per sample was kept for further analysis, while the other mL was subjected to subcellular fractionation. Specifically, cellular debris and nuclei were removed by centrifugation at 600 x g for 15 min at 4 °C, and the supernatants were centrifuged at 426,247 x g for 1 h at 4 °C in a TLA-100.2 rotor (Beckman Coulter, Inc.). Supernatants (cytosol) were collected, and pellets (membranes) were resuspended in 1 mL of the same homogenization buffer containing protease inhibitors.

2.3.4 Nuclear Protein Extraction

Primary mouse hepatocytes, 1 X 10^7 cells for each treatment, were collected in 2 mL of ice-cold homogenization buffer, and homogenized using a motor-driven Potter Elvehjem homogenizer at medium speed for 10 stokes. A drop of cells (~10 μl) was dripped onto a glass slide for examination under a compound light microscope to verify efficient lysis of the cells and intactness of the nucleus (a non-lysed cell appears as a dark nucleus surrounded by a halo of relatively bright cytoplasm). Nuclei were pelleted by centrifugation at 500 x g for 20 min at 4 °C, and the supernatants were transferred to a 1 mL polycarbonate ultracentrifuge tube suited for a TLA 100.2 rotor and centrifuged at 426,247 x g for 1 h at 4 °C to extract post-nuclear membranes, which were then resuspended in 100 μL RIPA buffer (Table 2.1.5) for immunoblotting analysis. Nuclear pellets were washed with the ice-cold homogenization buffer and briefly rinsed with hypertonic buffer (Table 2.1.5), then resuspended in 100 μl of hypertonic buffer by vigorous vortexing and incubated on a rocking platform on ice for 2 h. The mixtures were then centrifuged at 426,247 x g at 4 °C for 1 h in a TLA-100 rotor, and the supernatants (nuclear extracts) were collected for immunoblotting analysis.

2.3.5 Bradford Protein Assay

Protein concentration was determined with the Protein Assay Reagent (BioRad). Ten μL of each protein standard (albumin at 0, 0.0625, 0.125, 0.25 and 0.5 mg/mL) was added in duplicate to the first line of wells in a 96-well plate. Cells were homogenized by sonication at a medium speed (level 2.5) for 20 seconds. Ten μl of the cellular homogenates were loaded into each well in triplicate. Standards and samples of each well were then reacted with 200 μL of Protein

Assay Reagent diluted 1:5 for several minutes at room temperature. Measurements were read at an absorbance of 595 nm.

2.3.6 Radioisotopic Labeling

2.3.6.1 [^{3}H]-Labeling

Isolated primary mouse or human hepatocytes in DMEM or RPMI supplemented with 15% FBS and antibiotics (50 U/mL penicillin/streptomycin), respectively, were incubated for 4 h during which attachment to the collagen-coated dishes occurred. Then hepatocytes were washed three times with serum-free medium, 5 min per wash, and incubated for 4 h in 2 ml of serum-free medium containing 5 μCi of [^{3}H]oleic acid and 0.4 mM oleic acid/0.5% BSA, or 10 μCi of [^{3}H]acetic acid and 50 μM acetate. Some media and cells (Pulse incubations) were harvested, and lipids were extracted using chloroform-methanol (2:1, v/v) and resolved by thin-layer chromatography (TLC). Radioactivity in various lipid classes was determined by liquid scintillation counting. Cellular protein concentrations were determined by Bradford Protein Assay. Remaining cells were washed three times with serum-free medium, 5 min per wash, then incubated with 2 mL of serum-free medium for another 4 h or overnight (Chase incubations); cells and media were collected and lipids analyzed as described above. DGAT inhibitors alone or in combination were dissolved in DMEM and introduced 1 h before Pulse or Chase experiment as indicated in figure legends.

2.3.6.2 [^{14}C]- and [^{3}H]-Oleic Acid Double Labeling

Primary mouse hepatocytes attached to collagen-coated dishes were washed three times with serum-free DMEM, 5 min per wash, and incubated overnight (12-16 h) in 2 mL of DMEM containing 1 μCi of [^{14}C]oleic acid and 0.4 mM oleic acid/0.5% BSA ([^{14}C] labeling). Cells were then washed three times with 0.5%BSA DMEM, 5 min per wash, and incubated with supplement-free DMEM for 1 h in the presence or absence of DGAT1 and 2 inhibitors alone or in combination, followed by another incubation in 2 ml of DMEM containing 5 μCi of [^{3}H]oleic acid and 0.4 mM oleic acid/0.5% BSA for 4 h ([^{3}H] labeling). Media were collected, and cells were washed with PBS twice before harvest. Intracellular and secreted lipids were extracted using chloroform-methanol (2:1, v/v) and resolved by TLC. Radioactivity in [^{3}H]TG and [^{14}C]TG was determined by liquid scintillation counting, and normalized to cellular protein mass measured by Bradford Protein Assay.

2.3.6.3 [^{35}S]Methionine/Cysteine Labeling

Cultured hepatocytes were washed three times with DMEM, 5 min per wash, and incubated for 4 h in 2 mL of DMEM containing 0.4 mM oleic acid/0.5% BSA, or 50 μM acetate. Next, cells were washed three times with DMEM, 5 min per wash, and incubated with regular DMEM in the presence or absence of DGAT inhibitors alone or in combination for 1 h, then washed with Methionine/Cysteine-free DMEM (Table 2.1.5), 5 min per wash, and incubated for 1 h with [^{35}S]-Protein Labeling Mix (200 μCi/mL) in the Methionine/Cysteine-free DMEM (2 mL/dish). Media were then removed, and cells were briefly washed with DMEM before

incubation with DGAT inhibitors overnight (12-16 h). Finally media were collected for VLDL density analysis as described (see section 2.3.13).

2.3.7 FA Oxidation Measurement

Chase media obtained from [^{3}H]oleic acid and [^{3}H]acetic acid labeling studies were analyzed for the content of acid soluble metabolites (ASMs) resulting from FA β-oxidation. Thirty μL of 20% BSA and 16 μL of 70% perchloric acid were added to 200 μL of culture medium from each sample. Samples were then centrifuged at 21,130 x g for 5 min before an aliquot (50 μL) of the supernatant was used for liquid scintillation counting.

2.3.8 Lipid Extraction and Separation by TLC

For lipid extraction and isolation by TLC,[203] 4 mL of chloroform/methanol (2:1, v/v) with 100 μg of each non-radioactive lipid carrier (phosphatidylcholine, oleic acid, trioleoylglycerol and cholesteryl oleate) were added to 1 mL of cellular or medium sample and mixed thoroughly by vigorous vortexing. The mixture was then centrifuged at 425 x g for 5 min in a table top centrifuge (Eppendorf 5810R) to separate lipid and aqueous phases. The lower phase (lipid) was collected with a doubled Pasteur pipette and evaporated under N_2. The residue was dissolved in 100 μL of chloroform and loaded onto a 20 X 20 cm TLC plate, which was immediately placed in a neutral lipid solvent tank (heptane: isopropyl ether: acetic acid, 600:400:40) to resolve neutral lipids for ~1 h duration. Alternatively, before the plate was placed in the neutral lipid solvent tank, PL were resolved by placement first in a tank containing chloroform/methanol (2:1, v/v) to migrate

lipids to ~1.5 cm above the origin, TLC plates were then briefly dried and placed in a PL solvent tank (chloroform: methanol: acetic acid: H_2O, 500:300:80:40) for ~20 min. Plates were dried thoroughly in air before visualization.

2.3.9 Detection of (Non)-Radioactive Lipids

2.3.9.1 Semi-quantification of Lipids by Charring

TLC plates containing resolved lipids were thoroughly infiltrated with 3% cupric sulfate, followed by 8% phosphoric acid, and heating at 180°C for 10 min. Lipid spots were captured by G:BOX Chemi XX6 (Syngene, MD) with the upper white light on, then quantified by GeneTools (Version 4.03.00). TG spots were normalized to total PL.

2.3.9.2 Liquid Scintillation Counting

Lipids on TLC plates were visualized by staining overnight with iodine. Lipid spots were circled scraped onto weighing papers and transferred to scintillation vials. Five mL of the CytoScint scintillation cocktail (MP Biomedicals) were thoroughly mixed with each sample by vigorous vortexing. Radioactivity was measured by a scintillation counter (Beckman LS 6500).

2.3.10 Immunoblotting

Hepatocytes were harvested in 2 mL of cold-PBS and sonicated at medium speed (level 2.5) for 20 seconds. An aliquot (30 μL) of each sample was mixed with 10 μL of 4X SDS-polyacrylamide gel electrophoresis (PAGE) loading buffer (Table 2.1.5), and boiled for 5 min to denature protein. Samples were then loaded into

wells of a 10-well SDS polyacrylamide gel. The concentration of polyacrylamide in gels depended on the molecular mass of target proteins (10% for proteins of <150 kDa, 4% for proteins of >150 kDa). The proteins were stacked at 60 V and separated at 100 V using a BioRad Mini-PROTEAN 3 system. Proteins resolved by PAGE were transferred to Immobilon-P transfer membrane (PVDF) membranes (Millipore Canada) in transfer buffer for 2 h at a constant voltage of 100 V. Membranes were quickly rinsed with TTBS, blocked with 5% skim milk in TTBS for 1 h at room temperature, and washed with TTBS 3 times, 10 min per time. Next, the membranes were incubated with primary antibodies diluted in 3% BSA in TTBS overnight at 4°C. On the next day, membranes were washed with TTBS 3 X 10 min, followed by incubation with HRP-conjugated secondary antibodies diluted 1: 5,000 in 5% skim milk in TTBS for 1 h at room temperature. Finally, membranes were washed again under the same regimen, and immunoreactivity was detected by G:BOX Chemi XX6 (Syngene, MD) using Supersignal West Dura or Pierce ECL Western Blotting Detection Reagents (Thermo Scientific). Quantitative analyses were performed with GeneTools (Version 4.03.00). For apoB precipitation, 1 mL of medium of each sample was mixed with 60 μL of 50 mg/mL of Cab-O-Sil (fumed silica) and incubated on a test tube rotator at 4°C for 1 h. The media were then centrifuged at 15294 x g at 4 °C for 5 min in a table top centrifuge (Eppendorf 5817R). The supernatant was removed, and the pellet was resuspended with 40 μL of pre-warmed 4 X SDS-PAGE loading buffer. The proteins were analyzed by immunoblotting as described above.

2.3.11 mRNA Expression Analysis

2.3.11.1 RNA Isolation from Primary Hepatocytes

Cultured hepatocytes were briefly washed with PBS before 1 mL of Trizol reagent was applied to each dish to lyse cells. The mixture was then transferred to a RNAse-free tube and incubated at room temperature for 5 min, before 200 μL of chloroform were added. The aqueous phase containing RNA was collected after centrifugation at 13,000 x g at 4 °C for 15 min. RNA was precipitated with an equal volume of isopropanol and centrifugation at 13,000 x g at 4 °C for 15 min. The purified RNA was further washed with 1 mL of 75% RNAse-free ethanol to remove salts. The RNA was pelleted by centrifugation as above, dried at room temperature for several minutes, and dissolved in an appropriate amount of RNAse-free water. RNA concentration was determined by a NanoDrop 2000 spectrophotometer (Thermo Scientific).

2.3.11.2 Reverse Transcription

Two μg of RNA were incubated with DNAse 1/buffer mixture at room temperature for 15 min to remove any potentially remaining DNA contamination. DNAse 1 activity was terminated by heating at 65 °C for 10 min in the presence of EDTA to maintain the integrity of RNA. A total of 11 μl of the DNAse 1-digested RNA sample was mixed with 200 ng of Oligo dT primer, 45 ng of random hexamers and 10 mMols of dNTPs, and heated at 65 °C for 5 min. Meanwhile, the reverse transcriptase, Superscript III, was mixed with its 1X buffer and 0.1 μM DTT. The enzyme mixture was then added to the RNA substrate mixture. The

reverse transcription system (20 μL) was incubated at 50 °C for 50 min, followed by termination at 70 °C for 15 min.

2.3.11.3 Real-Time Polymerase Chain Reaction

Real-time quantitative polymerase chain reaction (qPCR) was performed with the Platinum SYBR Green qPCR SuperMix-UDG kit (Invitrogen) in the STEPONEPLUS Real-Time PCR System (Applied Biosystems). Twenty μl of cDNA were combined from all samples, and diluted 1:10, followed by serial 1:4 dilutions to generate four points in the standard curve. cDNA samples were diluted 200 times, and 4 μl of the diluted cDNA was used as template. Primers for tested genes are listed in Table 2.1.4. All target genes were normalized to a housekeeping gene, *Ppia*, encoding cyclophilin.

2.3.12 Lipoprotein Density Determination

A total of 2 ml medium was collected from hepatocytes incubated with [^{35}S]-Protein Labeling Mix (200 μCi/mL), and centrifuged at 425 x g at 4 °C for 5 min to precipitate cell debris. 1.8 mL of supernatant were combined with 100 μL of plasma from an overnight-fasted, chow-fed wild type female mouse, 100 μL of Complete Protease Inhibitor Cocktail (X20), and 0.97 g desiccated KBr. The mixture was gently placed into a 5.0-ml polypropylene Quick-Seal tube and overlaid with 3 mL of 0.9% NaCl. The fully filled Quick-Seal tube was then sealed by a pre-heated sealing machine (Laborgeraete-Beranek, Weinheim, Germany). The tubes were placed in a VTi 65.2 rotor, centrifuged at 416,000 x g for 1 h at 8 °C, and decelerated at the slowest speed (#9). The stratified tubes were carefully

held with a test tube clamp on an iron stand. A 18 G, 1.5 inch needle was inserted at the top of the tube and connected to a Mini-Peristaltic pump (Harvard Apparatus) set at a speed of 0.8 mL/min (slowest). A 23 G, 1 inch needle was used to punch a hole at the bottom of the tube to allow samples to drip in a density-dependent way. Ten fractions, 0.5 ml each, with densities ranging from 1.006 g/mL (fraction 10) to 1.21 g/mL (fraction 1), were collected into each tube. ApoB was precipitated by addition of Cab-O-Sil to each fraction and analyzed by electrophoresis on SDS-4% polyacrylamide gels. Proteins were transferred to PVDF membranes, which were exposed to Kodak BioMax MR films for 48 h before developing.

2.3.13 Confocal Fluorescence Scanning Microscopy

Mouse hepatocytes were plated onto collagen-coated coverslips in 6-well dishes at 2 X 10^5 cells/well, and incubated with DMEM containing 6 μM Bodipy FL C12 combined with 0.4 mM oleic acid/0.5% BSA for 4 h. Some cells were harvested at this point (Pulse), while other cells were washed three times with DMEM, and incubated for an additional 4 h in DMEM before fixation (Chase). DGAT inhibitors were introduced 1 h before Pulse or Chase incubation as indicated in figure legends. Cells were washed with PBS twice, 5 min per time, and fixed with 4% paraformaldehyde for 10 min. Cells were washed again with PBS, 2 X 5 min, and mounted onto glass slides with a small drop of Prolong Gold Antifade Reagent with DAPI, and stored in the dark overnight. The following day, slides were sealed with nail polish. Images were collected with a confocal laser scanning microscope (Leica TCS SP5, LAS AF Lite 3.2 software; Leica Microsystems, Wetzlar, Germany) equipped with a Leica PLAN APO 100X/1.44 oil M25

objective. The 488-nm laser line was used to image Bodipy FL C12, and emission signals were collected with a band pass 500–530 nm filter-IR blocking. Z-stacks covering entire cells were projected, and lipid droplet numbers and sizes were quantified and analyzed with ImageJ 1.48V.

McA cells stably expressing FLAG-tagged hepatic lipase were plated onto coverslips in 6-well dishes at a concentration of 1 X 10^5 cells/well, and incubated in DMEM containing 10% FBS, 10% HS, 50 U/mL penicillin/streptomycin and 250 μg/ml G418 overnight. On the next day, cells were washed with PBS twice, 5 min per time, and fixed with 4% paraformaldehyde for 10 min. Cells were washed again with PBS, 2 X 5 min, followed by an immunofluorescence staining procedure. First, free-aldehyde groups of the fixative were quenched by incubating cells with 50 mM NH_4Cl-PBS for 20 min at room temperature. Second, cells were permeabilized with 0.05% saponin in PBS for 15 min, then washed with TBS, 2 X 5 min, followed by another wash with TTBS for 5 min. Third, cells were blocked with 3% BSA in TTBS for 1 h at room temperature, followed by incubation with anti-Golgi α-Mannosidase II primary antibody diluted 1:500 in 3% BSA in TTBS on a low-speed tilting shaker at 4 °C overnight; cells were protected from light by wrapping them in foil. The following day, cells were washed with TTBS 3 times, 10 min each time, and incubated with Texas Red-conjugated donkey anti-rabbit secondary antibody diluted 1:100 in 3% BSA in TTBS for 1 h at room temperature in the dark, followed by 3 X 10 min washes with TTBS. Finally, cells were stained with 6 μM Bodipy 493/503 dye in PBS for 15 min, and washed with PBS, 2 X 5 min. Cells were briefly rinsed with ddH2O to remove remaining salts before they were mounted onto glass slides. Image collection and analysis were done as described above. In addition, a 561-nm laser

line (~ 30% relative intensity) was used to image Texas Red fluorescence, and signals were collected with a long-pass 615-nm filter.

2.3.14 Statistical Analysis

Data are presented as the mean ± SEM. Analysis was performed using GraphPad PRISM 4 software. Significant differences between groups were determined by one-way ANOVA followed by Bonferroni post-tests. $P<0.05$ was interpreted as significantly different.

CHAPTER III RESULTS, SUMMARY AND DISCUSSION

3.1 Overview

The assembly of secretion-competent VLDL is dependent on the provision of lipids, TG in particular. DGAT 1 and 2 catalyze the final step in mammalian TG biosynthesis, the two enzymes share no homology in primary amino acid sequence, and are encoded by genes belonging to distinct gene families.[71] The two DGATs perform non-redundant physiological functions, reflected by distinct phenotypes upon genetic or pharmacological inhibition of one DGAT.[125,131,138,140,204] While extensive investigation of DGATs has been undertaken in tissues such as adipose, small intestine and skin, less is known about their roles in hepatic TG synthesis and secretion. The majority (60-80%) of TG in VLDL is derived from re-esterification of lipolytic products in hepatocytes.[144,153] It has been shown that lipases involved in the hydrolysis of preformed TG include ER-localized carboxylesterase 1d/TGHand arylacetamide deacetylase,[189,190,192] however, it has not been determined which DGAT catalyzes the re-esterification of DG to support VLDL maturation.

Topological studies separated DGAT activities in hepatic microsomes into overt, cytosolic side-localized, and latent, lumenal side-localized.[115,205,206] This led to a hypothesis that the overt DGAT activity might be responsible for the synthesis of TG stored in cytosolic LDs, while the latent DGAT activity would mainly contribute to the formation of lumenal LDs, lipidation of primordial ApoB particles and maturation/expansion of VLDL.[207,208] DGAT1 is suggested to contain multiple transmembrane domains,[113] and have a dual topology within the ER of HepG2 cells, exhibiting comparable activities on both cytosolic and luminal sides of the ER membrane.[114] In contrast, DGAT2 was postulated to be intercalated into the ER bilayer through one or two transmembrane domains,

with both the N and C termini oriented toward the cytosol.[115] In addition to its ER localization, DGAT2 was found on the surface of LDs in *Caenorhabditis elegans* intestinal segments and *Drosophila melanogaster* Schneider 2 cells.[118,119,206] Thus, DGAT2 would be predicted to contribute to the overt activity. However, divergent DGAT1 and 2 topologies might not be sufficient to assign specific roles of these enzymes in channeling TG for distinct metabolic functions because there appears to be a functional crosstalk between TG residing in cytosolic LDs and ER lumenal LDs.[209,210]

To investigate the distinct contributions of the two DGATs to hepatic TG synthesis, deposition in LDs, and TG secretion in VLDL, I pharmacologically inhibited their activities in primary mouse and human hepatocytes with potent, highly selective small molecule inhibitors. Moreover, because some studies showed DGAT2 preferentially utilized endogenously synthesized FA to form TG in the HepG2 hepatoma cell line, whereas DGAT1 was primarily responsible for exogenous FA esterification,[114,139] I tracked lipids synthesized from FA made *de novo*, or from exogenously supplied oleic acid.

3.2 Results

3.2.1 DGAT1 and DGAT2 Can Compensate for Each Other to Synthesize TG.

To investigate individual DGAT function in TG synthesis in primary mouse hepatocytes, we inhibited DGAT1 or DGAT2 activities individually or together by small molecule inhibitors, then assessed *de novo* synthesis of TG by incubation

with [^{3}H]acetic acid and incorporation of exogenously supplied [^{3}H]oleic acid into TG. Cells were incubated with 50 μM [^{3}H]acetic acid or 0.4 mM [^{3}H]oleic acid, respectively. Cellular TG mass did not change after 4 h incubation with acetate, while it was augmented after 0.4 mM oleate supplementation (Figure 3-1), indicating that excess exogenous oleate contributed to significant enhancement of the hepatic TG pool, while FA synthesized *de novo* from acetate did not significantly increase intracellular TG content. TG synthesis from *de novo* synthesized FA (acetate precursor) was not affected by the inhibition of either DGAT1 or DGAT2 alone, and was slightly decreased in DGAT2-inactivated cells incubated with oleate. Inactivation of both DGAT1 and DGAT2 dramatically reduced TG synthesis (>80%) irrespective of whether FA was endogenously synthesized (Figure 3-2A) or supplied exogenously (Figure 3-3A). Moreover, DGAT inhibitors did not affect mRNA expression of either *Dgat1* or *Dgat2* (Figure 3-4). Therefore, DGAT1 and DGAT2 can compensate for each other to synthesize TG in mouse hepatocytes, though DGAT2 appears to be more efficient in esterifying exogenous FA.

3.2.2 Inhibition of DGATs Influences *sn*-1,2-DG and GPL Synthesis.

Sn-1,2-DG is at the pivotal junction of the Kennedy pathway of glycerolipid synthesis and can be converted to either PC, PE or TG. Destinations of *sn*-1,2-DG for energy storage as TG or membrane-forming PC and PE are controlled by enzymes, the DGATs and the CDP-choline/ethanolamine:*sn*-1,2-DG phosphocholine/phosphoethanolamine cytidylyltransferases

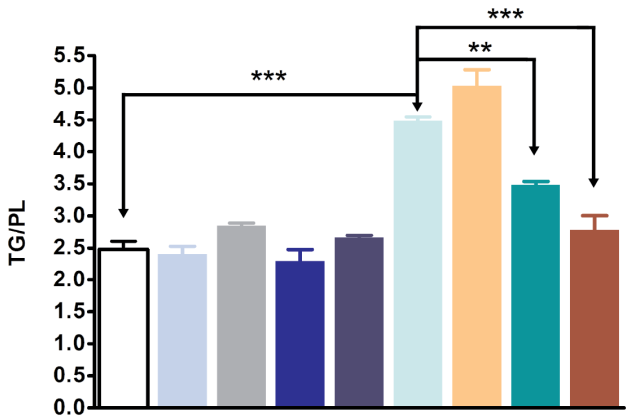

Acetate	-	+	+	+	+	-	-	-	-
Oleate	-	-	-	-	-	+	+	+	+
DGAT1inh	-	-	+	-	+	-	+	-	+
DGAT2inh	-	-	-	+	+	-	-	+	+

Figure 3-1. Influence of DGAT inhibition on intracellular TG mass under different treatments. Mouse hepatocytes were incubated in DMEM without any other addition (Blank), or with 0.4 mM oleate/0.5% BSA or with 50 μM acetate for 4 h, in the presence or absence of DGAT1 or DGAT2 inhibitors alone or in combination. TG levels were normalized to total PL. Data are presented as mean ± SEM. **P<0.01, ***P<0.001 between two groups indicated with downward-pointing arrows based on three independent biological replicates. Abbreviations: TG, triacylglycerol; PL, phospholipid.

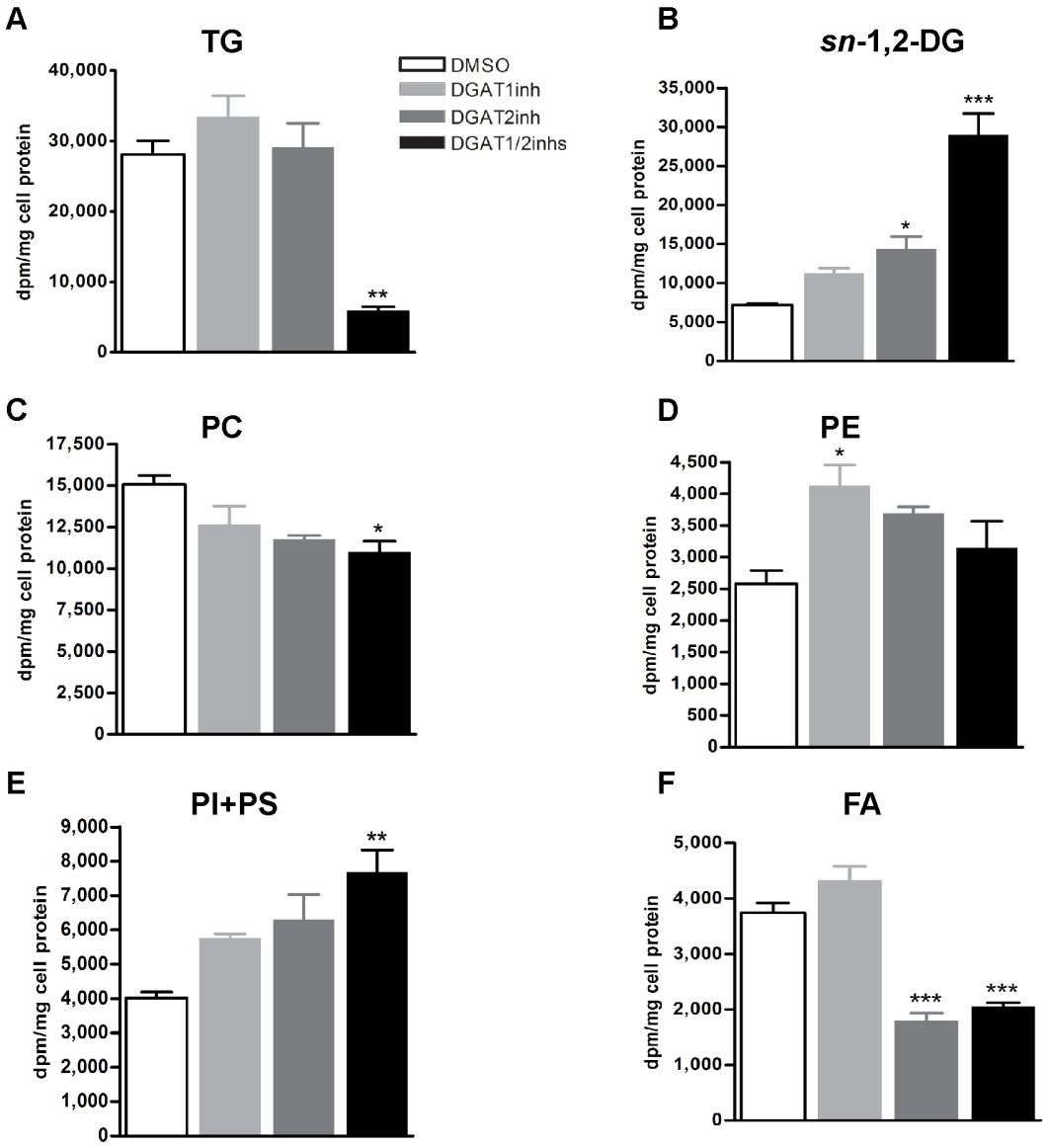

Figure 3-2. Influence of DGAT inhibition on various lipid species generated from *de novo* synthesized FA. Mouse hepatocytes were incubated in DMEM containing 10 µCi [^{3}H]acetic acid and 50 µM acetate for 4 h in the presence or absence of DGAT1 or DGAT2 inhibitors alone or in combination. Incorporation of [^{3}H]acetic acid into intracellular **A**, TG; **B**, sn-1,2-DG; **C**, PC; **D**, PE; **E**, combined PI and PS; **F**, FA; normalized to total cellular protein. Data are presented as mean ± SEM. *P<0.05, **P<0.01, ***P<0.001 versus control (DMSO) based on three independent biological replicates. Abbreviations: TG, triacylglycerol; DG, diacylglycerol; PC, phosphatidylcholine; PE, phosphatidylethanolamine; PI, phosphatidylinositol; PS, phosphatidylserine; FA, fatty acid.

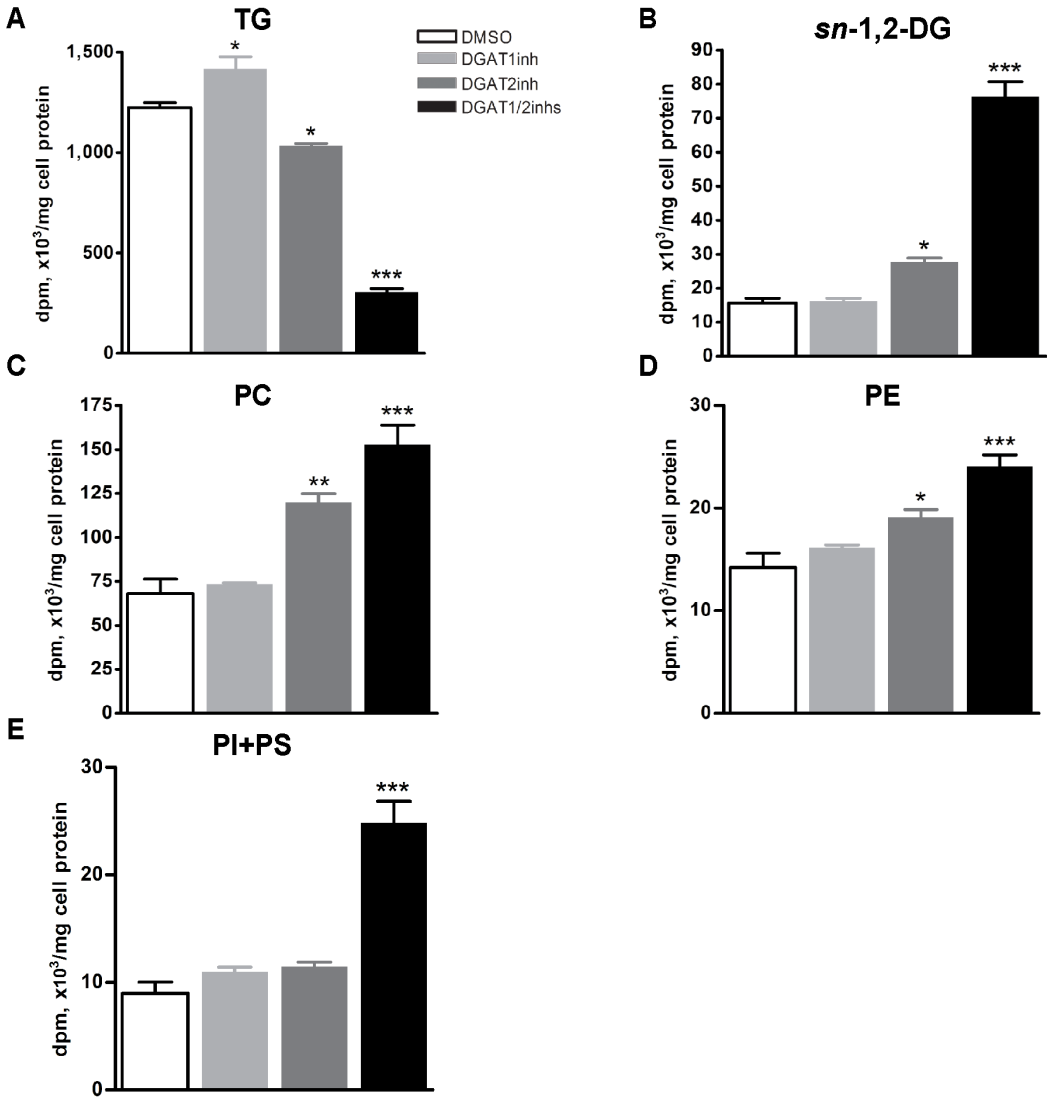

Figure 3-3. Influence of DGAT inhibition on various lipid species generated from exogenous oleic acid. Mouse hepatocytes were incubated in DMEM containing 5 μCi [^{3}H]oleic acid combined with 0.4 mM oleate/0.5% BSA for 4 h in the presence or absence of DGAT1 or DGAT2 inhibitors alone or in combination. Incorporation of [^{3}H]oleic acid into intracellular **A**, TG; **B**, *sn*-1,2-DG; **C**, PC; **D**, PE; **E**, combined PI and PS; normalized to total cellular protein. Data are presented as mean ± SEM. *P<0.05, **P<0.01, ***P<0.001 versus control (DMSO) based on three independent biological replicates. Abbreviations: TG, triacylglycerol; DG, diacylglycerol; PC, phosphatidylcholine; PE, phosphatidylethanolamine; PI, phosphatidylinositol; PS, phosphatidylserine.

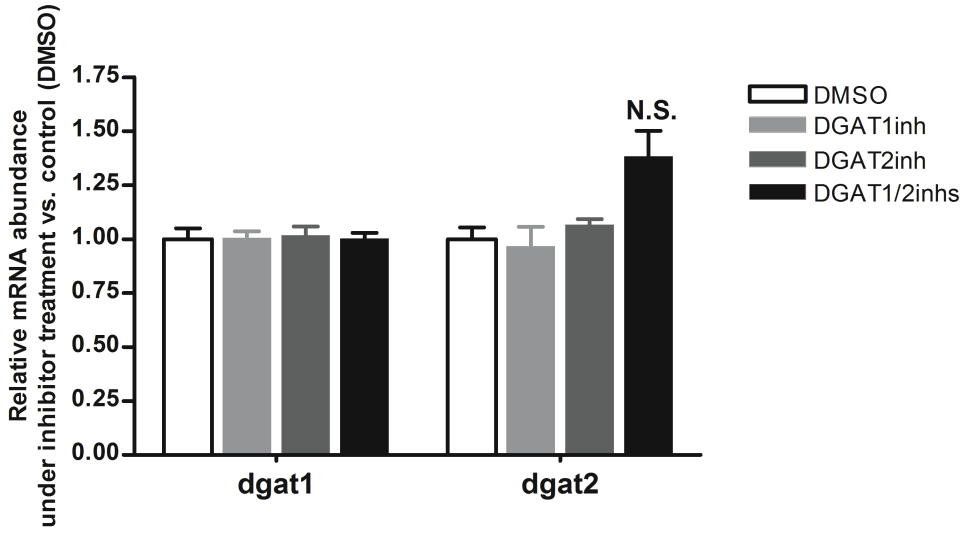

Figure 3-4. Inhibition of individual DGAT does not affect expression of their mRNAs. Mouse hepatocytes were incubated in DMEM containing 50 μM acetate for 4 h, in the presence or absence of DGAT1 or DGAT2 inhibitors alone or in combination. The abundance of *Dgat1* and *Dgat2* mRNA was determined by real-time qPCR. Data are presented as the ratio of *Dgat1* or *Dgat2* expression to *cyclophilin* expression. Values are normalized to DMSO (control) where the gene/*cyclophilin* ratio was set as 1. N.S. indicates no significant difference from the control based on three independent biological replicates.

respectively. I postulated that inhibition of DGAT1 or DGAT2 would reduce esterification of *sn*-1,2-DG to TG and increase channeling of *sn*-1,2-DG to GPL synthesis. Indeed, combined inhibition of DGAT1 and DGAT2 resulted in accumulation of *sn*-1,2-DG, which also occurred to a lesser but significant degree upon inhibition of DGAT2 but not DGAT1 alone (Figures 3-2B and 3-3B). These results suggest a more active role of DGAT2 in hepatic TG synthesis, in agreement with previous reports showing that reduction of *Dgat2*, but not *Dgat1*, expression by ASO decreased hepatic TG levels in high-fat diet-induced obese mice.[140,204]

While increased *sn*-1,2-DG availability from *de novo* lipogenesis (acetate) did not lead to enhanced PC or PE synthesis (Figure 3-2C-D), *sn*-1,2-DG produced from exogenous oleic acid was channeled to GPL synthesis (Figure 3-3C-D). Moreover, inactivation of both DGATs augmented the formation of PI and PS, regardless of the acyl donor (*de novo* synthesized or exogenous FA) (Figures 3-2E and 3-3E).

3.2.3 DGAT2 Promotes, Whereas DGAT1 Restricts Cytosolic LD Growth in Mouse Hepatocytes.

PC acts as a surfactant to prevent LD coalescence, and genetic ablation of CTP:phosphocholine cytidylyltransferase alpha, the rate-limiting enzyme in PC synthesis, results in giant LDs.[152,211,212] I therefore hypothesized that the observed increased PC synthesis from exogenous oleate (Figure 3-3C) would alter LD morphology. To test this hypothesis, LD biogenesis was stimulated by incubation of hepatocytes with oleate together with a trace of Bodipy FA analogue. The experimental protocol is laid out as presented in the schematic diagram [Figure 3-5A(1)], and representative images

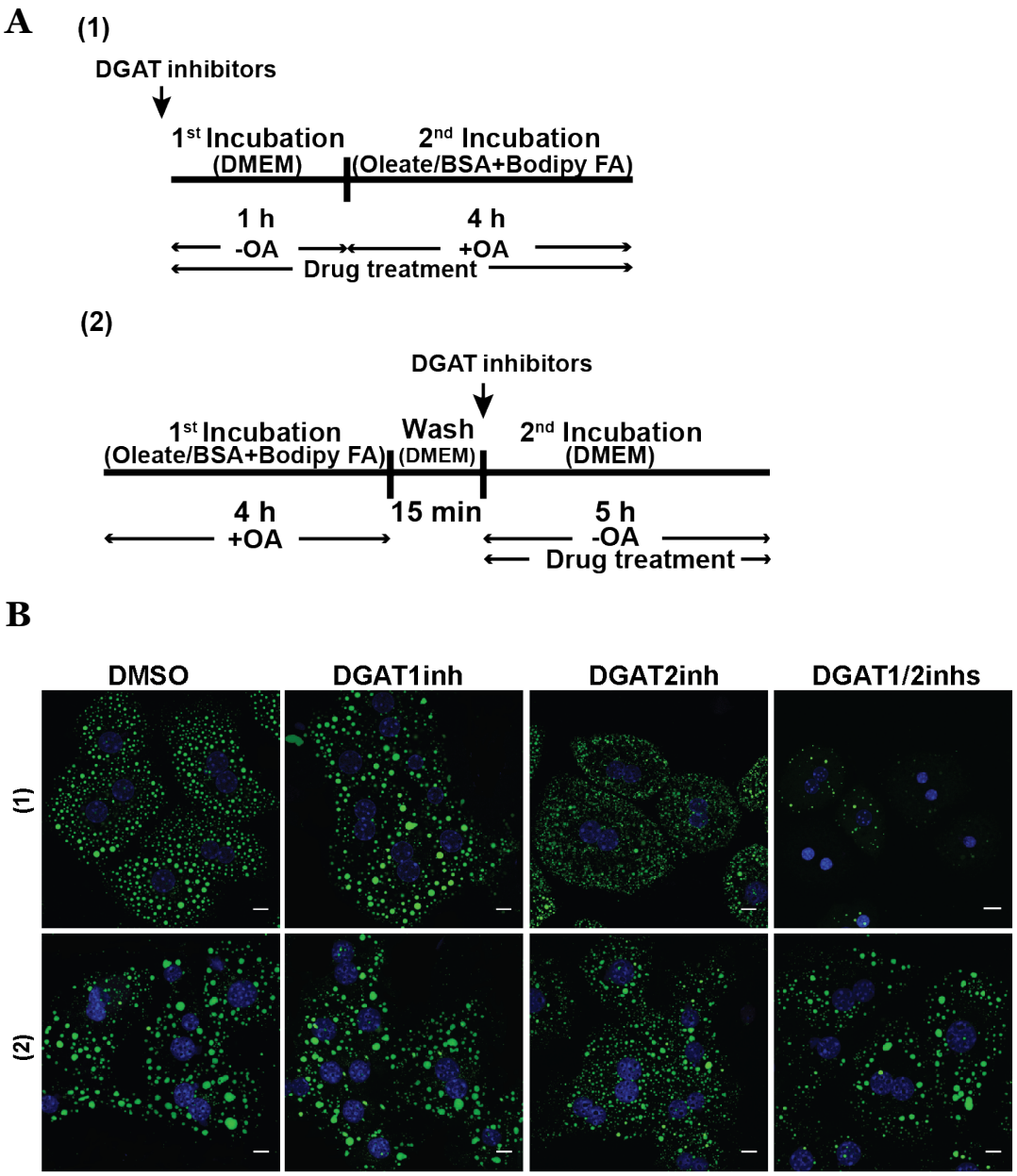

Figure 3-5. DGAT2 promotes, whereas DGAT1 restricts, cytosolic LD growth in mouse hepatocytes. A, Schematic diagrams of chronological orders of oleate + Bodipy FA incubations and drug treatments. DGAT inhibitors were introduced (1) before or (2) after incubation with oleate/BSA and Bodipy FA. **B**, Morphology of LDs in representative cells of each group. LDs were marked by fluorescently labeled lipids after incubation with Bodipy FL C12 (green), nuclei were counterstained with DAPI (blue). Confocal midsections are shown. Scale bar = 10 μm.

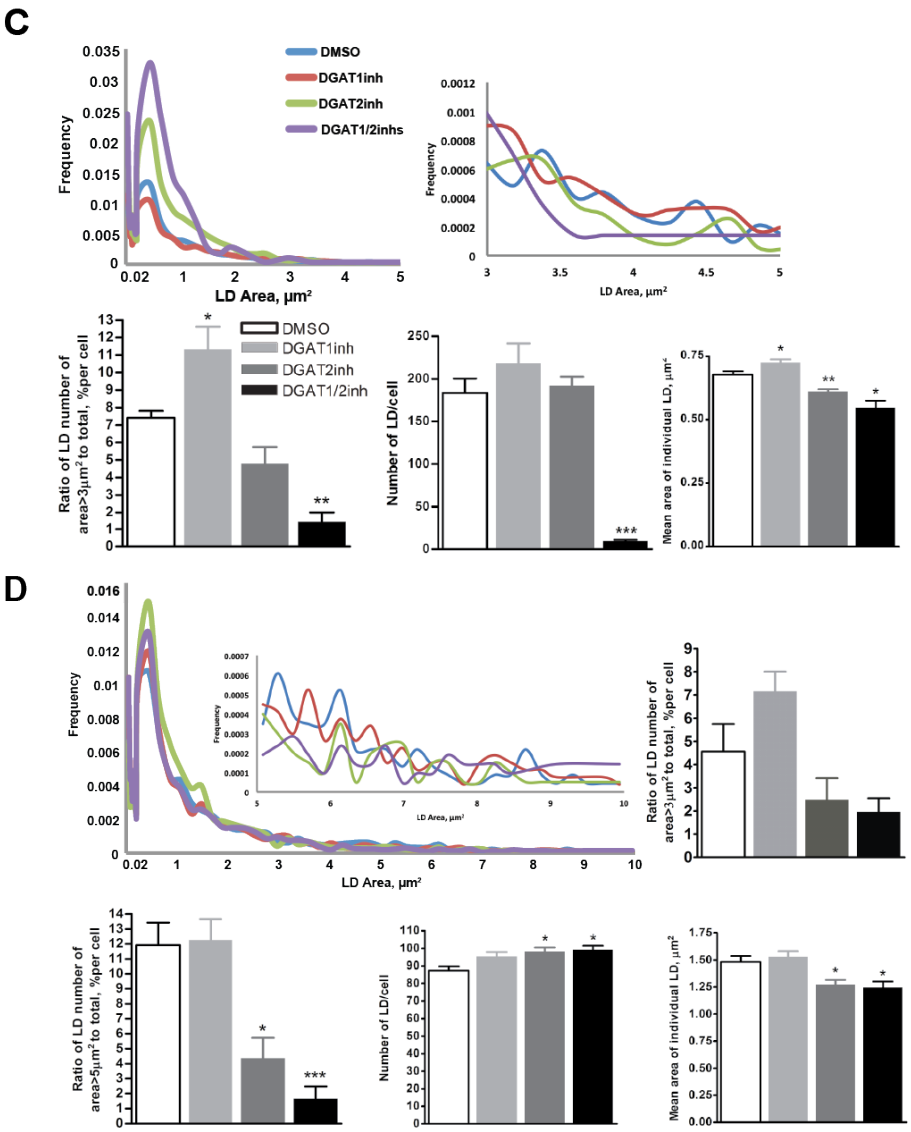

Figure 3-5. DGAT2 promotes, whereas DGAT1 restricts cytosolic LD growth in mouse hepatocytes. Quantification of LDs in 30 random cells of each group from (1) and (2) experiments. Z-stacks including entire cells were projected, in which sizes and numbers of LDs were determined by ImageJ 1.48V. **C,** Cells were analyzed from the (1) experiment. Distributions of LD areas between 0.02 to 5 µm² are shown in the first panel, with the tail region (3-5 µm²) enlarged. Ratios of LDs with areas larger than 3 µm² to the total in each cell are shown in the second panel. **D**, Cells were analyzed from the (2) experiment. Distributions of LD areas between 0.02 to 10 µm² are shown in the first panel with the tail region (5-10 µm²) enlarged. Ratios of LDs with areas larger than 3 and 5 µm² to the total in each cell are shown in the second and third panels, respectively. Numbers of LDs per cell and the mean areas of individual LDs are shown in the last two panels. Data are presented as mean ± SEM. *P<0.05, **P<0.01, ***P<0.001 versus control (DMSO) based on three independent biological replicates.

from this experiment are shown in the upper panel of Figure 3-5B. Thirty cells were analyzed in each group. The number of LDs per cell did not change unless both DGATs were inactivated. The mean area of an individual LD and the percentage of LDs with areas larger than 3 μm^2 were increased when DGAT1 was inhibited alone, and the frequency of small LDs (area <1 μm^2) was decreased upon DGAT1 inhibition, whereas DGAT2 inhibition tended to exert opposite effects (Figure 3-5C).

Next, we investigated whether any morphological changes would occur in LDs containing preformed TG, in other words, when DGAT activity was inhibited during TG turnover. The experimental protocol is shown in the schematic diagram [Figure 3-5A(2)] and representative images from this experiment are shown in the lower panel of Figure 3-5B. Thirty cells from each condition were analyzed. When DGAT2 or both DGATs were inhibited, the frequency of small LDs (area <1 μm^2) was increased, accompanied with a slight increase of the number of LDs per cell, while the mean area and the ratio of LDs with areas larger than 3 μm^2 tended to decrease, additionally, LDs with areas larger than 5 μm^2 accounted for a significantly decreased portion of the total LDs per cell (Figure 3-5D). DGAT1 inhibition alone exerted no significant influence on the size and number of preformed LDs (Figure 3-5D). The mean area of individual LD containing preformed as opposed to newly synthesized TG was larger, although the intracellular TG content did not change, suggesting that LD coalescence occurred during TG turnover.

3.2.4 Inhibition of DGAT2, but Not DGAT1, Reduces Lipogenic Gene Expression.

Because *Dgat2*$^{-/-}$ mice exhibited markedly diminished FA levels in the liver and plasma,[138] we examined the potential modulatory role of DGATs on *de novo* synthesis of FA by analyzing lipogenic gene expression and SREBP1c maturation. Messenger RNA

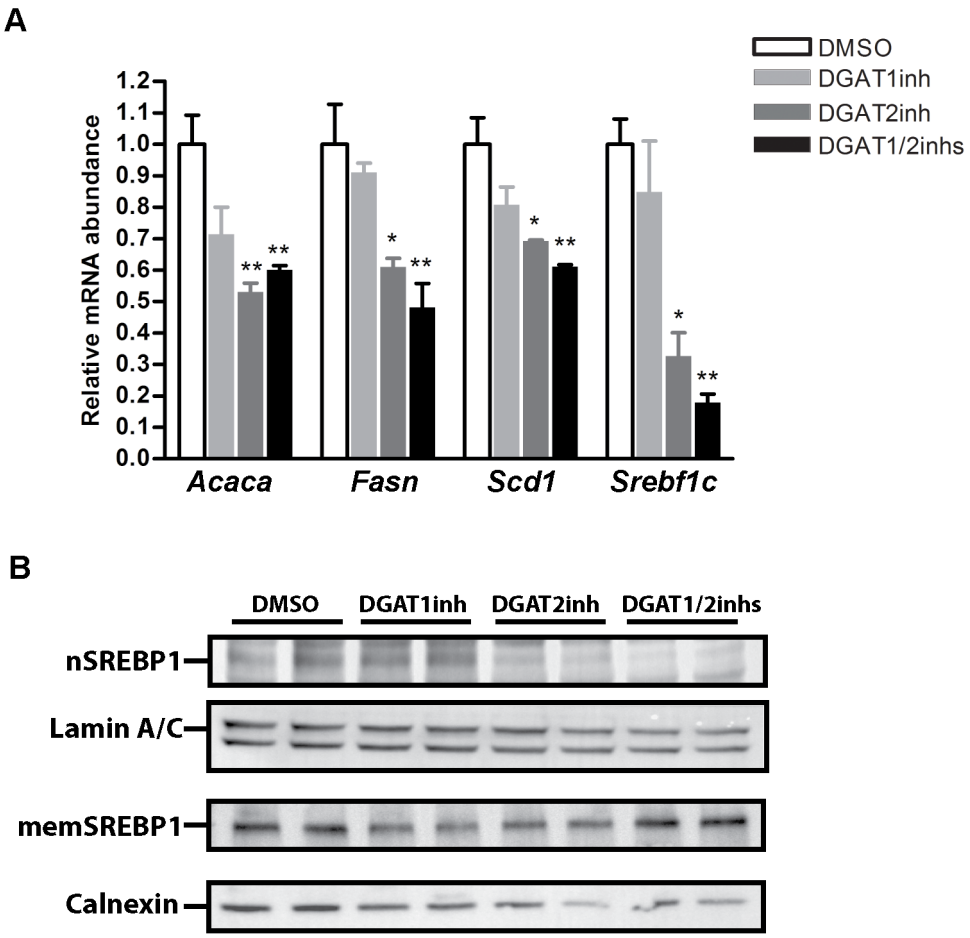

Figure 3-6. Inhibition of DGAT2, but not DGAT1, reduces lipogenic gene expression. Mouse hepatocytes were incubated in DMEM containing 50 μM acetate for 4 h, in the presence or absence of 5 μM DGAT1 or DGAT2 inhibitors alone or in combination. **A**, Quantitative PCR analysis of lipogenic gene expression. Data are presented as the ratio of expression of a given gene to *cyclophilin*. Values are normalized to control (DMSO) where the gene/*cyclophilin* ratio was set as 1. Data are presented as mean ± SEM. *P<0.05, **P<0.01, ***P<0.001 versus control (DMSO) of each gene based on three independent biological replicates. **B**, Immunoblotting of the mature form of SREBP1c in the nuclei (nSREBP1) and of full-length SREBP1c precursor in the membrane (memSREBP1). Lamin A/C and Calnexin served as loading controls for nuclei and ER membranes, respectively.

expression of genes involved in *de novo* lipogenesis (*Acaca*, *Fasn* and *Srebf1c*) and desaturation (*Scd1*) was significantly downregulated upon DGAT2 inhibition (Figure 3-6A). Nuclear localization of the master lipogenic transcriptional activator SREBP1c was diminished upon DGAT2 inactivation (Figure 3-6B). Because of the short time treatment with DGAT inhibitors (4 h), changes in protein expression and metabolism might may not be evident, and therefore, it was not surprising that the total amount of full-length SREBP1 precursor did not alter, and nor was *de novo* TG synthesis upon singular DGAT2 inactivation (Figure 3-2A). Nonetheless, metabolic changes might occur during prolonged treatment with DGAT inhibitors.

3.2.5 The TG Pool Generated by DGAT1 Is Preferentially Used for Supplying Substrates for Oxidation, Whereas DGAT2-derived TG Is More Favored for Secretion.

Though DGAT1 and DGAT2 can compensate for each other to synthesize TG, their distinct membrane topologies, interacting protein partners and subcellular localizations might imply different destinations and uses for their products.[71] Neutral lipids stored in the cytosol or ER lumen of hepatocytes are destined for distinct uses. TG present within the ER can be deposited into primordial apoB particles or resident ER lumenal LDs, both closely correlated with VLDL maturation,[153,213] while TG stored in cytosolic LDs provides FA for oxidation in mitochondria.[183,214] Thus, I first examined if DGAT1 or DGAT2 inactivation would affect intracellular TG distribution by analyzing the proportion of newly synthesized TG dispensed into cytosol and membranes. However, no change in the subcellular localization of synthesized TG was observed when either DGAT was inhibited (Figure 3-7). This is perhaps not surprising because the capacity of TG

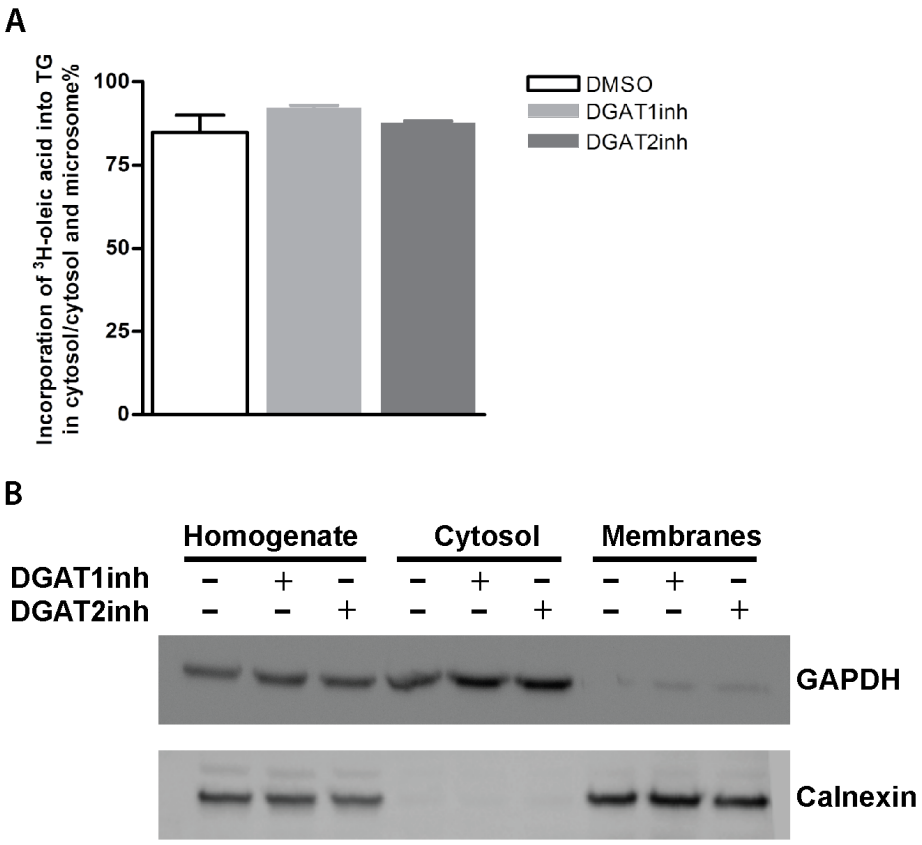

Figure 3-7. Inhibition of individual DGAT does not affect intracellular TG distribution. A, Percentage of TG synthesized from [^{3}H]oleic acid in cytosol. **B**, Purity of subcellular fractions. Immunoblotting with anti-mouse Calnexin (microsomal marker) and GAPDH (cytosolic marker) polyclonal antibodies were performed in total homogenate, cytosol and membrane fractions.

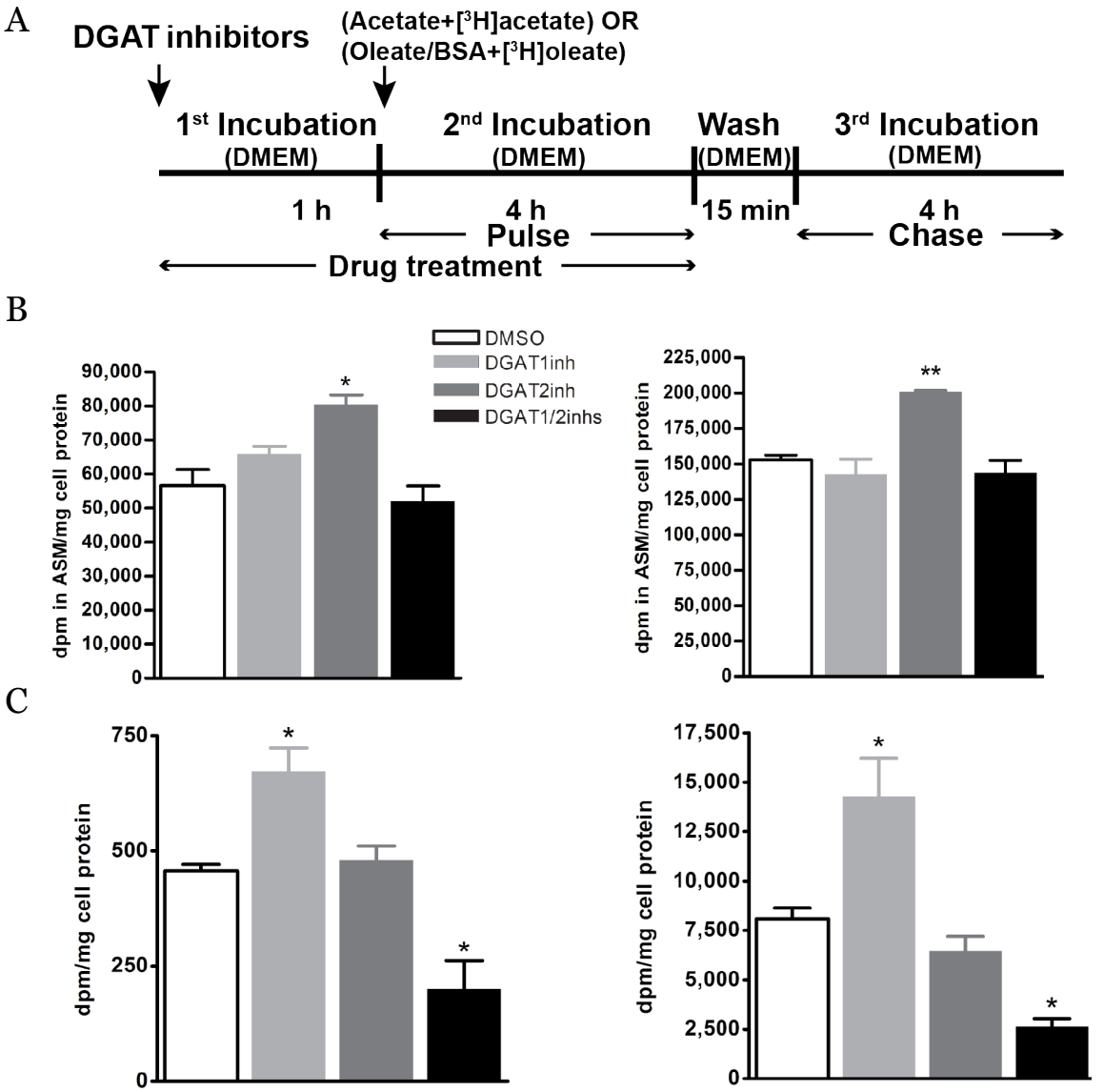

Figure 3-8. The TG pool generated by DGAT1 is preferentially used for supplying substrates for oxidation, whereas DGAT2-derived TG is more favored for secretion. Mouse hepatocytes were incubated in DMEM containing 10 μCi [^{3}H]acetic acid and 50 μM acetate, or containing 5 μCi [^{3}H]oleic acid and 0.4 mM oleate/0.5% BSA for 4 h, in the presence or absence of DGAT1 or DGAT2 inhibitors alone or in combination. Cells were then washed and incubated for an additional 4 h in DMEM without nutritional or pharmacological supplements before harvest. Media were collected for analysis of FA oxidation and TG secretion. **A**, Schematic diagram of chronological order of [^{3}H]-labeling and drug treatments. **B**, Radioactivity from [^{3}H]acetic acid (left) or [^{3}H]oleic acid (right) in acid soluble metabolites (ASMs) and **C**, secreted TG were determined by liquid scintillation counting and normalized to total cellular protein. Data are presented as mean ± SEM. *P<0.05, **P<0.01, ***P<0.001 versus control (DMSO) based on three independent biological replicates.

storage within the ER bilayer is limited, and TG stored in cytosolic and ER lumenal depots is intimately linked.[177,178,213]

We next addressed whether inactivation of DGATs directly influences TG utilization employing an experimental protocol shown in Figure 3-8A. After the "Chase" period, radioactivity in acid soluble metabolites (ASMs) and medium TG were measured, which indicated FA oxidation and VLDL secretion, respectively. Inhibition of DGAT2 (TG synthesized by DGAT1) augmented FA oxidation, while DGAT1 inhibition (TG synthesized by DGAT2) had no effect on FA oxidation (Figure 3-8B), suggesting that DGAT1-derived TG pool was preferentially used for FA oxidation. This observation is in agreement with previous studies in rats with diet-induced nonalcoholic fatty liver disease, where increased FA oxidation was also observed upon ASO-mediated decrease of *Dgat2* expression.[204] On the contrary, inhibition of DGAT1 (TG synthesized by DGAT2) increased TG secretion, on which DGAT2 inhibition had no effect (Figure 3-8C), thus suggesting DGAT2-derived TG pool was more efficiently channeled to VLDL assembly. In separate experiments, to validate that DGAT inhibitors were completely removed before the "Chase" period, cells were incubated with [^{3}H]acetic acid or [^{3}H]oleic acid during the "Chase" period. TG synthesis was nearly completely recovered, suggesting that the DGAT inhibitors were eliminated (Figure 3-9).

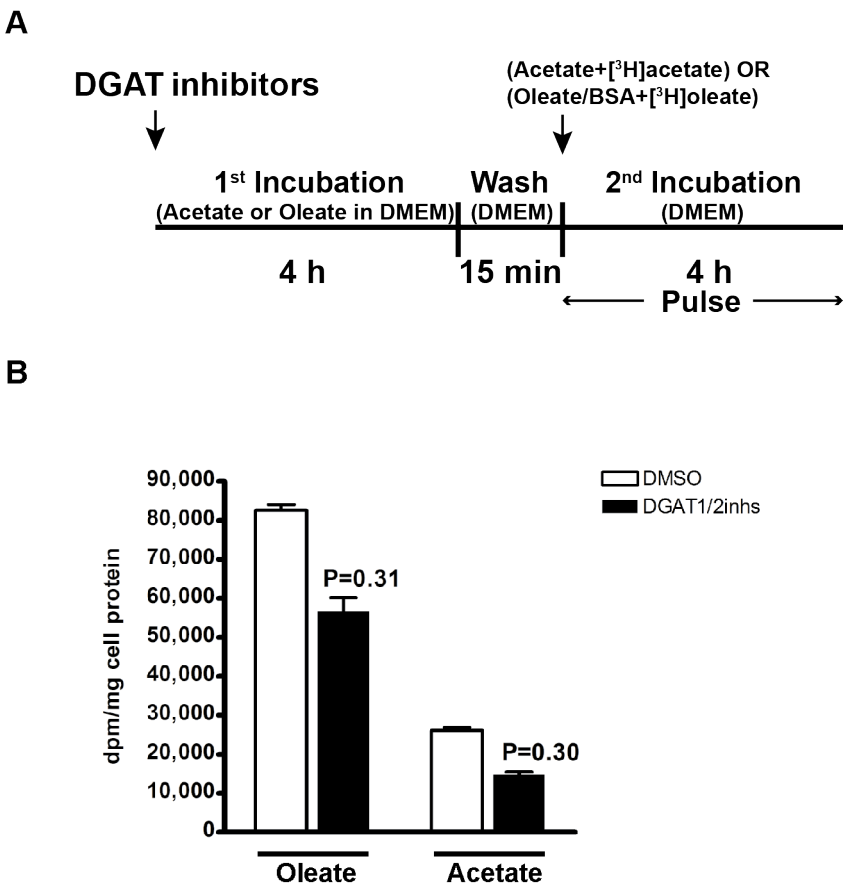

Figure 3-9. Validation of complete removal of DGAT inhibitors by regular washing. A, Schematic diagram of chronological orders of drug treatments and [3H] labeling. **B**, Incorporation of [3H]oleic acid or [3H]acetic acid into intracellular TG, normalized to total cellular protein. Data are presented as mean ± SEM. P values versus control (DMSO), determined by unpaired two-tailed t test, are indicated on top of the black bars.

3.2.6 Inhibition of DGAT2, but Not DGAT1, Reduces Re-esterification of Lipolytic Products and TG Secretion without An Effect on Extracellular apoB Levels in Mouse Hepatocytes.

To distinguish potentially different functions of DGAT1 and DGAT2 in providing TG for VLDL assembly by re-esterification of lipolytic products from preformed lipids, we introduced the DGAT inhibitors immediately before the "Chase" period, that is, after lipids were synthesized from radiolabeled precursors, as depicted in Figure 3-10A. Inhibition of DGAT2 dramatically reduced TG secretion, suggesting a prominent role for DGAT2 in the re-esterification of DG to form VLDL-destined TG, though DGAT1 might have a minor additive effect, since inhibition of both DGATs further dampened TG secretion (Figure 3-10B-C). Attenuation of VLDL-TG secretion was independent of MTP expression (Figure 3-11A-B). Additionally, there was no preference for FA origin used for the re-synthesis of VLDL-TG, because similar attenuation of VLDL secretion was observed when preformed TG was made *de novo* from acetate or from exogenously supplied oleate (Figure 3-10B-C).

More TG undergoes lipolysis than is required to support VLDL assembly, and excess re-esterified TG re-enters the intracellular TG storage pool.[169] However, it is technically challenging to segregate recycled TG from the pre-existing TG. To distinguish the pre-existing TG pool from the newly synthesized TG pool, a double labeling experiment was carried out in which the preformed TG was labeled with [^{14}C]oleic acid during an overnight incubation (Pulse), followed by a 4 h "Chase" period, during which the newly synthesized TG pool was labeled with [^{3}H]oleic acid. DGAT inhibitors were present only during the "Chase" period, during which pre-existing [^{14}C]TG was undergoing a lipolysis-

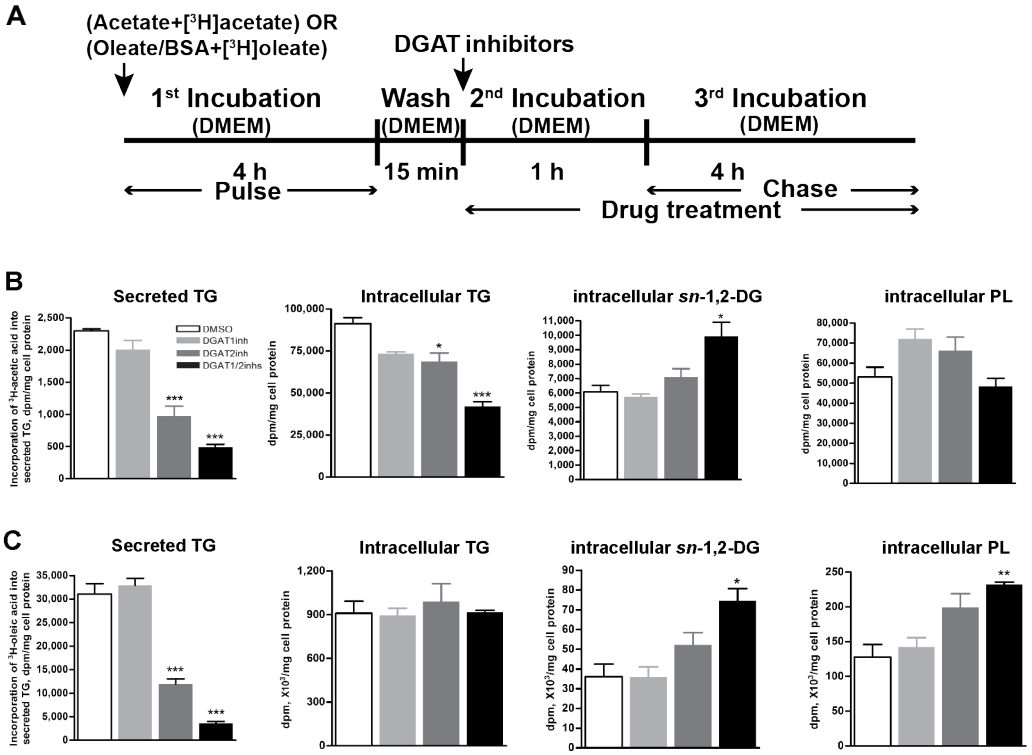

Figure 3-10. Inhibition of DGAT2, but not DGAT1, reduces re-esterification of lipolytic products and TG secretion without an effect on extracellular apoB levels in mouse hepatocytes. Mouse hepatocytes were incubated in DMEM containing 10 μCi [3H]acetic acid and 50 μM acetate, or 5 μCi [3H]oleic acid and 0.4 mM oleate/0.5% BSA for 4 h. Cells were then washed and incubated in DMEM for additional 4 h in the presence or absence of DGAT1 or DGAT2 inhibitors alone or in combination. Media were harvested and analyzed for TG and apoB secretion. Cells were collected and analyzed for intracellular lipids levels. **A**, Schematic diagram of the order of [3H]-labeling and drug treatments. Secreted and intracellular TG, intracellular *sn*-1,2-DG and phospholipid (PL) synthesized from **B**, [3H]acetic acid; **C**, [3H]oleic acid were determined. Statistical data are presented as the mean ± SEM. *P<0.05, **P<0.01, ***P<0.001 versus control (DMSO) based on three independent biological replicates.

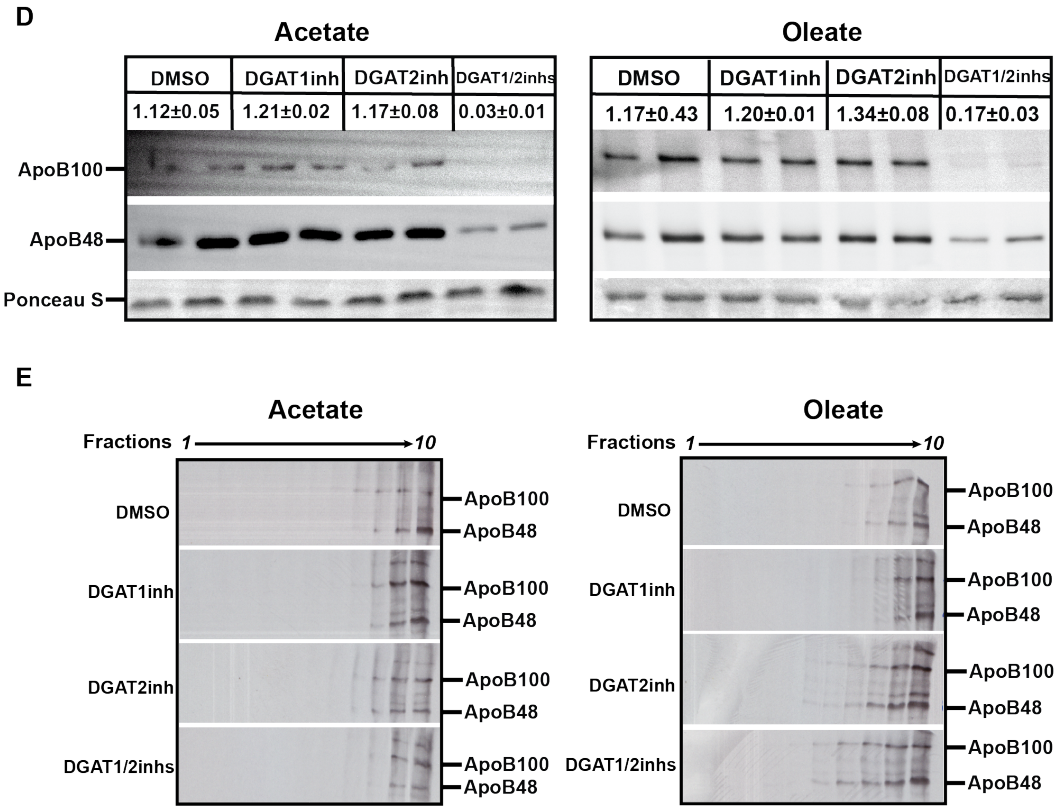

Figure 3-10. Inhibition of DGAT2, but not DGAT1, reduces re-esterification of lipolytic products and TG secretion without an effect on extracellular apoB levels in mouse hepatocytes. D, Immunoblot analysis of extracellular apoB48 and apoB100 levels. Extracellular apoB100 levels were quantified by GeneTools (Syngene Inc.), and normalized to the total protein load quantified by Ponceau S Red staining. **E**, [^{35}S]Met/Cys-labeled extracellular apoB100 and apoB48 of lipoproteins with densities ranging from 1.006 g/mL (Fraction 10) to 1.21 g/mL (Fraction 1), 10 fractions/treatment.

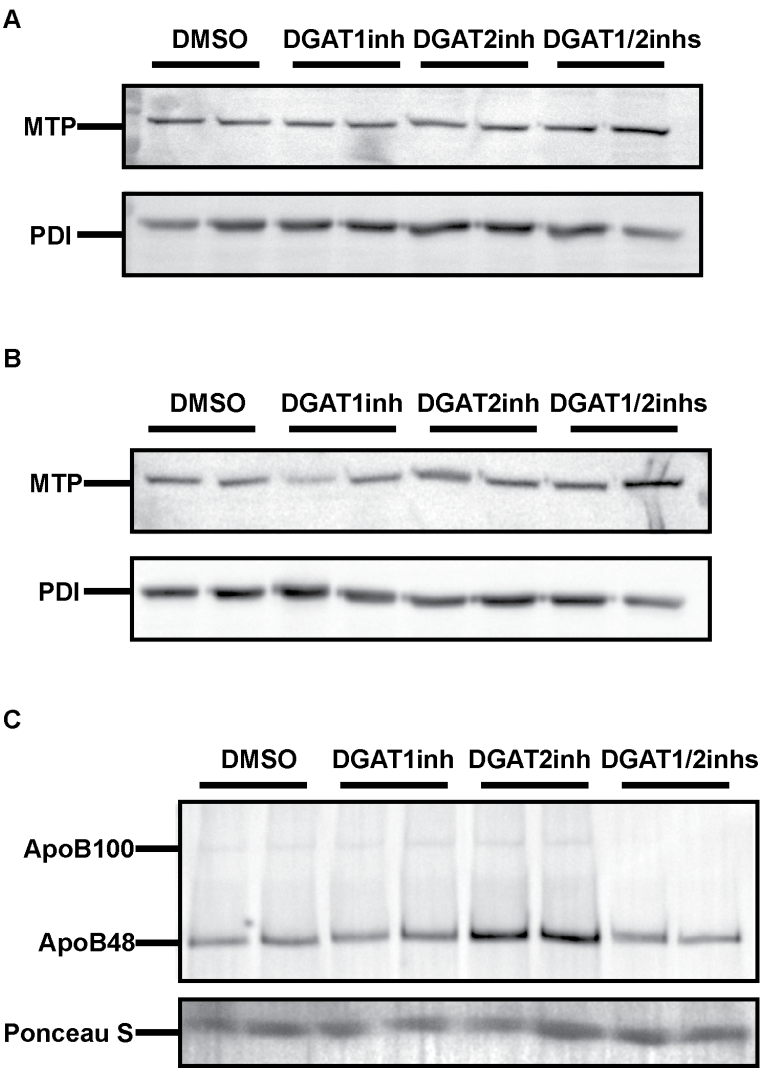

Figure 3-11. Inhibition of DGAT(s) does not affect MTP expression. Mouse hepatocytes were treated in the same way as illustrated in Figure 3-10A. MTP expression levels were detected by immunoblot analysis in cells incubated with **A**, 50 μM acetate or **B**, 0.4 mM oleate/0.5% BSA for 4 h in DMEM (Pulse), followed by an overnight (12-16 h) Chase. **C**, Extracellular apoB levels in cells pulsed in the absence of DGAT inhibitors and chased overnight in the presence or absence of DGATs inhibitors alone or in combination. Ponceau S Red staining served to control for protein loading.

re-esterification cycle while newly synthesized TG was [^{3}H]-labeled. DGAT2 inactivation decreased only the secretion of [^{14}C]TG but not [^{3}H]TG (Figure 3-12), further demonstrating a critical role for DGAT2 for VLDL secretion through re-esterification of lipolytic products of preformed TG.

Finally, we analyzed the effect of DGAT1 and DGAT2 inactivation on apoB secretion. The extracellular apoB48 and apoB100 levels were significantly decreased after simultaneous inhibition of both DGATs, but not when either of the two DGATs was inhibited alone (Figure 3-10D), and the lack of effect on apoB secretion was persistent even when neither acetate nor oleate was supplemented (Figure 3-11C). This suggested that DGAT2-inactivation leads to secretion of less lipidated and thus denser apoB. To test this possibility, we determined the lipoprotein densities after DGAT inhibition by density gradient centrifugation of secreted [^{35}S]-labeled apoB. ApoB100 and apoB48 shifted to fractions of higher densities when DGAT2 or both DGATs were inhibited (Figure 3-10E). However, this was more obvious in cells supplemented with oleate than acetate, possibly because incubation with acetate does not stimulate substantial TG synthesis and therefore VLDL secretion.

In conclusion, in mouse hepatocytes, DGAT2 plays the dominant role in the re-esterification process and acts as a driving force in facilitation of VLDL maturation, without altering extracellular apoB levels.

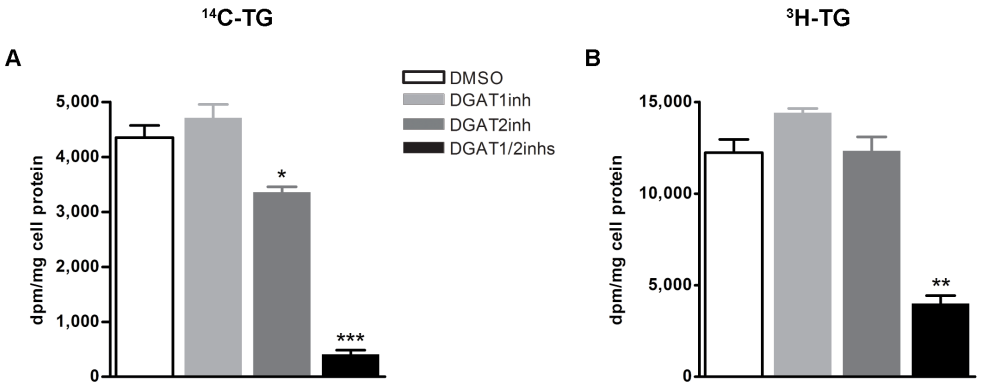

Figure 3-12. DGAT2 catalyzes re-esterification of lipolytic products from preformed TG destined for VLDL secretion. A, [^{14}C]oleic acid-labeled TG secretion. **B**, [^{3}H]oleic acid-labeled TG secretion. Secreted [^{14}C]TG was derived from preformed TG pools, whereas [^{3}H]TG was derived from newly synthesized TG.

3.2.7 DGAT1 and DGAT2 Regulate VLDL Secretion Similarly in Human and Mouse Hepatocytes.

While mouse hepatocytes secrete apoB48 and apoB100 lipoproteins, human hepatocytes secrete lipoproteins containing only apoB100, because apoB100 lacks APOBEC-1, the catalytic component of the *apoB* mRNA-editing complex. Studies in the HepG2 hepatoma cell line showed the length of the apoB molecule was proportional to the nascent lipoprotein core circumference,[215] thus determining lipoprotein sizes and compositions, which may also correlate to different metabolic fates and rates. Therefore, the presence of apoB48 and apoB100 on VLDL particles secreted from mouse hepatocytes adds a layer of complexity to the interpretation of lipoprotein metabolism. In light of this knowledge, I used human primary hepatocytes to further investigate DGAT1 and DGAT2 functions in VLDL secretion. I found that similar to mouse hepatocytes, DGAT2 in primary human hepatocytes was more important for VLDL maturation than DGAT1, since inhibition of DGAT2 alone significantly diminished TG secretion (Figure 3-13A). Moreover, a combination of both DGAT inhibitors nearly abrogated secretion of TG synthesized *de novo* from acetic acid (Figure 3-13A). I could not analyze the secretion of oleic acid-derived TG in human hepatocytes upon simultaneous inhibition of both DGATs owing to massive cell death under this particular circumstance, likely due to the toxic effects of excess free FA. Interestingly, different from mouse hepatocytes, extracellular apoB100 levels were invariable in acetate-supplemented human hepatocytes even when both DGATs were inhibited (Figure 3-13B). Based on lipoprotein density analysis, inhibition of DGAT2 or both DGATs decreased the buoyant density of apoB100-bound lipoproteins in human hepatocytes, similar to mouse

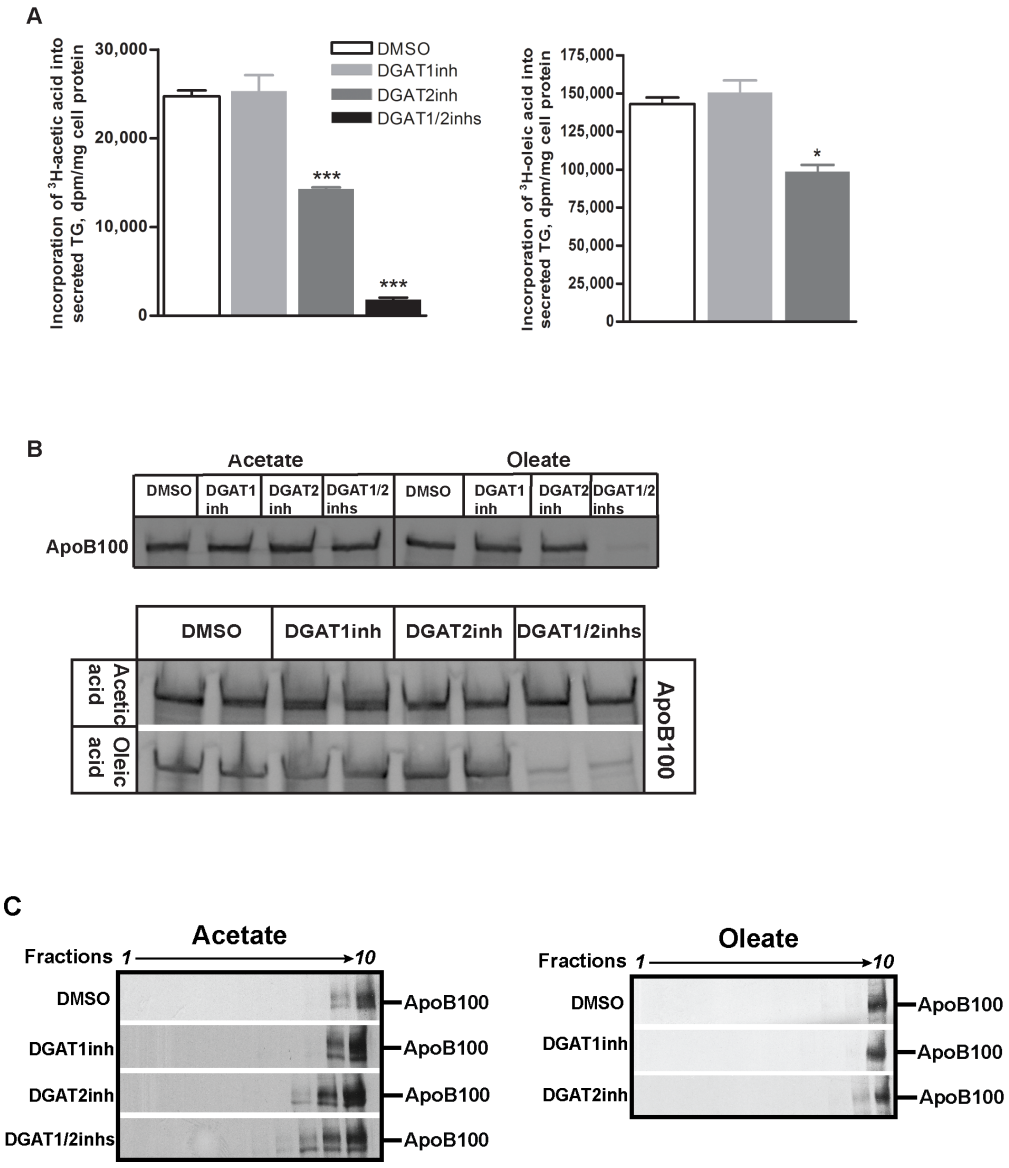

Figure 3-13. DGAT1 and DGAT2 regulate VLDL secretion similarly in human and mouse hepatocytes. Human hepatocytes were incubated in DMEM containing 10 μCi [^{3}H]acetic acid and 50 μM acetate, or 5 μCi [^{3}H]oleic acid and 0.4 mM oleate/0.5%BSA for 4 h (Pulse). Cells were then washed and incubated in DMEM for additional 4 h (Chase). DGAT1 and DGAT2 inhibitors were added to human hepatocytes in both the Pulse and Chase periods. Media were harvested and analyzed for TG and apoB secretion. **A**, Secretion of TG synthesized from [^{3}H]acetic acid (left) or [^{3}H]oleic acid (right). **B**, Immunoblot analysis of extracellular apoB100 levels. **C**, [^{35}S]Met/Cys-labeled extracellular apoB100 of lipoproteins with densities increasing from Fraction 10 to 1. Statistical data are presented as mean ± SEM. *P<0.05, ***P<0.001 versus control (DMSO) based on three independent biological replicates.

hepatocytes (Figure 3-13C). In conclusion, in human hepatocytes, we observed equivalent phenomena as in mouse hepatocytes with respect to the contribution of the two DGATs to VLDL-TG secretion in that DGAT2 was required for TG secretion, on which DGAT1 had a small additive effect. However, extracellular apoB100 levels remained constant even when both DGATs were inactivated.

3.3 Summary and Discussion

In this study I investigated the roles of DGAT1 and DGAT2 in lipid metabolism and VLDL secretion in primary mouse and human hepatocytes by inactivation of DGAT1 and DGAT2 with specific small molecule inhibitors alone or in combination. I found that in mouse hepatocytes, DGAT1 and DGAT2 can compensate for each other to synthesize TG, but the TG pool generated by DGAT1 was preferably used for supplying substrates for oxidation, whereas TG synthesized by DGAT2 was preferentially used for secretion in VLDL. Inhibition of DGAT2 or both DGATs resulted in accumulation of *sn*-1,2-DG that was diverted to various GPL species that also possessed distinct preferences for FA origins. Inhibition of DGAT2 (TG synthesized through DGAT1) significantly increased PC synthesis and slightly decreased TG synthesis from exogenous oleic acid and led to the formation of smaller LDs. On the contrary, inactivation of DGAT1 (TG synthesized by DGAT2) promoted LD expansion. The different impacts of DGAT1 and 2 on LD morphology in primary mouse hepatocytes are in good agreement with studies in McA cells, where overexpression of *Dgat1* led to the formation of small LDs around the cell periphery, whereas large LDs were more frequently observed in *Dgat2*-expressing cells.[118] In all, these results demonstrate a conserved role for DGATs in regulating LD size.

Inhibition of DGAT2 impaired lipogenic gene expression possibly through diminished nuclear presence of transcriptionally active mature SREBP1c. Finally, DGAT2, but not DGAT1, is required for re-esterification of lipolysis-derived DG to support VLDL maturation (lipidation). However, extracellular apoB content did not change in DGAT2-inactivated cells, indicating that similar numbers of lipoprotein particles were secreted but these particles were less lipidated. Importantly, the dominant role of DGAT2 in VLDL maturation was confirmed in primary human hepatocytes.

Previous studies reported discordant interpretations of results on the distinct contributions of DGATs to VLDL maturation, which may stem from the use of different animal and cellular models, dose and time course of virus injection and other experimental variables. First, some studies showed that adenovirus-mediated *Dgat1* overexpression in mice resulted in increased latent DGAT activity and a dilated ER, leading to enlarged VLDL with increased TG content.[216] This observation is in agreement with studies in McA cells where overexpression of human *Dgat1* increased secretion of TG-enriched VLDL.[217] However, other studies reported that while short-term overexpression of *Dgat1* or *Dgat2* resulted in increased hepatic TG mass, the rate of VLDL production was not affected.[218] Notably, an important role of DGAT1 was reported in the re-esterification of partial glycerides with exogenously derived FA, while DGAT2 was proposed to have limited effects on re-esterification.[114,219] However, these studies used the HepG2 hepatoma cell line, which has been shown to be deficient in the use of preformed TG for VLDL assembly, possibly due to the absence of lipases, such as carboxylesterase 1d/TGH and arylacetamide deacetylase.[188-190,210,220,221] Second, *Dgat1*-deficient mice fed a high-fat diet presented with much lower hepatic TG stores but normal plasma TG concentration when compared with

wild-type control mice,[125] and DGAT1 was found not to be essential for chylomicron formation in mice, as genetic ablation of *Dgat1* accumulated TG in large LDs of enterocytes and chylomicron-sized particles in the lumen of the ER and Golgi apparatus; albeit chylomicron secretion was delayed.[129] On the other hand, *Dgat2*-deficient mice had a very low plasma TG concentration immediately after birth,[138] which suggests an impairment in VLDL secretion; however, a liver-specific *Dgat2*$^{-/-}$ mouse model would be required to further test the role of DGAT2 in hepatic TG metabolism.

Another important question is the substrate preference of the two DGATs. Oleic acid supplementation mimics FA released from adipose tissue or circulating lipoproteins, while *de novo* synthesized FA from acetate represents carbohydrate metabolism. Both sources of FA can be esterified into TG for storage or packaged into VLDL particles for secretion. Though previous studies showed preference of DGAT2 for *de novo* synthesized FA as a substrate for TG production,[114,139] we did not observe any significant differences between DGAT1 and DGAT2 with respect to using endogenously (acetate) or exogenously (oleate) derived FA for TG synthesis or secretion.

Interestingly, inhibition of DGAT2 reduced the mature form of SREBP1 in the nucleus, which led to the decreased transcription of several lipogenic genes including *Acaca*, *Fasn*, *Scd1* and *Srebf1c* itself, while inhibition of DGAT1 had no effect on lipogenesis. A role for DGAT2 in the regulation of *de novo* FA synthesis was reported in HeLa cells where SCD1 was found to physically interact with DGAT2, thereby providing a pool of monounsaturated fatty acids for TG biosynthesis.[123] Because increased *Srebf1c* expression and FA synthesis in the liver contribute to the development of steatosis in rodent models of insulin-

resistance and obesity,[222] DGAT2 might be an excellent therapeutic target to alleviate lipid metabolic disorders. This potential pharmacological intervention is also supported by studies where attenuation of *Dgat2* expression in obese mice by ASO was shown to improve insulin resistance, steatosis and hyperlipidemia.[140,204] Notably, in our study, although DGAT2 inhibition significantly decreased TG secretion, VLDL particle numbers was not affected, resulting in less buoyant VLDL. As a consequence, this smaller and denser VLDL appears more like LDL, which is proportional to the levels of "bad cholesterol", and highly atherogenic.

Inhibition of both DGAT1 and DGAT2 activities resulted in extensive cellular death of primary human hepatocytes supplemented with oleic acid and followed by prolonged (>12 h) Chase. Cell death could be possibly due to excess free FA that might have accumulated in the ER as a result of not being able to be (re)esterified to TG for storage or secretion. Excess free FA elicits profound changes in ER membrane phospholipids, which is followed by ER deformation and leakage of protein-folding chaperones to the cytosol.[223,224] In addition, alterations in mitochondrial membrane PL and activation of NADPH oxidase by DG through protein kinase C-dependent pathways produce reactive oxygen species, release cytochrome c and result in mitochondrial dysfunction.[225]

Currently, it is not clear how the cytosolic topology of the DGAT2 active site 6contributes to VLDL assembly. ER-localized DGAT2 should contribute only to the overt DGAT activity. However, pharmacological inhibition of DGAT2 by Niacin decreased both overt and latent DGAT activities by 30%.[226] Highly conserved motifs of DGAT2 (YFP and HPHG) residing in the ER lumen or membrane, respectively, play essential roles in the enzyme is catalysis.[227]

Therefore, integration of DGAT1 and DGAT2 function with their topologies requires further experimentation. A working model of the contributions of DGAT1 and DGAT2 to lipid metabolism in hepatocytes is presented in Figure 3.14.

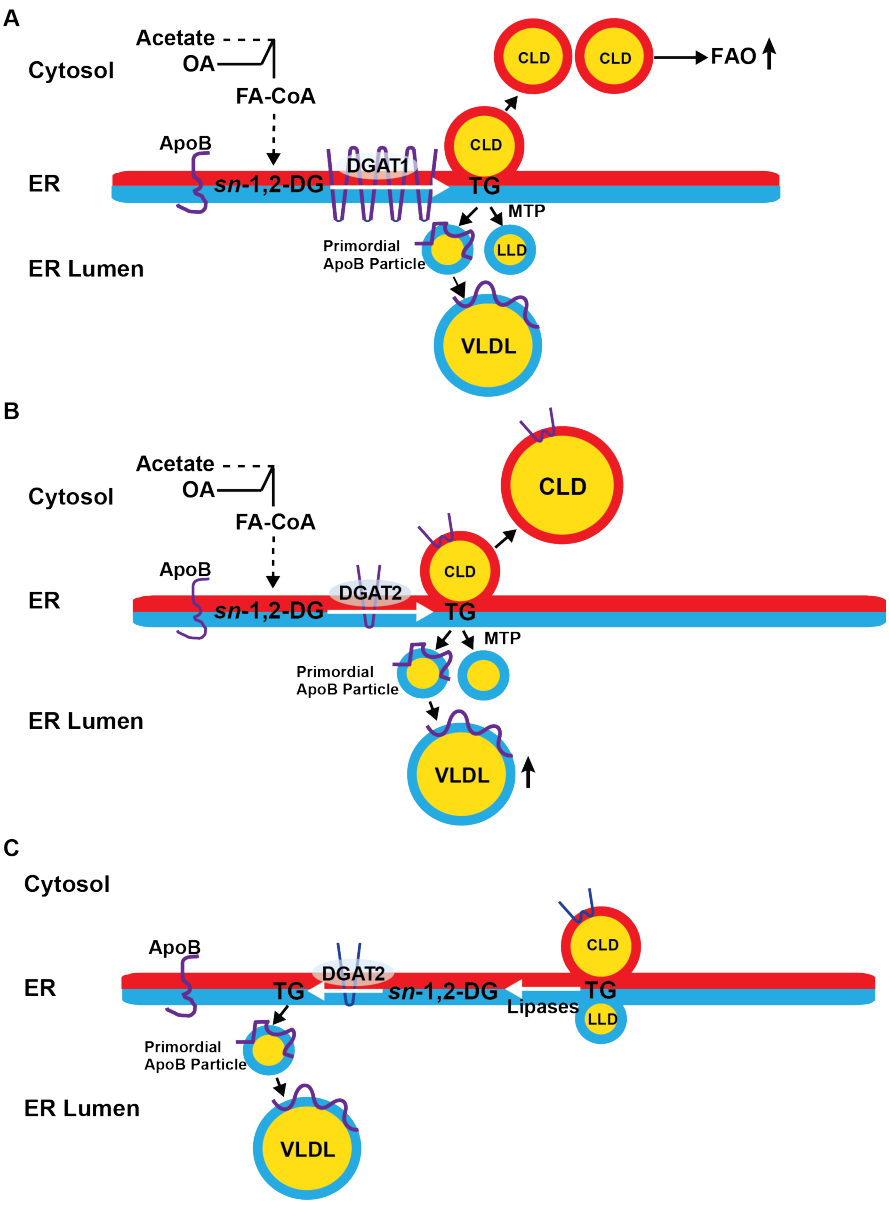

Figure 3-14. A working model illustrating the contributions of DGAT1 and DGAT2 to TG metabolism in hepatocytes. DGAT1 and DGAT2 can compensate for each other to synthesize TG from FA made *de novo* (acetate) or exogenously supplied (oleate). **A**, DGAT1 is a polytopic ER membrane protein. LDs incorporating DGAT1-generated TG are efficiently used for supplying substrates for FA oxidation, and are less capable of expansion. **B**, DGAT2 intercalates into the ER phospholipid bilayer and CLD phospholipid monolayer via a long hydrophobic region. TG synthesized by DGAT2 preferentially contributes to VLDL assembly. CLD-bound DGAT2 catalyzes LD expansion. **C**, DGAT2 is required for VLDL maturation (lipidation) by catalyzing re-esterification of DG originating from lipolysis of pre-existing TG pools. Abbreviations: CLD, cytosolic lipid droplet; FAO, fatty acid oxidation; LLD, lumenal lipid droplet; MTP, microsomal triglyceride transfer protein.

CHAPTER IV FUTURE PERSPECTIVES

4.1 The Relationship between DGATs and ER-Localized Lipases

VLDL assembly has been proposed to occur in two distinct steps: the first step is the co-translational and co-translocational lipidation of apoB to form a primordial apoB particle, and the second is to further lipidate it to generate mature secretion-competent VLDL. The post-translational lipidation of apoB during the second step of VLDL maturation was experimentally verified, as TG-rich VLDL appeared in the lumen of microsomes about 15 min after apoB synthesis.[228]

The first step requires a ER lumenal protein, MTP, that transfers TG present within the ER to lipid-free apoB. The location of the second step remains controversial. Some kinetic studies found the rates of TG and apoB movement within Golgi cisternae were different,[229] lipoprotein diameters seemed to increase during transit through *cis* and *trans* Golgi stacks, and no visible lipoprotein particles were detected by transmission electron microscopy in the ER of McA cells, suggesting Golgi-localized lipid acquisition during VLDL maturation.[228] However, by trapping apoB100 lipoproteins in subcellular organelles with different inhibitors of vesicular transport, followed by subcellular fractionation, another group suggested it is in the ER and not in the Golgi of McA cells that the poorly lipidated lipoproteins are converted to TG-rich VLDL.[230] Moreover, considering that the majority of TG assembled into secretion-competent VLDL is derived from the hydrolysis-re-esterification cycle, and hydrolysis relies on ER-localized lipases such as TGH and arylacetamide deacetylase,[186,189-192] it remains unexplained as to from where the substrates for TG resynthesis would come in the Golgi-localized lipidation model. In our study, we found DGAT2 played the

predominant role in VLDL secretion. DGAT2 has been reported to localize on the ER and on the surface of cytosolic LDs in certain cell models. Based on the potential correspondence in subcellular localization between DGAT2 and the ER-localized lipases, I postulate that DGAT2 may function downstream of TGH or other uncharacterized ER-localized lipases, and esterify the lipolytic products for VLDL assembly.

In order to test this hypothesis, I performed some preliminary experiments. First, to examine if DGAT2 catalyzes the re-esterification of DG substrates derived from TGH, I treated *Tgh*-global knockout primary mouse hepatocytes with DGAT inhibitors under the same protocol laid out in Figure 3-10A. If TGH acts upstream of DGAT2, hydrolyzing preformed TG to provide substrates for DGAT2, then inactivation of DGAT2 in the absence of TGH should not lead to further decrease in TG secretion. However, DGAT2 inhibitor efficiently dampened TG secretion in TGH-deficient mouse hepatocytes just as it did in wild-type hepatocytes (Figure 4-1A). Furthermore, DGAT1 inhibitor exerted an additive effect on TG secretion, similar to what was observed in wild-type hepatocytes (Figure 4-1A). This initial test appeared to rule out the possibility that TGH is the executive enzyme upstream of DGAT2; other lipases may be involved in hydrolyzing preformed TG to supply substrates for DGAT2-catalyzed TG resynthesis for VLDL secretion.

Therefore, to demonstrate the potential existence of other lipases, we treated wild-type mouse hepatocytes with DGAT inhibitors in combination with a pan-lipase inhibitor, diethyl-p-nitrophenylphosphate (E600) that specifically and irreversibly reacts with the catalytic serine residue of almost all known esterases/lipases.[231] As a result, although E600 alone dramatically attenuated TG

secretion, simultaneous addition of DGAT2 inhibitor appeared to reduce further TG secretion (Figure 4-1B). However, no definite conclusion could be made based on the current data, as the difference between E600 alone and E600 together with DGAT2 inhibitor was not statistically significant. Moreover, DGAT1 inhibitor failed to exert any additional negative effects on TG secretion (Figure 4-1B), possibly due to limitations of measurement. Alternatively, the residual amount of radioactivity (~8000 dpm/mg cell protein) upon treatment of two DGAT inhibitors and E600 might imply other pathways for VLDL maturation independent of the hydrolysis-re-esterification cycle.

To test whether the limitations lie in the measurement, mouse hepatocytes were treated with serial doses of Golgicide A (GCA), an inhibitor of Golgi maintenance and bidirectional trafficking. The expected results were that the highest dose (10 μM) of GCA would eliminate secretory trafficking, thus abrogating VLDL secretion. Indeed, 10 μM of GCA was sufficient to abolish TG secretion in McA cells, and the background amount of radioactivity was around 800 dpm/mg cell protein (Figure 4-2C), about 10-fold less than that upon treatment with a combination of two DGAT inhibitors and E600, thus ruling out the limitation imposed by the methodology.

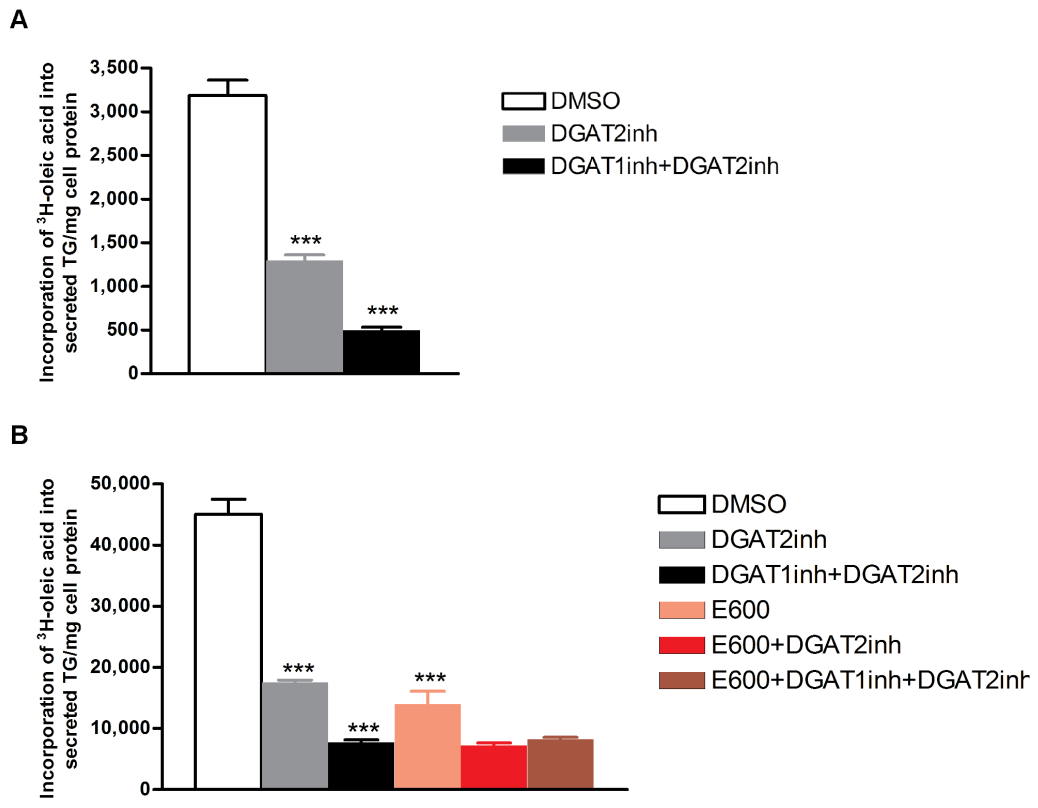

Figure 4-1. Potential lipases that hydrolyze preformed TG to supply substrates for DGAT2. Primary hepatocytes from **A,** *Tgh*$^{-/-}$ and **B,** wild type mice were incubated with [^{3}H]-oleic acid for 4 h, followed by another 4 h-treatment with vehicle (DMSO) or experimental drugs as indicated in the figure legends. The amounts of radioactivity incorporated into secreted TG were measured, and normalized to cellular protein mass. Data are presented as mean ± SEM. ***P<0.001 versus control (DMSO) based on three independent biological replicates.

4.2 Arf/COPI Machinery Modulates Cytosolic LD Turnover And VLDL Secretion in McA Cells

Hepatic TG, once synthesized, is distributed into three types of LDs: cytosolic LDs, ER lumenal LDs and primordial apoB particles that subsequently mature into secretion-competent VLDL. Directionality of TG transport into the cytosol or the ER lumen is probably regulated by LD-coat proteins, such as perilipins, and ER-localized proteins involved in TG transfer, LD biogenesis and accumulation, such as MTP. Cytosolic and lumenal LDs differ significantly in their associated proteins and lipid compositions. Lumenal LDs exhibit a lower ratio of TG to PL , suggesting relatively small size on average compared to cytosolic LDs.[209] Gel filtration chromatography and agarose gel electrophoresis analysis also revealed that these apoB-free lipid particles are heterogeneous with sizes ranging from HDL (8 nm) to VLDL (>50 nm), suggesting different stages of biogenesis and metabolism.[209] Interestingly, MTP was highly concentrated with small-size lumenal LDs, while apoE was dominantly associated with large ones, and TGH presented in fractions of various sizes, but particularly enriched in medium-sized lumenal LDs.[209] Moreover, MTP and apoE, but not TGH, were also found in the apoB-containing lumenal lipoproteins.[209] Substantial evidence has demonstrated the indispensable role of MTP in VLDL assembly and non-apoB lumenal LD formation.[48,176,232,233] Genetic ablation of apoE in mice resulted in TG accumulation in the liver with impaired VLDL secretion.[234-236] All this information implies an intimate relationship between apoB-free lumenal LDs and apoB-containing lipoproteins, and lumenal LDs may provide lipid substrates for VLDL assembly, though the cellular mechanisms are unclear.[153]

On the other hand, considering the lipid storage capacity within the ER lumen is relatively limited when compared to cytosolic LDs (Figure 3-7), and lipids stored in the cytosol and ER lumen of hepatocytes are in a constant dynamic interchange,[209,210], and a variety of cytosolic LD-associated proteins such as perilipin 2, CIDEB and ABHD5, affect VLDL secretion,[177-181,237] I hypothesized that cytosolic LDs may also supply TG substrates for VLDL secretion. However, VLDL assembly appears to be independent of lipolysis by cytosolic lipases, such as ATGL or hormone-sensitive lipase, because hepatic overexpression or deletion of these lipases did not influence VLDL secretion.[183,185,214] Transfer of bilayer-disrupting hydrophobic TG from cytosolic LDs *en bloc* across the ER membrane would be energetically unfavourable. In contrast, DG is a non-ionic amphiphilic molecule with an unesterified hydroxyl group as the small hydrophilic head and two acyl chains as the lipophilic tails. DG is highly motile within membranes and functions as a fluidifier and cosurfactant of PL to decrease surface tension.[150] Therefore, cytosolic TG may be hydrolyzed by ER-localized lipases, and the resulting DG is then re-esterified by DGAT2 to TG used for VLDL assembly. Notably, TGH, localized to ER lumen, has been demonstrated to regulate VLDL secretion, and may function as a lipase to mobilize preformed stored TG.[186,189,190] However, the mechanisms of how cytosolic LDs connect to the ER to supply TG substrates for ER-localized lipases are largely unknown. Recent studies have shown that the Arf1/COPI machinery can bud LDs of nano-scales from PL-covered oil/water interfaces *in vitro*.[121] *In vivo* studies in *Drosophila* S2 cells and mammalian NRK cells have found the Arf1/COPI complex to be localized on cellular LDs, and confirmed the Arf1/COPI-dependent formation and segregation of nano-LDs from existing LDs.[120] These nano-LDs exhibited a high surface (PL) to volume (neutral lipids) ratio, partitioning of which led to decreased amounts of

PL on their parent LDs. Because PL function as a surfactant to stabilize LD emulsions, depletion of them results in higher surface tension of the parent-LDs and a propensity of these PL-deficient LDs to hemi-fuse and form bridges with the ER.[120] These ER-LD bridges were required for LD targeting of some enzymes involved in TG synthesis and metabolism, such as ATGL, GPAT4 and DGAT2.[120]

To extend this study further, I proposed that the Arf1/COPI complex-triggered LD-ER membrane junctions to enable cytosolic TG translocation into the ER lumen. Inhibition of the Arf1/COPI machinery may prevent cytosolic LDs from contacting ER membranes, thus blocking cytosolic TG supply to VLDL assembly. In order to examine this hypothesis, GCA was used to selectively inhibit GBF1, a guanine nucleotide exchange factor of Arf, thus restricting Arf in its GDP-bound inactive form. Arf-GDP dissociates from membranes and is unable to recruit heptameric COPI complex to bud coated vesicles.[238] The key is to determine a concentration of GCA that inhibits the Arf1/COPI-mediated nano-LD budding and thus the LD-ER linkage without affecting Golgi integrity and normal membrane trafficking and secretory pathways. McA cells stably transfected with a FLAG-tagged secretory protein (hepatic lipase) were employed to determine a specific concentration of GCA that could potentially decrease apoB and VLDL-TG secretion, while maintaining FLAG-tagged hepatic lipase secretion. GCA was introduced in a Chase period after a 4 h-incubation with oleic acid (Pulse), and four different concentrations of GCA (0, 1, 5 and 10 μM) were tested in McA cells expressing FLAG-tagged hepatic lipase. The experimental procedure is presented in Figure 4-2A. Results show that only at a concentration of 5 μM of GCA was the apoB secretion drastically decreased and a normal secretory pathway maintained (Figure 4-2B). Moreover, TG secretion was remarkably reduced at 5 μM of GCA (Figure 4-2C), while cellular TG levels remained

unchanged (Figure 4-2D). Surprisingly, the preformed intracellular TG was significantly decreased upon treatment with 10 μM of GCA (Figure 4-2D).

To further confirm that the Golgi apparatus was intact from a morphological point of view, the Golgi was visualized by immunostaining with a polyclonal antibody against mannosidase II, a key enzyme in *N*-glycan processing, essentially localized on the Golgi membrane. McA cells stably transfected with FLAG-hepatic lipase were incubated with oleic acid for 4 hours, followed by GCA treatments under the same protocol as shown in Figure 4-2A. As a result, no obvious changes were observed with respect to Golgi morphology after treatment with 1 or 5 μM GCA compared to that of 0 μM GCA; in constrast, 10 μM GCA seemed to collapse the Golgi, as no recognizable juxta-nuclear signal was detected. Representative images are shown in Figure 4-3. The images support previous functional studies, as 10 μM of GCA also abolished normal secretory transport of FLAG-hepatic lipase. LDs were counterstained with Bodipy 493/503, exhibiting comparable morphologies in the absence or presence of 1 or 5 μM of GCA during the Chase period; cells treated with 10 μM of GCA might exhibit decreased LD numbers (Figure 4-3). Statistical analysis would be required to confirm the morphological changes of the Golgi and LDs.

In conclusion, I found inhibition of the Arf1/COPI machinery by 5 μM of GCA in McA cells drastically decreased apoB and TG secretion, while maintaining a normal Arf1/COPI-dependent secretory pathway and the integrity of Golgi apparatus. Our next step is to demonstrate the Arf1/COPI complex is required to establish a connection between cytosolic LD and the ER, through which TG molecules stored in the cytosol of hepatocytes could be translocated into the ER lumen and mobilized to supply substrates for VLDL assembly. Technically, ER-

LD bridges could be visualized by ultrathin section electron microscopy. The majority of cytosolic LDs is expected to dislodge from the ER membrane at a certain concentration (5 μM) of GCA. Moreover, in section 3.2.5, we demonstrated that DGAT1 and DGAT2 generated66 separate LD pools that were preferentially utilized for distinct metabolic pathways, either for oxidation or secretion, respectively. Thus it would be interesting to further investigate whether the Arf1/COPI complex mediates an ER junction with both DGAT1- and DGAT2-derived pools of cytosolic LDs and if so, whether the Arf1/COPI complex can distinguish between these two pools of cytosolic LDs for differential metabolic uses. To answer these questions, individual DGAT inhibitors combined with serial doses of GCA could be applied during TG synthesis in hepatocytes, and FA oxidation and VLDL secretion could be analyzed. The idea is to form LDs via one form of DGATs, and test how inhibition of the Arf1/COPI machinery would affect their metabolism.

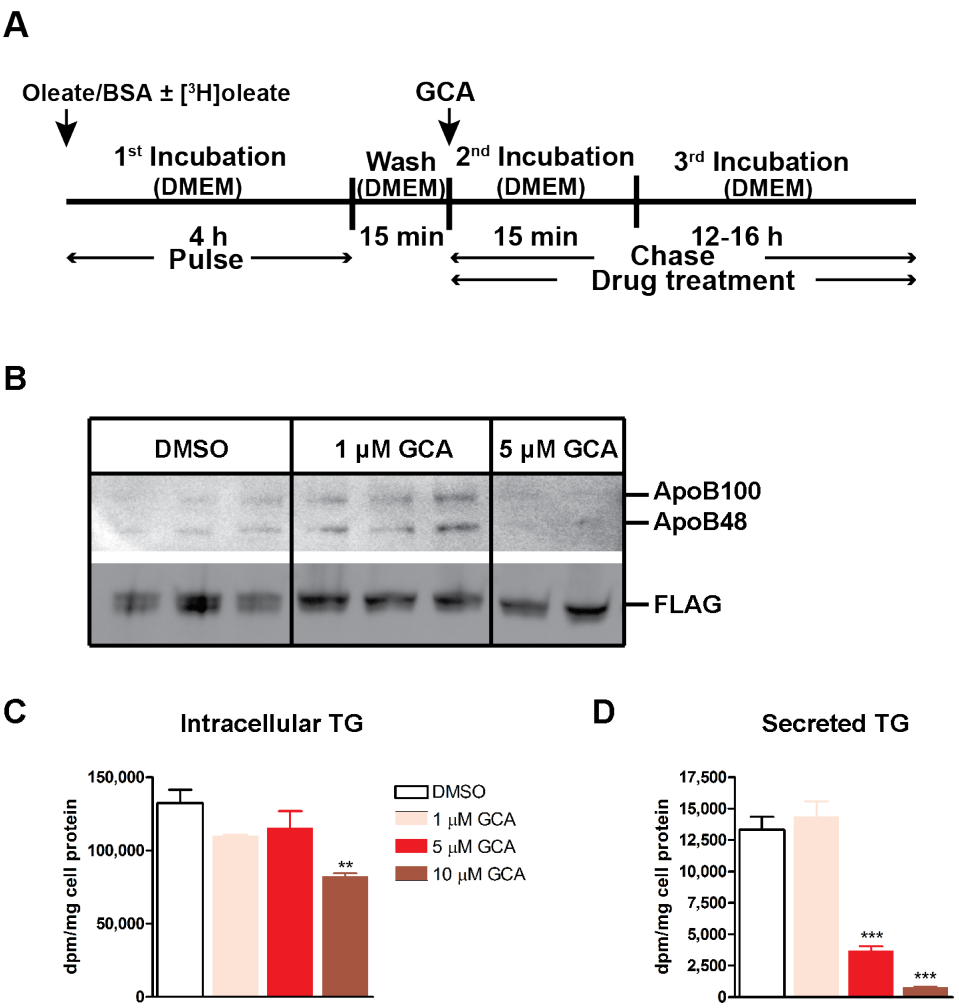

Figure 4-2. GCA at 5 μM concentration impaires VLDL secretion but not normal secretory pathways in McA cells. McA cells stably transfected with FLAG-tagged hepatic lipase were incubated with oleate/BSA for 4 h, or in the radioisotope labeling experiment, with oleate/BSA and [^{3}H]-oleate. Cells were then washed and chased with GCA overnight (12-16 h) after a short period of preincubation. The experimental procedure is laid out in panel **A. B,** Immunoblotting against apoB and FLAG in the medium. Total proteins were precipitated by TCA. **C,** The amounts of radioactivity incorporated into intracellular and secreted TG were measured, and normalized to cellular protein mass. Data are presented as mean ± SEM. **P<0.01, ***P<0.001 versus control (DMSO) based on three independent biological replicates.

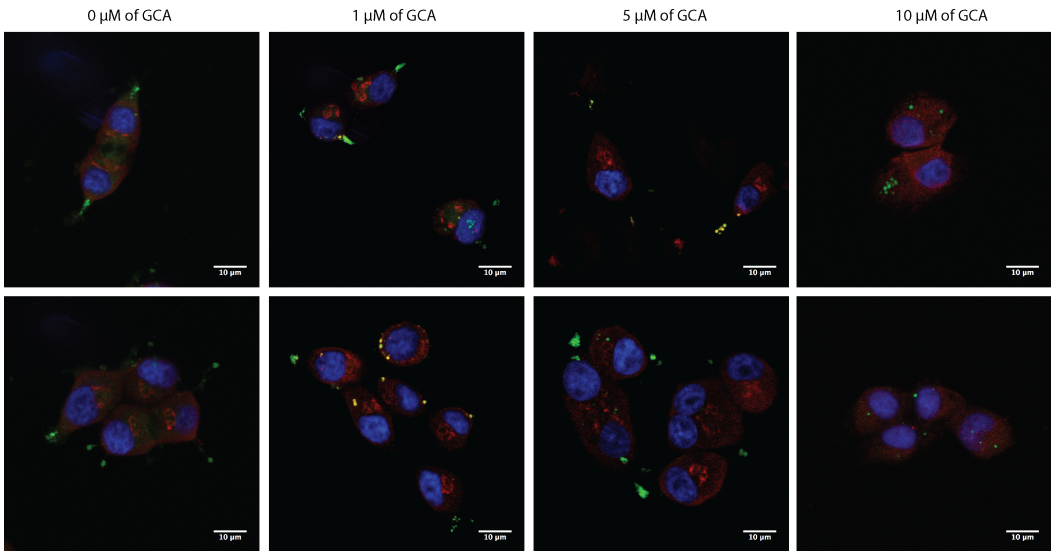

Figure 4-3. Golgi morphology upon treatment with GCA at different concentrations. McA cells stably transfected with FLAG-tagged hepatic lipase were treated as illustrated in Figure 4-2A. Two representative images in each condition are shown. Localization of the Golgi membrane protein α-Mannosidase II is revealed in red color following immunostaining. Lipid droplets were stained with Bodipy 493/503, and shown in green color. Nuclei were stained with DAPI, and shown in blue. Z-stacks were collected and displayed as projections. Each image contains ~10 slices, 0.1 µm per slice, scale bar=10 µm.

REFERENCES

1. Despres JP, Moorjani S, Lupien PJ, Tremblay A, Nadeau A, Bouchard C. Regional distribution of body fat, plasma lipoproteins, and cardiovascular disease. *Arteriosclerosis*. Jul-Aug 1990;10(4):497-511.
2. Kissebah AH, Krakower GR. Regional adiposity and morbidity. *Physiological reviews*. Oct 1994;74(4):761-811.
3. Gil-Campos M, Canete RR, Gil A. Adiponectin, the missing link in insulin resistance and obesity. *Clinical nutrition*. Oct 2004;23(5):963-974.
4. Barnett AH, Kumar S. Obesity and diabetes (2nd ed.). Chichester, West Sussex, U.K.: Wiley-Blackwell. 2009.
5. Abdul-Ghani MA, DeFronzo RA. Pathogenesis of insulin resistance in skeletal muscle. *Journal of biomedicine & biotechnology*. 2010;2010:476279.
6. DeFronzo RA, Gunnarsson R, Bjorkman O, Olsson M, Wahren J. Effects of insulin on peripheral and splanchnic glucose metabolism in noninsulin-dependent (type II) diabetes mellitus. *The Journal of clinical investigation*. Jul 1985;76(1):149-155.
7. DeFronzo RA, Tripathy D. Skeletal muscle insulin resistance is the primary defect in type 2 diabetes. *Diabetes care*. Nov 2009;32 Suppl 2:S157-163.
8. Thiebaud D, Jacot E, DeFronzo RA, Maeder E, Jequier E, Felber JP. The effect of graded doses of insulin on total glucose uptake, glucose oxidation, and glucose storage in man. *Diabetes*. Nov 1982;31(11):957-963.
9. Shulman GI. Cellular mechanisms of insulin resistance. *The Journal of clinical investigation*. Jul 2000;106(2):171-176.
10. Cusi K, Maezono K, Osman A, et al. Insulin resistance differentially affects the PI 3-kinase- and MAP kinase-mediated signaling in human muscle. *The Journal of clinical investigation*. Feb 2000;105(3):311-320.
11. Krook A, Bjornholm M, Galuska D, et al. Characterization of signal transduction and glucose transport in skeletal muscle from type 2 diabetic patients. *Diabetes*. Feb 2000;49(2):284-292.
12. Yu C, Chen Y, Cline GW, et al. Mechanism by which fatty acids inhibit insulin activation of insulin receptor substrate-1 (IRS-1)-associated phosphatidylinositol 3-kinase activity in muscle. *The Journal of biological chemistry*. Dec 27 2002;277(52):50230-50236.
13. Chavez JA, Holland WL, Bar J, Sandhoff K, Summers SA. Acid ceramidase overexpression prevents the inhibitory effects of saturated fatty acids on insulin signaling. *The Journal of biological chemistry*. May 20 2005;280(20):20148-20153.
14. Itani SI, Ruderman NB, Schmieder F, Boden G. Lipid-induced insulin resistance in human muscle is associated with changes in diacylglycerol, protein kinase C, and IkappaB-alpha. *Diabetes*. Jul 2002;51(7):2005-2011.
15. Summers SA. Ceramides in insulin resistance and lipotoxicity. *Progress in lipid research*. Jan 2006;45(1):42-72.
16. Hirosumi J, Tuncman G, Chang L, et al. A central role for JNK in obesity and insulin resistance. *Nature*. Nov 21 2002;420(6913):333-336.
17. Petersen KF, Dufour S, Befroy D, Garcia R, Shulman GI. Impaired mitochondrial activity in the insulin-resistant offspring of patients with type 2 diabetes. *The New England journal of medicine*. Feb 12 2004;350(7):664-671.

18. Solinas G, Naugler W, Galimi F, Lee MS, Karin M. Saturated fatty acids inhibit induction of insulin gene transcription by JNK-mediated phosphorylation of insulin-receptor substrates. *Proceedings of the National Academy of Sciences of the United States of America*. Oct 31 2006;103(44):16454-16459.
19. Tan CY, Vidal-Puig A. Adipose tissue expandability: the metabolic problems of obesity may arise from the inability to become more obese. *Biochemical Society transactions*. Oct 2008;36(Pt 5):935-940.
20. Miyazaki Y, Mahankali A, Matsuda M, et al. Improved glycemic control and enhanced insulin sensitivity in type 2 diabetic subjects treated with pioglitazone. *Diabetes care*. Apr 2001;24(4):710-719.
21. Bullen JW, Jr., Bluher S, Kelesidis T, Mantzoros CS. Regulation of adiponectin and its receptors in response to development of diet-induced obesity in mice. *American journal of physiology. Endocrinology and metabolism*. Apr 2007;292(4):E1079-1086.
22. Considine RV, Sinha MK, Heiman ML, et al. Serum immunoreactive-leptin concentrations in normal-weight and obese humans. *The New England journal of medicine*. Feb 1 1996;334(5):292-295.
23. Flier JS. Diabetes. The missing link with obesity? *Nature*. Jan 18 2001;409(6818):292-293.
24. Yadav A, Kataria MA, Saini V, Yadav A. Role of leptin and adiponectin in insulin resistance. *Clinica chimica acta; international journal of clinical chemistry*. Feb 18 2013;417:80-84.
25. Yamauchi T, Kamon J, Waki H, et al. The fat-derived hormone adiponectin reverses insulin resistance associated with both lipoatrophy and obesity. *Nature medicine*. Aug 2001;7(8):941-946.
26. Alberti KG, Zimmet P, Shaw J, Group IDFETFC. The metabolic syndrome--a new worldwide definition. *Lancet*. Sep 24-30 2005;366(9491):1059-1062.
27. Fabbrini E, Sullivan S, Klein S. Obesity and nonalcoholic fatty liver disease: biochemical, metabolic, and clinical implications. *Hepatology*. Feb 2010;51(2):679-689.
28. Farrell GC, van Rooyen D, Gan L, Chitturi S. NASH is an Inflammatory Disorder: Pathogenic, Prognostic and Therapeutic Implications. *Gut and liver*. Apr 2012;6(2):149-171.
29. Sheth SG, Gordon FD, Chopra S. Nonalcoholic steatohepatitis. *Annals of internal medicine*. Jan 15 1997;126(2):137-145.
30. Henao-Mejia J, Elinav E, Jin C, et al. Inflammasome-mediated dysbiosis regulates progression of NAFLD and obesity. *Nature*. Feb 9 2012;482(7384):179-185.
31. Day CP, James OF. Steatohepatitis: a tale of two "hits"? *Gastroenterology*. Apr 1998;114(4):842-845.
32. Sanyal AJ, Campbell-Sargent C, Mirshahi F, et al. Nonalcoholic steatohepatitis: association of insulin resistance and mitochondrial abnormalities. *Gastroenterology*. Apr 2001;120(5):1183-1192.
33. Pardina E, Baena-Fustegueras JA, Catalan R, et al. Increased expression and activity of hepatic lipase in the liver of morbidly obese adult patients in relation to lipid content. *Obesity surgery*. Jul 2009;19(7):894-904.
34. Westerbacka J, Kolak M, Kiviluoto T, et al. Genes involved in fatty acid partitioning and binding, lipolysis, monocyte/macrophage recruitment,

and inflammation are overexpressed in the human fatty liver of insulin-resistant subjects. *Diabetes*. Nov 2007;56(11):2759-2765.
35. Fabbrini E, Magkos F, Mohammed BS, et al. Intrahepatic fat, not visceral fat, is linked with metabolic complications of obesity. *Proceedings of the National Academy of Sciences of the United States of America*. Sep 8 2009;106(36):15430-15435.
36. Greco D, Kotronen A, Westerbacka J, et al. Gene expression in human NAFLD. *American journal of physiology. Gastrointestinal and liver physiology*. May 2008;294(5):G1281-1287.
37. Donnelly KL, Smith CI, Schwarzenberg SJ, Jessurun J, Boldt MD, Parks EJ. Sources of fatty acids stored in liver and secreted via lipoproteins in patients with nonalcoholic fatty liver disease. *The Journal of clinical investigation*. May 2005;115(5):1343-1351.
38. Mayes PA. Intermediary metabolism of fructose. *The American journal of clinical nutrition*. Nov 1993;58(5 Suppl):754S-765S.
39. Ouyang X, Cirillo P, Sautin Y, et al. Fructose consumption as a risk factor for non-alcoholic fatty liver disease. *Journal of hepatology*. Jun 2008;48(6):993-999.
40. Chakravarthy MV, Pan Z, Zhu Y, et al. "New" hepatic fat activates PPARalpha to maintain glucose, lipid, and cholesterol homeostasis. *Cell metabolism*. May 2005;1(5):309-322.
41. Sunny NE, Parks EJ, Browning JD, Burgess SC. Excessive hepatic mitochondrial TCA cycle and gluconeogenesis in humans with nonalcoholic fatty liver disease. *Cell metabolism*. Dec 7 2011;14(6):804-810.
42. Bugianesi E, Gastaldelli A, Vanni E, et al. Insulin resistance in non-diabetic patients with non-alcoholic fatty liver disease: sites and mechanisms. *Diabetologia*. Apr 2005;48(4):634-642.
43. Kohjima M, Enjoji M, Higuchi N, et al. Re-evaluation of fatty acid metabolism-related gene expression in nonalcoholic fatty liver disease. *International journal of molecular medicine*. Sep 2007;20(3):351-358.
44. Caldwell SH, Swerdlow RH, Khan EM, et al. Mitochondrial abnormalities in non-alcoholic steatohepatitis. *Journal of hepatology*. Sep 1999;31(3):430-434.
45. Perez-Carreras M, Del Hoyo P, Martin MA, et al. Defective hepatic mitochondrial respiratory chain in patients with nonalcoholic steatohepatitis. *Hepatology*. Oct 2003;38(4):999-1007.
46. Cortez-Pinto H, Chatham J, Chacko VP, Arnold C, Rashid A, Diehl AM. Alterations in liver ATP homeostasis in human nonalcoholic steatohepatitis: a pilot study. *Jama*. Nov 3 1999;282(17):1659-1664.
47. Raabe M, Flynn LM, Zlot CH, et al. Knockout of the abetalipoproteinemia gene in mice: reduced lipoprotein secretion in heterozygotes and embryonic lethality in homozygotes. *Proceedings of the National Academy of Sciences of the United States of America*. Jul 21 1998;95(15):8686-8691.
48. Raabe M, Veniant MM, Sullivan MA, et al. Analysis of the role of microsomal triglyceride transfer protein in the liver of tissue-specific knockout mice. *The Journal of clinical investigation*. May 1999;103(9):1287-1298.

49. Cai D, Yuan M, Frantz DF, et al. Local and systemic insulin resistance resulting from hepatic activation of IKKβ and NF-κB. *Nature medicine*. Feb 2005;11(2):183-190.
50. Fessler MB, Rudel LL, Brown JM. Toll-like receptor signaling links dietary fatty acids to the metabolic syndrome. *Current opinion in lipidology*. Oct 2009;20(5):379-385.
51. Tacke F, Luedde T, Trautwein C. Inflammatory pathways in liver homeostasis and liver injury. *Clinical reviews in allergy & immunology*. Feb 2009;36(1):4-12.
52. Masaki T, Chiba S, Tatsukawa H, et al. Adiponectin protects LPS-induced liver injury through modulation of TNFα in KK-Ay obese mice. *Hepatology*. Jul 2004;40(1):177-184.
53. Stanton MC, Chen SC, Jackson JV, et al. Inflammatory Signals shift from adipose to liver during high fat feeding and influence the development of steatohepatitis in mice. *Journal of inflammation*. 2011;8:8.
54. Poirier P, Giles TD, Bray GA, et al. Obesity and cardiovascular disease: pathophysiology, evaluation, and effect of weight loss: an update of the 1997 American Heart Association Scientific Statement on Obesity and Heart Disease from the Obesity Committee of the Council on Nutrition, Physical Activity, and Metabolism. *Circulation*. Feb 14 2006;113(6):898-918.
55. Bloch S, Couderc R. [Apolipoprotein B and LDL cholesterol: which parameter(s) should be included in the assessment of cardiovascular risk?]. *Annales de biologie clinique*. Sep-Oct 1998;56(5):539-544.
56. Van Gaal LF, Mertens IL, De Block CE. Mechanisms linking obesity with cardiovascular disease. *Nature*. Dec 14 2006;444(7121):875-880.
57. Chan DC, Watts GF, Redgrave TG, Mori TA, Barrett PH. Apolipoprotein B-100 kinetics in visceral obesity: associations with plasma apolipoprotein C-III concentration. *Metabolism: clinical and experimental*. Aug 2002;51(8):1041-1046.
58. Jonkers IJ, Smelt AH, Hattori H, et al. Decreased PLTP mass but elevated PLTP activity linked to insulin resistance in HTG: effects of bezafibrate therapy. *Journal of lipid research*. Aug 2003;44(8):1462-1469.
59. Garg A. Clinical review#: Lipodystrophies: genetic and acquired body fat disorders. *The Journal of clinical endocrinology and metabolism*. Nov 2011;96(11):3313-3325.
60. Savage DB, Tan GD, Acerini CL, et al. Human metabolic syndrome resulting from dominant-negative mutations in the nuclear receptor peroxisome proliferator-activated receptor-gamma. *Diabetes*. Apr 2003;52(4):910-917.
61. Rubio-Cabezas O, Puri V, Murano I, et al. Partial lipodystrophy and insulin resistant diabetes in a patient with a homozygous nonsense mutation in CIDEC. *EMBO molecular medicine*. Aug 2009;1(5):280-287.
62. Gandotra S, Lim K, Girousse A, Saudek V, O'Rahilly S, Savage DB. Human frame shift mutations affecting the carboxyl terminus of perilipin increase lipolysis by failing to sequester the adipose triglyceride lipase (ATGL) coactivator AB-hydrolase-containing 5 (ABHD5). *The Journal of biological chemistry*. Oct 7 2011;286(40):34998-35006.
63. Gandotra S, Le Dour C, Bottomley W, et al. Perilipin deficiency and autosomal dominant partial lipodystrophy. *The New England journal of medicine*. Feb 24 2011;364(8):740-748.

64. Shackleton S, Lloyd DJ, Jackson SN, et al. LMNA, encoding lamin A/C, is mutated in partial lipodystrophy. *Nature genetics*. Feb 2000;24(2):153-156.
65. Capanni C, Mattioli E, Columbaro M, et al. Altered pre-lamin A processing is a common mechanism leading to lipodystrophy. *Human molecular genetics*. Jun 1 2005;14(11):1489-1502.
66. Chen W, Yechoor VK, Chang BH, Li MV, March KL, Chan L. The human lipodystrophy gene product Berardinelli-Seip congenital lipodystrophy 2/seipin plays a key role in adipocyte differentiation. *Endocrinology*. Oct 2009;150(10):4552-4561.
67. Krahmer N, Farese RV, Jr., Walther TC. Balancing the fat: lipid droplets and human disease. *EMBO molecular medicine*. Jul 2013;5(7):905-915.
68. Tian Y, Bi J, Shui G, et al. Tissue-autonomous function of Drosophila seipin in preventing ectopic lipid droplet formation. *PLoS genetics*. Apr 2011;7(4):e1001364.
69. Fei W, Shui G, Gaeta B, et al. Fld1p, a functional homologue of human seipin, regulates the size of lipid droplets in yeast. *The Journal of cell biology*. Feb 11 2008;180(3):473-482.
70. Huang-Doran I, Sleigh A, Rochford JJ, O'Rahilly S, Savage DB. Lipodystrophy: metabolic insights from a rare disorder. *The Journal of endocrinology*. Dec 2010;207(3):245-255.
71. Yen CL, Stone SJ, Koliwad S, Harris C, Farese RV, Jr. Thematic review series: glycerolipids. DGAT enzymes and triacylglycerol biosynthesis. *Journal of lipid research*. Nov 2008;49(11):2283-2301.
72. Coleman RA, Lee DP. Enzymes of triacylglycerol synthesis and their regulation. *Progress in lipid research*. Mar 2004;43(2):134-176.
73. Coleman RA, Mashek DG. Mammalian triacylglycerol metabolism: synthesis, lipolysis, and signaling. *Chemical reviews*. Oct 12 2011;111(10):6359-6386.
74. Yang LY, Kuksis A. Apparent convergence (at 2-monoacylglycerol level) of phosphatidic acid and 2-monoacylglycerol pathways of synthesis of chylomicron triacylglycerols. *Journal of lipid research*. Jul 1991;32(7):1173-1186.
75. Yen CL, Stone SJ, Cases S, Zhou P, Farese RV, Jr. Identification of a gene encoding MGAT1, a monoacylglycerol acyltransferase. *Proceedings of the National Academy of Sciences of the United States of America*. Jun 25 2002;99(13):8512-8517.
76. Yen CL, Farese RV, Jr. MGAT2, a monoacylglycerol acyltransferase expressed in the small intestine. *The Journal of biological chemistry*. May 16 2003;278(20):18532-18537.
77. Yen CL, Cheong ML, Grueter C, et al. Deficiency of the intestinal enzyme acyl CoA:monoacylglycerol acyltransferase-2 protects mice from metabolic disorders induced by high-fat feeding. *Nature medicine*. Apr 2009;15(4):442-446.
78. Nelson DW, Gao Y, Yen MI, Yen CL. Intestine-specific deletion of acyl-CoA:monoacylglycerol acyltransferase (MGAT) 2 protects mice from diet-induced obesity and glucose intolerance. *The Journal of biological chemistry*. Jun 20 2014;289(25):17338-17349.
79. Banh T, Nelson DW, Gao Y, Huang TN, Yen MI, Yen CL. Adult-onset deficiency of acyl CoA:monoacylglycerol acyltransferase 2 protects mice

from diet-induced obesity and glucose intolerance. *Journal of lipid research*. Feb 2015;56(2):379-389.
80. Cheng D, Nelson TC, Chen J, et al. Identification of acyl coenzyme A:monoacylglycerol acyltransferase 3, an intestinal specific enzyme implicated in dietary fat absorption. *The Journal of biological chemistry*. Apr 18 2003;278(16):13611-13614.
81. Muoio DM, Seefeld K, Witters LA, Coleman RA. AMP-activated kinase reciprocally regulates triacylglycerol synthesis and fatty acid oxidation in liver and muscle: evidence that sn-glycerol-3-phosphate acyltransferase is a novel target. *The Biochemical journal*. Mar 15 1999;338 (Pt 3):783-791.
82. Gonzalez-Baro MR, Lewin TM, Coleman RA. Regulation of Triglyceride Metabolism. II. Function of mitochondrial GPAT1 in the regulation of triacylglycerol biosynthesis and insulin action. *American journal of physiology. Gastrointestinal and liver physiology*. May 2007;292(5):G1195-1199.
83. Nagle CA, An J, Shiota M, et al. Hepatic overexpression of glycerol-sn-3-phosphate acyltransferase 1 in rats causes insulin resistance. *The Journal of biological chemistry*. May 18 2007;282(20):14807-14815.
84. Neschen S, Morino K, Hammond LE, et al. Prevention of hepatic steatosis and hepatic insulin resistance in mitochondrial acyl-CoA:glycerol-sn-3-phosphate acyltransferase 1 knockout mice. *Cell metabolism*. Jul 2005;2(1):55-65.
85. Pellon-Maison M, Montanaro MA, Lacunza E, et al. Glycerol-3-phosphate acyltranferase-2 behaves as a cancer testis gene and promotes growth and tumorigenicity of the breast cancer MDA-MB-231 cell line. *PloS one*. 2014;9(6):e100896.
86. Shiromoto Y, Kuramochi-Miyagawa S, Daiba A, et al. GPAT2, a mitochondrial outer membrane protein, in piRNA biogenesis in germline stem cells. *Rna*. Jun 2013;19(6):803-810.
87. Cao J, Li JL, Li D, Tobin JF, Gimeno RE. Molecular identification of microsomal acyl-CoA:glycerol-3-phosphate acyltransferase, a key enzyme in de novo triacylglycerol synthesis. *Proceedings of the National Academy of Sciences of the United States of America*. Dec 26 2006;103(52):19695-19700.
88. Shan D, Li JL, Wu L, et al. GPAT3 and GPAT4 are regulated by insulin-stimulated phosphorylation and play distinct roles in adipogenesis. *Journal of lipid research*. Jul 2010;51(7):1971-1981.
89. Cao J, Perez S, Goodwin B, et al. Mice deleted for GPAT3 have reduced GPAT activity in white adipose tissue and altered energy and cholesterol homeostasis in diet-induced obesity. *American journal of physiology. Endocrinology and metabolism*. May 15 2014;306(10):E1176-1187.
90. Vergnes L, Beigneux AP, Davis R, Watkins SM, Young SG, Reue K. Agpat6 deficiency causes subdermal lipodystrophy and resistance to obesity. *Journal of lipid research*. Apr 2006;47(4):745-754.
91. West J, Tompkins CK, Balantac N, et al. Cloning and expression of two human lysophosphatidic acid acyltransferase cDNAs that enhance cytokine-induced signaling responses in cells. *DNA and cell biology*. Jun 1997;16(6):691-701.
92. Eberhardt C, Gray PW, Tjoelker LW. Human lysophosphatidic acid acyltransferase. cDNA cloning, expression, and localization to

chromosome 9q34.3. *The Journal of biological chemistry*. Aug 8 1997;272(32):20299-20305.
93. Agarwal AK, Arioglu E, De Almeida S, et al. AGPAT2 is mutated in congenital generalized lipodystrophy linked to chromosome 9q34. *Nature genetics*. May 2002;31(1):21-23.
94. Schmidt JA, Yvone GM, Brown WJ. Membrane topology of human AGPAT3 (LPAAT3). *Biochemical and biophysical research communications*. Jul 9 2010;397(4):661-667.
95. Schmidt JA, Brown WJ. Lysophosphatidic acid acyltransferase 3 regulates Golgi complex structure and function. *The Journal of cell biology*. Jul 27 2009;186(2):211-218.
96. Koeberle A, Shindou H, Harayama T, Yuki K, Shimizu T. Polyunsaturated fatty acids are incorporated into maturating male mouse germ cells by lysophosphatidic acid acyltransferase 3. *FASEB journal : official publication of the Federation of American Societies for Experimental Biology*. Jan 2012;26(1):169-180.
97. Yuki K, Shindou H, Hishikawa D, Shimizu T. Characterization of mouse lysophosphatidic acid acyltransferase 3: an enzyme with dual functions in the testis. *Journal of lipid research*. May 2009;50(5):860-869.
98. Ghosh AK, Ramakrishnan G, Chandramohan C, Rajasekharan R. CGI-58, the causative gene for Chanarin-Dorfman syndrome, mediates acylation of lysophosphatidic acid. *The Journal of biological chemistry*. Sep 5 2008;283(36):24525-24533.
99. Reue K, Dwyer JR. Lipin proteins and metabolic homeostasis. *Journal of lipid research*. Apr 2009;50 Suppl:S109-114.
100. Peterfy M, Phan J, Xu P, Reue K. Lipodystrophy in the fld mouse results from mutation of a new gene encoding a nuclear protein, lipin. *Nature genetics*. Jan 2001;27(1):121-124.
101. Reue K. The lipin family: mutations and metabolism. *Current opinion in lipidology*. Jun 2009;20(3):165-170.
102. Phan J, Reue K. Lipin, a lipodystrophy and obesity gene. *Cell metabolism*. Jan 2005;1(1):73-83.
103. Harris TE, Huffman TA, Chi A, et al. Insulin controls subcellular localization and multisite phosphorylation of the phosphatidic acid phosphatase, lipin 1. *The Journal of biological chemistry*. Jan 5 2007;282(1):277-286.
104. Grimsey N, Han GS, O'Hara L, Rochford JJ, Carman GM, Siniossoglou S. Temporal and spatial regulation of the phosphatidate phosphatases lipin 1 and 2. *The Journal of biological chemistry*. Oct 24 2008;283(43):29166-29174.
105. Gropler MC, Harris TE, Hall AM, et al. Lipin 2 is a liver-enriched phosphatidate phosphohydrolase enzyme that is dynamically regulated by fasting and obesity in mice. *The Journal of biological chemistry*. Mar 13 2009;284(11):6763-6772.
106. Weiss SB, Kennedy EP, Kiyasu JY. The enzymatic synthesis of triglycerides. *The Journal of biological chemistry*. Jan 1960;235:40-44.
107. Cases S, Smith SJ, Zheng YW, et al. Identification of a gene encoding an acyl CoA:diacylglycerol acyltransferase, a key enzyme in triacylglycerol synthesis. *Proceedings of the National Academy of Sciences of the United States of America*. Oct 27 1998;95(22):13018-13023.

108. Lardizabal KD, Mai JT, Wagner NW, Wyrick A, Voelker T, Hawkins DJ. DGAT2 is a new diacylglycerol acyltransferase gene family: purification, cloning, and expression in insect cells of two polypeptides from Mortierella ramanniana with diacylglycerol acyltransferase activity. *The Journal of biological chemistry*. Oct 19 2001;276(42):38862-38869.
109. Cases S, Stone SJ, Zhou P, et al. Cloning of DGAT2, a second mammalian diacylglycerol acyltransferase, and related family members. *The Journal of biological chemistry*. Oct 19 2001;276(42):38870-38876.
110. Turchetto-Zolet AC, Maraschin FS, de Morais GL, et al. Evolutionary view of acyl-CoA diacylglycerol acyltransferase (DGAT), a key enzyme in neutral lipid biosynthesis. *BMC evolutionary biology*. 2011;11:263.
111. Yen CL, Monetti M, Burri BJ, Farese RV, Jr. The triacylglycerol synthesis enzyme DGAT1 also catalyzes the synthesis of diacylglycerols, waxes, and retinyl esters. *Journal of lipid research*. Jul 2005;46(7):1502-1511.
112. Ables GP, Yang KJ, Vogel S, et al. Intestinal DGAT1 deficiency reduces postprandial triglyceride and retinyl ester excursions by inhibiting chylomicron secretion and delaying gastric emptying. *Journal of lipid research*. Nov 2012;53(11):2364-2379.
113. McFie PJ, Stone SL, Banman SL, Stone SJ. Topological orientation of acyl-CoA:diacylglycerol acyltransferase-1 (DGAT1) and identification of a putative active site histidine and the role of the n terminus in dimer/tetramer formation. *The Journal of biological chemistry*. Nov 26 2010;285(48):37377-37387.
114. Wurie HR, Buckett L, Zammit VA. Evidence that diacylglycerol acyltransferase 1 (DGAT1) has dual membrane topology in the endoplasmic reticulum of HepG2 cells. *The Journal of biological chemistry*. Oct 21 2011;286(42):36238-36247.
115. Stone SJ, Levin MC, Farese RV, Jr. Membrane topology and identification of key functional amino acid residues of murine acyl-CoA:diacylglycerol acyltransferase-2. *The Journal of biological chemistry*. Dec 29 2006;281(52):40273-40282.
116. Stone SJ, Levin MC, Zhou P, Han J, Walther TC, Farese RV, Jr. The endoplasmic reticulum enzyme DGAT2 is found in mitochondria-associated membranes and has a mitochondrial targeting signal that promotes its association with mitochondria. *The Journal of biological chemistry*. Feb 20 2009;284(8):5352-5361.
117. McFie PJ, Banman SL, Kary S, Stone SJ. Murine diacylglycerol acyltransferase-2 (DGAT2) can catalyze triacylglycerol synthesis and promote lipid droplet formation independent of its localization to the endoplasmic reticulum. *The Journal of biological chemistry*. Aug 12 2011;286(32):28235-28246.
118. Wilfling F, Wang H, Haas JT, et al. Triacylglycerol synthesis enzymes mediate lipid droplet growth by relocalizing from the ER to lipid droplets. *Developmental cell*. Feb 25 2013;24(4):384-399.
119. Xu N, Zhang SO, Cole RA, et al. The FATP1-DGAT2 complex facilitates lipid droplet expansion at the ER-lipid droplet interface. *The Journal of cell biology*. Sep 3 2012;198(5):895-911.
120. Wilfling F, Thiam AR, Olarte MJ, et al. Arf1/COPI machinery acts directly on lipid droplets and enables their connection to the ER for protein targeting. *eLife*. 2014;3:e01607.

121. Thiam AR, Antonny B, Wang J, et al. COPI buds 60-nm lipid droplets from reconstituted water-phospholipid-triacylglyceride interfaces, suggesting a tension clamp function. *Proceedings of the National Academy of Sciences of the United States of America*. Aug 13 2013;110(33):13244-13249.
122. Jin Y, McFie PJ, Banman SL, Brandt C, Stone SJ. Diacylglycerol acyltransferase-2 (DGAT2) and monoacylglycerol acyltransferase-2 (MGAT2) interact to promote triacylglycerol synthesis. *The Journal of biological chemistry*. Oct 10 2014;289(41):28237-28248.
123. Man WC, Miyazaki M, Chu K, Ntambi J. Colocalization of SCD1 and DGAT2: implying preference for endogenous monounsaturated fatty acids in triglyceride synthesis. *Journal of lipid research*. Sep 2006;47(9):1928-1939.
124. Harris CA, Haas JT, Streeper RS, et al. DGAT enzymes are required for triacylglycerol synthesis and lipid droplets in adipocytes. *Journal of lipid research*. Apr 2011;52(4):657-667.
125. Smith SJ, Cases S, Jensen DR, et al. Obesity resistance and multiple mechanisms of triglyceride synthesis in mice lacking Dgat. *Nature genetics*. May 2000;25(1):87-90.
126. Chen HC, Ladha Z, Smith SJ, Farese RV, Jr. Analysis of energy expenditure at different ambient temperatures in mice lacking DGAT1. *American journal of physiology. Endocrinology and metabolism*. Jan 2003;284(1):E213-218.
127. Chen HC, Smith SJ, Ladha Z, et al. Increased insulin and leptin sensitivity in mice lacking acyl CoA:diacylglycerol acyltransferase 1. *The Journal of clinical investigation*. Apr 2002;109(8):1049-1055.
128. Liu L, Shi X, Bharadwaj KG, et al. DGAT1 expression increases heart triglyceride content but ameliorates lipotoxicity. *The Journal of biological chemistry*. Dec 25 2009;284(52):36312-36323.
129. Buhman KK, Smith SJ, Stone SJ, et al. DGAT1 is not essential for intestinal triacylglycerol absorption or chylomicron synthesis. *The Journal of biological chemistry*. Jul 12 2002;277(28):25474-25479.
130. Schober G, Arnold M, Birtles S, et al. Diacylglycerol acyltransferase-1 inhibition enhances intestinal fatty acid oxidation and reduces energy intake in rats. *Journal of lipid research*. May 2013;54(5):1369-1384.
131. Cao J, Zhou Y, Peng H, et al. Targeting Acyl-CoA:diacylglycerol acyltransferase 1 (DGAT1) with small molecule inhibitors for the treatment of metabolic diseases. *The Journal of biological chemistry*. Dec 2 2011;286(48):41838-41851.
132. Lin HV, Chen D, Shen Z, et al. Diacylglycerol acyltransferase-1 (DGAT1) inhibition perturbs postprandial gut hormone release. *PloS one*. 2013;8(1):e54480.
133. Chandak PG, Obrowsky S, Radovic B, et al. Lack of acyl-CoA:diacylglycerol acyltransferase 1 reduces intestinal cholesterol absorption and attenuates atherosclerosis in apolipoprotein E knockout mice. *Biochimica et biophysica acta*. Dec 2011;1811(12):1011-1020.
134. Haas JT, Winter HS, Lim E, et al. DGAT1 mutation is linked to a congenital diarrheal disorder. *The Journal of clinical investigation*. Dec 2012;122(12):4680-4684.

135. Hiramine Y, Tanabe T. Characterization of acyl-coenzyme A:diacylglycerol acyltransferase (DGAT) enzyme of human small intestine. *Journal of physiology and biochemistry*. Jun 2011;67(2):259-264.
136. Liu L, Zhang Y, Chen N, Shi X, Tsang B, Yu YH. Upregulation of myocellular DGAT1 augments triglyceride synthesis in skeletal muscle and protects against fat-induced insulin resistance. *The Journal of clinical investigation*. Jun 2007;117(6):1679-1689.
137. Koliwad SK, Streeper RS, Monetti M, et al. DGAT1-dependent triacylglycerol storage by macrophages protects mice from diet-induced insulin resistance and inflammation. *The Journal of clinical investigation*. Mar 2010;120(3):756-767.
138. Stone SJ, Myers HM, Watkins SM, et al. Lipopenia and skin barrier abnormalities in DGAT2-deficient mice. *The Journal of biological chemistry*. Mar 19 2004;279(12):11767-11776.
139. Qi J, Lang W, Geisler JG, et al. The use of stable isotope-labeled glycerol and oleic acid to differentiate the hepatic functions of DGAT1 and 2. *Journal of lipid research*. Jun 2012;53(6):1106-1116.
140. Yu XX, Murray SF, Pandey SK, et al. Antisense oligonucleotide reduction of DGAT2 expression improves hepatic steatosis and hyperlipidemia in obese mice. *Hepatology*. Aug 2005;42(2):362-371.
141. Liu Y, Millar JS, Cromley DA, et al. Knockdown of acyl-CoA:diacylglycerol acyltransferase 2 with antisense oligonucleotide reduces VLDL TG and ApoB secretion in mice. *Biochimica et biophysica acta*. Mar 2008;1781(3):97-104.
142. Monetti M, Levin MC, Watt MJ, et al. Dissociation of hepatic steatosis and insulin resistance in mice overexpressing DGAT in the liver. *Cell metabolism*. Jul 2007;6(1):69-78.
143. Sahini N, Borlak J. Recent insights into the molecular pathophysiology of lipid droplet formation in hepatocytes. *Progress in lipid research*. Apr 2014;54:86-112.
144. Wiggins D, Gibbons GF. The lipolysis/esterification cycle of hepatic triacylglycerol. Its role in the secretion of very-low-density lipoprotein and its response to hormones and sulphonylureas. *The Biochemical journal*. Jun 1 1992;284 (Pt 2):457-462.
145. Welte MA. Proteins under new management: lipid droplets deliver. *Trends in cell biology*. Aug 2007;17(8):363-369.
146. Herker E, Ott M. Unique ties between hepatitis C virus replication and intracellular lipids. *Trends in endocrinology and metabolism*. Jun 2011;22(6):241-248.
147. Walther TC, Farese RV, Jr. Lipid droplets and cellular lipid metabolism. *Annual review of biochemistry*. 2012;81:687-714.
148. Hartler J. Assessment of lipidomic species in hepatocyte lipid droplets from stressed mouse models. Scientific Data. Dec 23 2014;1:140051
149. Chitraju C, Trotzmuller M, Hartler J, et al. Lipidomic analysis of lipid droplets from murine hepatocytes reveals distinct signatures for nutritional stress. *Journal of lipid research*. Oct 2012;53(10):2141-2152.
150. Thiam AR, Farese RV, Jr., Walther TC. The biophysics and cell biology of lipid droplets. *Nature reviews molecular cell biology*. Dec 2013;14(12):775-786.
151. Ploegh HL. A lipid-based model for the creation of an escape hatch from the endoplasmic reticulum. *Nature*. Jul 26 2007;448(7152):435-438.

152. Krahmer N, Guo Y, Wilfling F, et al. Phosphatidylcholine synthesis for lipid droplet expansion is mediated by localized activation of CTP:phosphocholine cytidylyltransferase. *Cell metabolism*. Oct 5 2011;14(4):504-515.
153. Lehner R, Lian J, Quiroga AD. Lumenal lipid metabolism: implications for lipoprotein assembly. *Arteriosclerosis, thrombosis, and vascular biology*. May 2012;32(5):1087-1093.
154. Murphy S, Martin S, Parton RG. Quantitative analysis of lipid droplet fusion: inefficient steady state fusion but rapid stimulation by chemical fusogens. *PloS one*. 2010;5(12):e15030.
155. Ozeki S, Cheng J, Tauchi-Sato K, Hatano N, Taniguchi H, Fujimoto T. Rab18 localizes to lipid droplets and induces their close apposition to the endoplasmic reticulum-derived membrane. *Journal of cell science*. Jun 15 2005;118(Pt 12):2601-2611.
156. Martin S, Driessen K, Nixon SJ, Zerial M, Parton RG. Regulated localization of Rab18 to lipid droplets: effects of lipolytic stimulation and inhibition of lipid droplet catabolism. *The Journal of biological chemistry*. Dec 23 2005;280(51):42325-42335.
157. Bartz R, Zehmer JK, Zhu M, et al. Dynamic activity of lipid droplets: protein phosphorylation and GTP-mediated protein translocation. *Journal of proteome research*. Aug 2007;6(8):3256-3265.
158. Soni KG, Mardones GA, Sougrat R, Smirnova E, Jackson CL, Bonifacino JS. Coatomer-dependent protein delivery to lipid droplets. *Journal of cell science*. Jun 1 2009;122(Pt 11):1834-1841.
159. Guo Y, Walther TC, Rao M, et al. Functional genomic screen reveals genes involved in lipid-droplet formation and utilization. *Nature*. May 29 2008;453(7195):657-661.
160. Abu-Elheiga L, Brinkley WR, Zhong L, Chirala SS, Woldegiorgis G, Wakil SJ. The subcellular localization of acetyl-CoA carboxylase 2. *Proceedings of the National Academy of Sciences of the United States of America*. Feb 15 2000;97(4):1444-1449.
161. Thampy KG, Wakil SJ. Regulation of acetyl-coenzyme A carboxylase. II. Effect of fasting and refeeding on the activity, phosphate content, and aggregation state of the enzyme. *The Journal of biological chemistry*. May 5 1988;263(13):6454-6458.
162. Berg JM, Tymoczko JL, Stryer L. *Biochemistry*. 5th ed. New York: W. H. Freeman and CO.; 2002.
163. Shimomura I, Shimano H, Korn BS, Bashmakov Y, Horton JD. Nuclear sterol regulatory element-binding proteins activate genes responsible for the entire program of unsaturated fatty acid biosynthesis in transgenic mouse liver. *The Journal of biological chemistry*. Dec 25 1998;273(52):35299-35306.
164. Liang G, Yang J, Horton JD, Hammer RE, Goldstein JL, Brown MS. Diminished hepatic response to fasting/refeeding and liver X receptor agonists in mice with selective deficiency of sterol regulatory element-binding protein-1c. *The Journal of biological chemistry*. Mar 15 2002;277(11):9520-9528.
165. Shimano H, Horton JD, Shimomura I, Hammer RE, Brown MS, Goldstein JL. Isoform 1c of sterol regulatory element binding protein is less active than isoform 1a in livers of transgenic mice and in cultured cells. *The Journal of clinical investigation*. Mar 1 1997;99(5):846-854.

166. Okita RT, Okita JR. Cytochrome P450 4A fatty acid omega hydroxylases. *Current drug metabolism*. Sep 2001;2(3):265-281.
167. Reddy JK, Hashimoto T. Peroxisomal beta-oxidation and peroxisome proliferator-activated receptor alpha: an adaptive metabolic system. *Annual review of nutrition*. 2001;21:193-230.
168. Yang LY, Kuksis A, Myher JJ, Steiner G. Origin of triacylglycerol moiety of plasma very low density lipoproteins in the rat: structural studies. *Journal of lipid research*. Jan 1995;36(1):125-136.
169. Gibbons GF, Wiggins D. Intracellular triacylglycerol lipase: its role in the assembly of hepatic very-low-density lipoprotein (VLDL). *Advances in enzyme regulation*. 1995;35:179-198.
170. Levy E, Stan S, Delvin E, et al. Localization of microsomal triglyceride transfer protein in the Golgi: possible role in the assembly of chylomicrons. *The Journal of biological chemistry*. May 10 2002;277(19):16470-16477.
171. Wetterau JR, Combs KA, Spinner SN, Joiner BJ. Protein disulfide isomerase is a component of the microsomal triglyceride transfer protein complex. *The Journal of biological chemistry*. Jun 15 1990;265(17):9800-9807.
172. Swift LL, Zhu MY, Kakkad B, et al. Subcellular localization of microsomal triglyceride transfer protein. *Journal of lipid research*. Oct 2003;44(10):1841-1849.
173. Tietge UJ, Bakillah A, Maugeais C, Tsukamoto K, Hussain M, Rader DJ. Hepatic overexpression of microsomal triglyceride transfer protein (MTP) results in increased in vivo secretion of VLDL triglycerides and apolipoprotein B. *Journal of lipid research*. Nov 1999;40(11):2134-2139.
174. Rustaeus S, Stillemark P, Lindberg K, Gordon D, Olofsson SO. The microsomal triglyceride transfer protein catalyzes the post-translational assembly of apolipoprotein B-100 very low density lipoprotein in McA-RH7777 cells. *The Journal of biological chemistry*. Feb 27 1998;273(9):5196-5203.
175. Pan M, Liang Js JS, Fisher EA, Ginsberg HN. The late addition of core lipids to nascent apolipoprotein B100, resulting in the assembly and secretion of triglyceride-rich lipoproteins, is independent of both microsomal triglyceride transfer protein activity and new triglyceride synthesis. *The Journal of biological chemistry*. Feb 8 2002;277(6):4413-4421.
176. Kulinski A, Rustaeus S, Vance JE. Microsomal triacylglycerol transfer protein is required for lumenal accretion of triacylglycerol not associated with ApoB, as well as for ApoB lipidation. *The Journal of biological chemistry*. Aug 30 2002;277(35):31516-31525.
177. Magnusson B, Asp L, Bostrom P, et al. Adipocyte differentiation-related protein promotes fatty acid storage in cytosolic triglycerides and inhibits secretion of very low-density lipoproteins. *Arteriosclerosis, thrombosis, and vascular biology*. Jul 2006;26(7):1566-1571.
178. Ye J, Li JZ, Liu Y, et al. Cideb, an ER- and lipid droplet-associated protein, mediates VLDL lipidation and maturation by interacting with apolipoprotein B. *Cell metabolism*. Feb 2009;9(2):177-190.
179. Caviglia JM, Sparks JD, Toraskar N, et al. ABHD5/CGI-58 facilitates the assembly and secretion of apolipoprotein B lipoproteins by McA RH7777

rat hepatoma cells. *Biochimica et biophysica acta*. Mar 2009;1791(3):198-205.
180. Brown JM, Chung S, Das A, Shelness GS, Rudel LL, Yu L. CGI-58 facilitates the mobilization of cytoplasmic triglyceride for lipoprotein secretion in hepatoma cells. *Journal of lipid research*. Oct 2007;48(10):2295-2305.
181. Brown JM, Betters JL, Lord C, et al. CGI-58 knockdown in mice causes hepatic steatosis but prevents diet-induced obesity and glucose intolerance. *Journal of lipid research*. Nov 2010;51(11):3306-3315.
182. Guo F, Ma Y, Kadegowda AK, et al. Deficiency of liver Comparative Gene Identification-58 causes steatohepatitis and fibrosis in mice. *Journal of lipid research*. Aug 2013;54(8):2109-2120.
183. Wu JW, Wang SP, Alvarez F, et al. Deficiency of liver adipose triglyceride lipase in mice causes progressive hepatic steatosis. *Hepatology*. Jul 2011;54(1):122-132.
184. Ong KT, Mashek MT, Bu SY, Mashek DG. Hepatic ATGL knockdown uncouples glucose intolerance from liver TAG accumulation. *FASEB journal : official publication of the Federation of American Societies for Experimental Biology*. Jan 2013;27(1):313-321.
185. Reid BN, Ables GP, Otlivanchik OA, et al. Hepatic overexpression of hormone-sensitive lipase and adipose triglyceride lipase promotes fatty acid oxidation, stimulates direct release of free fatty acids, and ameliorates steatosis. *The Journal of biological chemistry*. May 9 2008;283(19):13087-13099.
186. Gilham D, Alam M, Gao W, Vance DE, Lehner R. Triacylglycerol hydrolase is localized to the endoplasmic reticulum by an unusual retrieval sequence where it participates in VLDL assembly without utilizing VLDL lipids as substrates. *Molecular biology of the cell*. Feb 2005;16(2):984-996.
187. Gilham D, Ho S, Rasouli M, Martres P, Vance DE, Lehner R. Inhibitors of hepatic microsomal triacylglycerol hydrolase decrease very low density lipoprotein secretion. *FASEB journal : official publication of the Federation of American Societies for Experimental Biology*. Sep 2003;17(12):1685-1687.
188. Lehner R, Vance DE. Cloning and expression of a cDNA encoding a hepatic microsomal lipase that mobilizes stored triacylglycerol. *The Biochemical journal*. Oct 1 1999;343 Pt 1:1-10.
189. Wei E, Ben Ali Y, Lyon J, et al. Loss of TGH/Ces3 in mice decreases blood lipids, improves glucose tolerance, and increases energy expenditure. *Cell metabolism*. Mar 3 2010;11(3):183-193.
190. Lian J, Wei E, Wang SP, et al. Liver specific inactivation of carboxylesterase 3/triacylglycerol hydrolase decreases blood lipids without causing severe steatosis in mice. *Hepatology*. Dec 2012;56(6):2154-2162.
191. Gibbons GF, Islam K, Pease RJ. Mobilisation of triacylglycerol stores. *Biochimica et biophysica acta*. Jan 3 2000;1483(1):37-57.
192. Trickett JI, Patel DD, Knight BL, Saggerson ED, Gibbons GF, Pease RJ. Characterization of the rodent genes for arylacetamide deacetylase, a putative microsomal lipase, and evidence for transcriptional regulation. *The Journal of biological chemistry*. Oct 26 2001;276(43):39522-39532.

193. Gusarova V, Brodsky JL, Fisher EA. Apolipoprotein B100 exit from the endoplasmic reticulum (ER) is COPII-dependent, and its lipidation to very low density lipoprotein occurs post-ER. *The Journal of biological chemistry*. Nov 28 2003;278(48):48051-48058.
194. Jones B, Jones EL, Bonney SA, et al. Mutations in a Sar1 GTPase of COPII vesicles are associated with lipid absorption disorders. *Nature genetics*. May 2003;34(1):29-31.
195. Pellett PA, Dietrich F, Bewersdorf J, Rothman JE, Lavieu G. Inter-Golgi transport mediated by COPI-containing vesicles carrying small cargoes. *eLife*. 2013;2:e01296.
196. Orci L, Stamnes M, Ravazzola M, et al. Bidirectional transport by distinct populations of COPI-coated vesicles. *Cell*. Jul 25 1997;90(2):335-349.
197. Asp L, Magnusson B, Rutberg M, Li L, Boren J, Olofsson SO. Role of ADP ribosylation factor 1 in the assembly and secretion of ApoB-100-containing lipoproteins. *Arteriosclerosis, thrombosis, and vascular biology*. Mar 2005;25(3):566-570.
198. Rustaeus S, Lindberg K, Boren J, Olofsson SO. Brefeldin A reversibly inhibits the assembly of apoB containing lipoproteins in McA-RH7777 cells. *The Journal of biological chemistry*. Dec 1 1995;270(48):28879-28886.
199. Brown HA, Gutowski S, Moomaw CR, Slaughter C, Sternweis PC. ADP-ribosylation factor, a small GTP-dependent regulatory protein, stimulates phospholipase D activity. *Cell*. Dec 17 1993;75(6):1137-1144.
200. Asp L, Claesson C, Boren J, Olofsson SO. ADP-ribosylation factor 1 and its activation of phospholipase D are important for the assembly of very low density lipoproteins. *The Journal of biological chemistry*. Aug 25 2000;275(34):26285-26292.
201. Pathre P, Shome K, Blumental-Perry A, et al. Activation of phospholipase D by the small GTPase Sar1p is required to support COPII assembly and ER export. *The EMBO journal*. Aug 15 2003;22(16):4059-4069.
202. Yao ZM, Vance DE. The active synthesis of phosphatidylcholine is required for very low density lipoprotein secretion from rat hepatocytes. *The Journal of biological chemistry*. Feb 25 1988;263(6):2998-3004.
203. Folch J, Lees M, Sloane Stanley GH. A simple method for the isolation and purification of total lipides from animal tissues. *The Journal of biological chemistry*. May 1957;226(1):497-509.
204. Choi CS, Savage DB, Kulkarni A, et al. Suppression of diacylglycerol acyltransferase-2 (DGAT2), but not DGAT1, with antisense oligonucleotides reverses diet-induced hepatic steatosis and insulin resistance. *The Journal of biological chemistry*. Aug 3 2007;282(31):22678-22688.
205. Waterman IJ, Price NT, Zammit VA. Distinct ontogenic patterns of overt and latent DGAT activities of rat liver microsomes. *Journal of lipid research*. Sep 2002;43(9):1555-1562.
206. Abo-Hashema KA, Cake MH, Power GW, Clarke D. Evidence for triacylglycerol synthesis in the lumen of microsomes via a lipolysis-esterification pathway involving carnitine acyltransferases. *The Journal of biological chemistry*. Dec 10 1999;274(50):35577-35582.
207. Owen M, Zammit VA. Evidence for overt and latent forms of DGAT in rat liver microsomes. Implications for the pathways of triacylglycerol

incorporation into VLDL. *Biochemical Society transactions*. Feb 1997;25(1):21S.
208. Owen MR, Corstorphine CC, Zammit VA. Overt and latent activities of diacylglycerol acytransferase in rat liver microsomes: possible roles in very-low-density lipoprotein triacylglycerol secretion. *The Biochemical journal*. Apr 1 1997;323 (Pt 1):17-21.
209. Wang H, Gilham D, Lehner R. Proteomic and lipid characterization of apolipoprotein B-free luminal lipid droplets from mouse liver microsomes: implications for very low density lipoprotein assembly. *The Journal of biological chemistry*. Nov 9 2007;282(45):33218-33226.
210. Lankester DL, Brown AM, Zammit VA. Use of cytosolic triacylglycerol hydrolysis products and of exogenous fatty acid for the synthesis of triacylglycerol secreted by cultured rat hepatocytes. *Journal of lipid research*. Sep 1998;39(9):1889-1895.
211. Cornell R, Vance DE. Binding of CTP: phosphocholine cytidylyltransferase to large unilamellar vesicles. *Biochimica et biophysica acta*. May 13 1987;919(1):37-48.
212. Jacobs RL, Zhao Y, Koonen DP, et al. Impaired de novo choline synthesis explains why phosphatidylethanolamine N-methyltransferase-deficient mice are protected from diet-induced obesity. *The Journal of biological chemistry*. Jul 16 2010;285(29):22403-22413.
213. Higashi Y, Itabe H, Fukase H, Mori M, Fujimoto Y, Takano T. Transmembrane lipid transfer is crucial for providing neutral lipids during very low density lipoprotein assembly in endoplasmic reticulum. *The Journal of biological chemistry*. Jun 13 2003;278(24):21450-21458.
214. Ong KT, Mashek MT, Bu SY, Greenberg AS, Mashek DG. Adipose triglyceride lipase is a major hepatic lipase that regulates triacylglycerol turnover and fatty acid signaling and partitioning. *Hepatology*. Jan 2011;53(1):116-126.
215. Kim E, Young SG. Genetically modified mice for the study of apolipoprotein B. *Journal of lipid research*. Apr 1998;39(4):703-723.
216. Yamazaki T, Sasaki E, Kakinuma C, Yano T, Miura S, Ezaki O. Increased very low density lipoprotein secretion and gonadal fat mass in mice overexpressing liver DGAT1. *The Journal of biological chemistry*. Jun 3 2005;280(22):21506-21514.
217. Liang JJ, Oelkers P, Guo C, et al. Overexpression of human diacylglycerol acyltransferase 1, acyl-coa:cholesterol acyltransferase 1, or acyl-CoA:cholesterol acyltransferase 2 stimulates secretion of apolipoprotein B-containing lipoproteins in McA-RH7777 cells. *The Journal of biological chemistry*. Oct 22 2004;279(43):44938-44944.
218. Millar JS, Stone SJ, Tietge UJ, et al. Short-term overexpression of DGAT1 or DGAT2 increases hepatic triglyceride but not VLDL triglyceride or apoB production. *Journal of lipid research*. Oct 2006;47(10):2297-2305.
219. Wurie HR, Buckett L, Zammit VA. Diacylglycerol acyltransferase 2 acts upstream of diacylglycerol acyltransferase 1 and utilizes nascent diglycerides and de novo synthesized fatty acids in HepG2 cells. *The FEBS journal*. Sep 2012;279(17):3033-3047.
220. Wu X, Shang A, Jiang H, Ginsberg HN. Low rates of apoB secretion from HepG2 cells result from reduced delivery of newly synthesized triglyceride to a "secretion-coupled" pool. *Journal of lipid research*. Jun 1996;37(6):1198-1206.

221. Gibbons GF, Khurana R, Odwell A, Seelaender MC. Lipid balance in HepG2 cells: active synthesis and impaired mobilization. *Journal of lipid research*. Oct 1994;35(10):1801-1808.
222. Shimomura I, Bashmakov Y, Horton JD. Increased levels of nuclear SREBP-1c associated with fatty livers in two mouse models of diabetes mellitus. *The Journal of biological chemistry*. Oct 15 1999;274(42):30028-30032.
223. Brookheart RT, Michel CI, Schaffer JE. As a matter of fat. *Cell metabolism*. Jul 2009;10(1):9-12.
224. Listenberger LL, Han X, Lewis SE, et al. Triglyceride accumulation protects against fatty acid-induced lipotoxicity. *Proceedings of the National Academy of Sciences of the United States of America*. Mar 18 2003;100(6):3077-3082.
225. Inoguchi T, Li P, Umeda F, et al. High glucose level and free fatty acid stimulate reactive oxygen species production through protein kinase C--dependent activation of NAD(P)H oxidase in cultured vascular cells. *Diabetes*. Nov 2000;49(11):1939-1945.
226. Ganji SH, Tavintharan S, Zhu D, Xing Y, Kamanna VS, Kashyap ML. Niacin noncompetitively inhibits DGAT2 but not DGAT1 activity in HepG2 cells. *Journal of lipid research*. Oct 2004;45(10):1835-1845.
227. Liu Q, Siloto RM, Snyder CL, Weselake RJ. Functional and topological analysis of yeast acyl-CoA:diacylglycerol acyltransferase 2, an endoplasmic reticulum enzyme essential for triacylglycerol biosynthesis. *The Journal of biological chemistry*. Apr 15 2011;286(15):13115-13126.
228. Tran K, Thorne-Tjomsland G, DeLong CJ, et al. Intracellular assembly of very low density lipoproteins containing apolipoprotein B100 in rat hepatoma McA-RH7777 cells. *The Journal of biological chemistry*. Aug 23 2002;277(34):31187-31200.
229. Bamberger MJ, Lane MD. Possible role of the Golgi apparatus in the assembly of very low density lipoprotein. *Proceedings of the National Academy of Sciences of the United States of America*. Apr 1990;87(7):2390-2394.
230. Yamaguchi J, Gamble MV, Conlon D, Liang JS, Ginsberg HN. The conversion of apoB100 low density lipoprotein/high density lipoprotein particles to apoB100 very low density lipoproteins in response to oleic acid occurs in the endoplasmic reticulum and not in the Golgi in McA RH7777 cells. *The Journal of biological chemistry*. Oct 24 2003;278(43):42643-42651.
231. Müller G, Petry S. *Lipases and phospholipases in drug development : from biochemistry to molecular pharmacology*. Weinheim, Germany: Wiley-VCH ; John Wiley; 2004.
232. Hussain MM, Shi J, Dreizen P. Microsomal triglyceride transfer protein and its role in apoB-lipoprotein assembly. *Journal of lipid research*. Jan 2003;44(1):22-32.
233. Rava P, Ojakian GK, Shelness GS, Hussain MM. Phospholipid transfer activity of microsomal triacylglycerol transfer protein is sufficient for the assembly and secretion of apolipoprotein B lipoproteins. *The Journal of biological chemistry*. Apr 21 2006;281(16):11019-11027.
234. Kuipers F, Jong MC, Lin Y, et al. Impaired secretion of very low density lipoprotein-triglycerides by apolipoprotein E- deficient mouse

hepatocytes. *The Journal of clinical investigation*. Dec 1 1997;100(11):2915-2922.
235. Mensenkamp AR, Havekes LM, Romijn JA, Kuipers F. Hepatic steatosis and very low density lipoprotein secretion: the involvement of apolipoprotein E. *Journal of hepatology*. Dec 2001;35(6):816-822.
236. Mensenkamp AR, Van Luyn MJ, Havinga R, et al. The transport of triglycerides through the secretory pathway of hepatocytes is impaired in apolipoprotein E deficient mice. *Journal of hepatology*. Apr 2004;40(4):599-606.
237. Lass A, Zimmermann R, Haemmerle G, et al. Adipose triglyceride lipase-mediated lipolysis of cellular fat stores is activated by CGI-58 and defective in Chanarin-Dorfman Syndrome. *Cell metabolism*. May 2006;3(5):309-319.
238. D'Souza-Schorey C, Chavrier P. ARF proteins: roles in membrane traffic and beyond. *Nature reviews. Molecular cell biology*. May 2006;7(5):347-358.